ANNALS
OF THE UNIVERSITY OF PETROŞANI

ELECTRICAL ENGINEERING

VOL. 14 (XXXXI)

CONTENTS

THE MODELING AND SIMULATION THE CONTROL SYSTEM OF SMALL DEFORMATIONS OF A ONE-DIMENSIONAL BAR

Olimpiu STOICUȚA[1], Corneliu MÂNDRESCU[2]

Abstract: The paper presents the modeling and simulation of the control system of small deformations that can occur in one-dimensional bar from the experience of traction-compression.

Key words: modeling, simulation, control system, small deformations, one-dimensional bar.

1. INTRODUCTION

The paper presents a control system of elasto-plastic deformations in case of the one-dimensional experiences. Control system is made using a press INSTROM, series 5900. The control by the force of the INSTROM electromechanical press is achieved through an induction motor. The induction motor speed is controlled through a system of the vector control, by the sensorless type, that contains in its loop a extended Luenberger observer. The INSTROM electromechanical press and block diagram of the process to be automated are shown in the figure 1.

2. THE MATHEMATIC MODEL OF THE PROCESS

The constitutive equations are formulated below a material particle x of the body Ω, where $\Omega = [a,b]$, which is deformed.

We introduce the following assumptions characteristic of the constitutive framework of the hardenind mixed model for von Mises flow theory.

The rate of strain tensor $\dot{\varepsilon}(x,t) = \varepsilon[\dot{u}(x,t)]$ can be descomposed into the rate of

---

[1] *Ph.D. Assist. Professor, University of Petrosani,* stoicuta_olimpiu@yahoo.com
[2] *Ph.D. Assoc. Professor, University of Petrosani,* c_mandrescu@yahoo.com

strain elastic and the rate of strain plastic, denoted by $\dot{\varepsilon}^e$ and $\dot{\varepsilon}^p$, respectively, according to he relation:

$$\dot{\varepsilon} = \dot{\varepsilon}^e + \dot{\varepsilon}^p \tag{1}$$

The constitutive elastic equation is defined by the relation:

$$\dot{\sigma} = \mathcal{E} \cdot \dot{\varepsilon}^e \tag{2}$$

where $\dot{\sigma}$ is the rate of Cauchy stress tensor, and $\mathcal{E}$ is the tensor of elastic moduli.

The irreversible properties of the material are described by the function of plasticity:

$$\mathcal{F}(\sigma, \alpha, k) = \left| \sigma_{11} - \alpha_{11} \right| - \left[Q \cdot (1 - e^{-b \cdot k}) + \sigma_Y \right] \tag{3}$$

where α is the isotropic hardening tensorial variable, and k is the scalar hardening variable.

The rate of strain plastic tensor is described by the flow rule:

$$\dot{\varepsilon}^p = \lambda \cdot \frac{\partial \mathcal{F}(\sigma, \alpha, k)}{\partial \sigma} \tag{4}$$
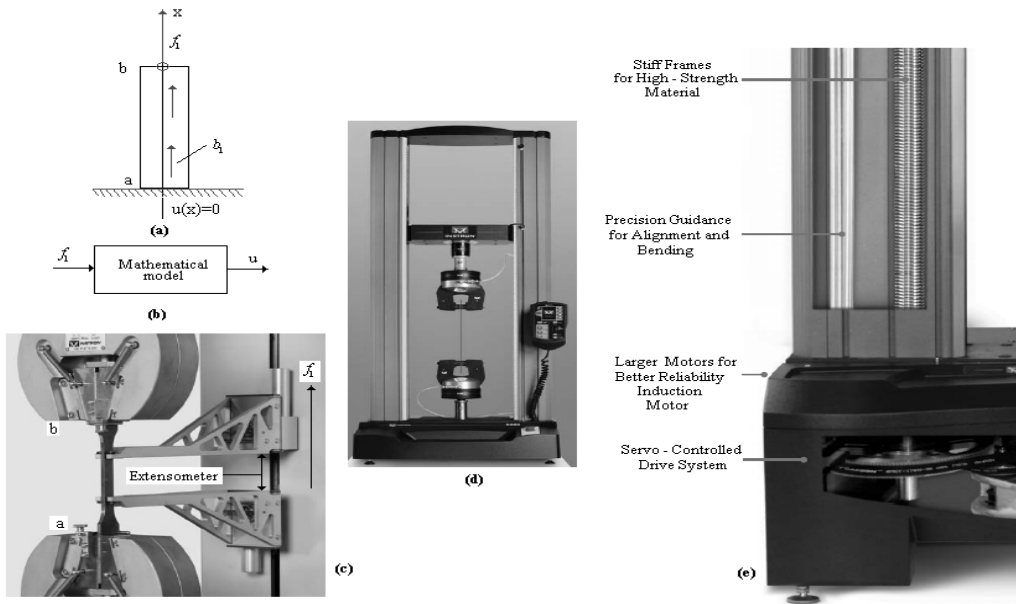
Fig. 1. The block diagram of the INSTROM electromecanical press [12]
a) The block diagram helpful for the determination of the mathematical model of the process;
b) The mathematical model of the process under the under the input-output systemic form;
c) The extensometer used for the mesurement by the uniaxial displacement;
d) The INSTROM electromecanical press;
e) The principal subsystem of the INSTROM electromecanical press

where the parameter λ, referred to as the plastic multiplier, is asumed to obey the following Kuhn-Tucker (complenmentarity) conditions:

$$\lambda \geq 0, \quad \mathcal{F} \leq 0, \quad \lambda \cdot \mathcal{F} = 0 \ \text{ with } \ \lambda \cdot \dot{\mathcal{F}} = 0 \tag{5}$$

The variation of the hardening tensorial variable α is given by the rule formulated by Armstrong, Frederik [1]:

$$\dot{\alpha} = C \cdot \dot{\varepsilon}^p - \gamma \cdot \alpha \cdot \dot{k} \tag{6}$$

where the rate of the scalar hardening variable k is given by the relation:

$$\dot{k} = \sqrt{2/3} \cdot \lambda \tag{7}$$

We attached the folowing initially conditions:

$$\sigma(0) = 0, \ \varepsilon(0) = 0, \ \varepsilon^p(0) = 0, \ \alpha(0) = 0, \ k(0) = 0 \tag{8}$$

the relation (4) becomes:

$$\dot{\varepsilon}_{11}^p = \lambda \cdot \frac{\sigma_{11} - \alpha_{11}}{Q \cdot (1 - e^{-b \cdot k}) + \sigma_Y} \tag{9}$$

and the constitutive equation of the variation of the hardening tensorial variable:

$$\dot{\alpha}_{11} = \lambda \cdot \left(C \cdot \frac{\sigma_{11} - \alpha_{11}}{Q \cdot (1 - e^{-b \cdot k}) + \sigma_Y} - \sqrt{\frac{2}{3}} \cdot \gamma \cdot \alpha_{11} \right) \tag{10}$$

where C and γ is an positive material constants.

We consider, the constitutive equation of the rate of stress tensor σ, given by the relation (3):

$$\dot{\sigma}_{11} = E \cdot \varepsilon_{11}(\dot{u}) - E \cdot \lambda \cdot \frac{\sigma_{11} - \alpha_{11}}{Q \cdot (1 - e^{-b \cdot k}) + \sigma_Y} \tag{11}$$

where $\varepsilon_{11}(\dot{u}) = d\dot{u}/dx$ with $\dot{u} = du/dt$, and E is the Young modulus.

The plastic multiplier λ are explicitly computed as:

$$\lambda = \frac{\langle \beta \rangle}{h} \cdot \mathcal{H}(\mathcal{F}) \tag{12}$$

with:

$$\beta = \frac{E \cdot \varepsilon(\dot{u}) \cdot (\sigma_{11} - \alpha_{11})}{Q \cdot (1 - e^{-b \cdot k}) + \sigma_Y} \tag{13}$$

$$h = E + C - \sqrt{\frac{2}{3}} \cdot \gamma \cdot \alpha_{11} \frac{\sigma_{11} - \alpha_{11}}{Q \cdot (1 - e^{-b \cdot k}) + \sigma_Y} + \sqrt{\frac{2}{3}} \cdot Q \cdot b \cdot e^{-b \cdot k} \tag{14}$$

with the supposition that $h > 0$, and $\mathcal{H}(\mathcal{F})$ the Heaviside function [4], [9].

Thus, the differential equation system obtained, are:

$$\begin{cases} \dfrac{d\varepsilon_{11}{}^p}{dt} = \dfrac{\beta}{h} \cdot \dfrac{\sigma_{11}-\alpha_{11}}{Q\cdot(1-e^{-b\cdot k})+\sigma_Y} \cdot \mathcal{H}(\mathcal{F}) \\[3mm] \dfrac{d\alpha_{11}}{dt} = \dfrac{\beta}{h} \cdot \left(C\dfrac{\sigma_{11}-\alpha_{11}}{Q\cdot(1-e^{-b\cdot k})+\sigma_Y} - \sqrt{\dfrac{2}{3}}\cdot\gamma\cdot\alpha_{11} \right)\cdot\mathcal{H}(\mathcal{F}) \\[3mm] \dfrac{d\sigma_{11}}{dt} = E\cdot\varepsilon_{11}(\dot u) - E\cdot\dfrac{\beta}{h}\cdot\dfrac{\sigma_{11}-\alpha_{11}}{Q\cdot(1-e^{-b\cdot k})+\sigma_Y}\cdot\mathcal{H}(\mathcal{F}) \\[3mm] \dfrac{dk}{dt} = \sqrt{\dfrac{2}{3}}\cdot\dfrac{\beta}{h}\cdot\mathcal{H}(\mathcal{F}) \end{cases} \qquad (15)$$

where β and h is given by the relation (13), respectively (14).

We further assume that the boundary of the body $\partial\Omega = \Gamma$ is divided in two parts denoted Γ_u and Γ_σ, with

$$\overline{\Gamma_u \cup \Gamma_\sigma} = \Gamma \text{ and } \Gamma_u \cap \Gamma_\sigma = \varnothing \qquad (16)$$

The motion (eqilibrum) equation is by the form:

$$div\left[\sigma_{11}(x,t)\right]+b_1(x,t)=0 \text{ in } \Omega\times I \qquad (17)$$

where $b_1 \in \mathbb{R}$ is the masic force, and $I = [0,T]$ is time interval of interest.

The kinematic equations, or boundary conditions is by the form:

$$\sigma_{11}\cdot n = f_1 \text{ on } \Gamma_\sigma\times I \text{ and } u=0 \text{ on } \Gamma_u\times I \qquad (18)$$

where n is the unit normal of the body Ω, and $f_1(x,t)$ is given function.

When we take the time derivative in (17), and (18) we have:

$$\begin{cases} div\left[\dfrac{d\sigma_{11}(x,t)}{dt}\right]+\dfrac{db_1(x,t)}{dt}=0 \text{ pe } \Omega\times I \\[3mm] \dfrac{d\sigma_{11}(x,t)}{dt}\cdot n = \dfrac{df_1(x,t)}{dt} \quad \text{pe } \Gamma_\sigma\times I \\[3mm] \dfrac{du(x,t)}{dt}=0 \quad \text{pe } \Gamma_u\times I \end{cases} \qquad (19)$$

We multiply the forst equation by the relation (19), with an certain displacement $w(x,t)$ and aplliyng integration to the domain Ω, we obtain:

$$\int_\Omega \dfrac{d}{dx}\left[\dfrac{d\sigma_{11}}{dt}\right]\cdot w\cdot dx + \int_\Omega \dfrac{db_1}{dt}\cdot w\cdot dx = 0 \qquad (20)$$

We apply Green's formula by the relation (20) and we have:

$$\left[\dfrac{d\sigma_{11}}{dt}\cdot n\cdot w\right]\bigg|_\Gamma - \int_\Omega \dfrac{d\sigma_{11}}{dt}\cdot\dfrac{dw}{dx}\cdot dx + \int_\Omega \dfrac{db_1}{dt}\cdot w\cdot dx = 0 \qquad (21)$$

Given the relation (20), the first term of the left member of relation (21) becomes:

$$\left[\frac{d\sigma_{11}}{dt} \cdot n \cdot w\right]_{\Gamma} = \left[\frac{df_1}{dt} \cdot w\right]_{\Gamma_\sigma} + \left[\frac{d\sigma_{11}}{dt} \cdot n \cdot w\right]_{\Gamma_u} \qquad (22)$$

Substitution of the constitutive equation (11) and the relation (22), into relation (23) gives:

$$\int_\Omega E \cdot \frac{d\dot{u}}{dx} \cdot \frac{dw}{dx} \cdot dx - \int_\Omega E \cdot \lambda \cdot \frac{\sigma_{11} - \alpha_{11}}{Q \cdot (1 - e^{-b \cdot k}) + \sigma_Y} \cdot \frac{dw}{dx} \cdot dx = \int_\Omega \frac{db_1}{dt} \cdot w \cdot dx + \left[\frac{df_1}{dt} w\right]_{\Gamma_\sigma} \qquad (23)$$

where $\varepsilon_{11}(\dot{u}) = d\dot{u}/dx$ and $\varepsilon_{11}(w) = dw/dx$.

If introduction the expresion of the plastic multiplier into relation (12), and we make calculations, then this becomes:

$$\int_\Omega \left[E \cdot \left(1 - E^{e \cdot p}\right)\right] \frac{d\dot{u}}{dx} \cdot \frac{dw}{dx} \cdot dx = \int_\Omega \frac{db_1}{dt} \cdot w \cdot dx + \left[\frac{df_1}{dt} \cdot w\right]_{\Gamma_\sigma} \qquad (24)$$

where:

$$E^{e \cdot p} = E \cdot \left(1 - sign(\beta) \cdot \frac{E}{h} \cdot \left(\frac{\sigma_{11} - \alpha_{11}}{Q \cdot (1 - e^{-b \cdot k}) + \sigma_Y}\right)^2 \cdot \mathcal{H}(\mathcal{F})\right) \qquad (25)$$

The relation (24) becomes:

$$\int_\Omega \varepsilon_{11}(w)^T \cdot E^{e \cdot p} \cdot \varepsilon_{11} \cdot (\dot{u}) \cdot dx = \int_\Omega w^T \cdot \dot{b}_1 \cdot dx + \left[w^T \cdot \dot{f}_1\right]_{\Gamma_\sigma} \qquad (26)$$

The relation (26) represent actually, the variational representation of the elasto-plastic probleme, in the onedimensional case.

The matematical model of this process is described by the differential equation system (15) and by the integral equation (26). The initial conditions of this model are given by the relation (8).

From the above, is observed as for the determination of the displacement $u(x,t)$, in the condition where is given the traction force $f_1(x,t)$ and the masic force $b_1(x,t)$, we have need by the resolve the integral equation (26) by the finite element method in tandem with the resolve the differential equation system by the Euler method. This method of solving the system of equations (15) and (26) was described in the work of Simo [10].

The mathematical model presented above, is simulated with S-Function Block of the Matlab Simulink. In cadre of this block is implemented the J. C. Simo [10] algorithm for the resolve the mathematic model of the process to by automated.

3. THE VECTOR CONTROL SYSTEM

The block diagram of the control system of the mechanical angular speed ω_r of the induction engine with a direct orientation after the rotor flux (DFOC), is presented in figure 2.

In figure 2 were marked with B1 the control block of the speed control system with direct orientation after the rotor flux (DFOC) and with B2 the extended Luenberger estimator block (ELO).

Some of the equations that define the vector control system are given by the elements which compose the field orientation block and consist of:

• stator voltage decoupling block (C_1U_s):

$$\begin{cases} u^*_{ds\lambda_r} = \dfrac{1}{b^*_{11}} \cdot \left[b^*_{11} \cdot v^*_{ds\lambda_r} - h_1 \right] \\[2mm] u^*_{qs\lambda_r} = \dfrac{1}{b^*_{11}} \cdot \left[b^*_{11} \cdot v^*_{qs\lambda_r} + h_2 \right] \end{cases} \tag{27}$$

where:

$$\begin{cases} h_1 = a^*_{13} \cdot |\psi_r| + a^*_{31} \cdot \dfrac{\hat{i}^2_{qs\lambda_r}}{|\psi_r|} + z_p \cdot \hat{\omega}_r \cdot \hat{i}_{qs\lambda_r} \\[3mm] h_2 = a^*_{14} \cdot z_p \cdot \hat{\omega}_r \cdot |\psi_r| + a^*_{31} \cdot \dfrac{\hat{i}_{ds\lambda_r} \cdot \hat{i}_{qs\lambda_r}}{|\psi_r|} + z_p \cdot \hat{\omega}_r \cdot \hat{i}_{ds\lambda_r} \end{cases} \tag{28}$$

Fig. 2. The block diagram of the vector control system which contains an ELO loop

• PI flux controller (PI_ψ) defined by the K_ψ proportionality constant and the T_ψ integration time:

$$\frac{dx_6}{dt} = \psi^*_r - |\psi_r|; \quad i^*_{ds\lambda_r} = \frac{K_\psi}{T_\psi} \cdot x_6 + K_\psi \cdot \left(\psi^*_r - |\psi_r| \right) \tag{29}$$

- couple PI controller (PI_Me) defined by the K_M proportionality constant and the T_M integration time:

$$\frac{dx_7}{dt} = M_e^* - M_e \; ; \quad i_{qs\lambda_r}^* = \frac{K_M}{T_M} \cdot x_7 + K_M \cdot \left(M_e^* - M_e \right) \tag{30}$$

- mechanical angular speed PI regulator (PI_W) defined by the K_ω proportionality constant and the T_ω integration time:

$$\frac{dx_8}{dt} = \omega_r^* - \hat{\omega}_r \; ; \quad M_e^* = \frac{K_\omega}{T_\omega} \cdot x_8 + K_\omega \cdot \left(\omega_r^* - \hat{\omega}_r \right) \tag{31}$$

- current PI controller (PI_I) defined by the K_i proportionality constant and the T_i integration time:

$$\frac{dx_9}{dt} = i_{ds\lambda_r}^* - \hat{i}_{ds\lambda_r} \; ; \quad v_{ds\lambda_r}^* = \frac{K_i}{T_i} \cdot x_9 + K_i \cdot \left(i_{ds\lambda_r}^* - \hat{i}_{ds\lambda_r} \right) \tag{32}$$

$$\frac{dx_{10}}{dt} = i_{qs\lambda_r}^* - \hat{i}_{qs\lambda_r} \; ; \quad v_{qs\lambda_r}^* = \frac{K_i}{T_i} \cdot x_{10} + K_i \cdot \left(i_{qs\lambda_r}^* - \hat{i}_{qs\lambda_r} \right) \tag{33}$$

- Flux analyzer (AF):

$$|\psi_r| = \sqrt{\hat{\psi}_{dr}^2 + \hat{\psi}_{qr}^2} \; ; \quad \sin \lambda_r = \frac{\hat{\psi}_{qr}}{|\psi_r|} \; ; \cos \lambda_r = \frac{\hat{\psi}_{dr}}{|\psi_r|} \tag{34}$$

- The calculate of the couple block (C1Me):

$$M_e = K_a \cdot |\psi_r| \cdot \hat{i}_{qs\lambda_r} \; ; \quad K_a = \frac{3}{2} \cdot z_p \cdot \frac{L_m^*}{L_r^*} \tag{35}$$

where: z_p is the pole pairs number.

- Extended Luenberger Observer: the equations that define the rotor flux Luenberger observer are described in the equation:

$$\frac{d}{dt} \hat{x}(t) = A(t) \cdot \hat{x}(t) + B \cdot u(t) + L(t) \cdot \left(y(t) - \hat{y}(t) \right) \tag{36}$$

where:

$$\hat{x}(t) = \begin{bmatrix} \hat{i}_{ds}(t) & \hat{i}_{qs}(t) & \hat{\psi}_{dr}(t) & \hat{\psi}_{qr}(t) \end{bmatrix}^T \; ; \quad \hat{y}(t) = \begin{bmatrix} \hat{i}_{ds}(t) & \hat{i}_{qs}(t) \end{bmatrix}^T \; ;$$

$$u(t) = \begin{bmatrix} u_{ds}(t) & u_{qs}(t) \end{bmatrix}^T \; ; \quad y(t) = \begin{bmatrix} i_{ds}(t) & i_{qs}(t) \end{bmatrix}^T \; ;$$

$$A(t) = \begin{bmatrix} a_{11}^* & 0 & a_{13}^* & a_{14}^* \cdot z_p \cdot \omega_r(t) \\ 0 & a_{11}^* & -a_{14}^* \cdot z_p \cdot \omega_r(t) & a_{13}^* \\ a_{31}^* & 0 & a_{33}^* & -z_p \cdot \omega_r(t) \\ 0 & a_{31}^* & z_p \cdot \omega_r(t) & a_{33}^* \end{bmatrix}$$

$$B = \begin{bmatrix} b_{11}^* & 0 & 0 & 0 \\ 0 & b_{11}^* & 0 & 0 \end{bmatrix}^T \; ; \; L = \begin{bmatrix} l_{11} & l_{12} & l_{21} & l_{22} \\ -l_{12} & l_{11} & -l_{22} & l_{21} \end{bmatrix}^T \; ;$$

$$l_{11} = (1-k) \cdot \left(a_{11}^* + a_{33}^* \right); l_{12} = z_p \cdot \omega_r \cdot (1-k); l_{22} = -\gamma \cdot l_{12}; l_{21} = \left(a_{31}^* + \gamma \cdot a_{11}^* \right) \cdot \left(1 - k^2 \right) - \gamma \cdot l_{11}$$

$$\gamma = \frac{\sigma^* \cdot L_s^* \cdot L_r^*}{L_m^*} \; ; \; a_{11}^* = -\left(\frac{1}{T_s^* \cdot \sigma^*} + \frac{1-\sigma^*}{T_r^* \cdot \sigma^*} \right) \; ; \; a_{13}^* = \frac{L_m^*}{L_s^* \cdot L_r^* \cdot T_r^* \cdot \sigma^*} \; ; \; a_{14}^* = \frac{L_m^*}{L_s^* \cdot L_r^* \cdot \sigma^*} \; ;$$

$$a_{31}^* = \frac{L_m^*}{T_r^*} \; ; \; a_{33}^* = -\frac{1}{T_r^*} \; ; b_{11}^* = \frac{1}{L_s^* \cdot \sigma^*} \; ; \; T_s^* = \frac{L_s^*}{R_s^*} \; ; \; T_r^* = \frac{L_r^*}{R_r^*} \; ; \; \sigma^* = 1 - \frac{\left(L_m^* \right)^2}{L_s^* \cdot L_r^*} \; .$$

In the relations above, are marked with "*" the identified electrical sizes of the induction motor.

The block diagram of the Extended Luenberger Observer (ELO) is presented in figure 3.

The adaptive mechanics of the extended Luenberger observer is defined by the following expression:

$$\widehat{\omega}_r = K_R \cdot e_f + K_i \cdot \int e_f \, dt \tag{37}$$
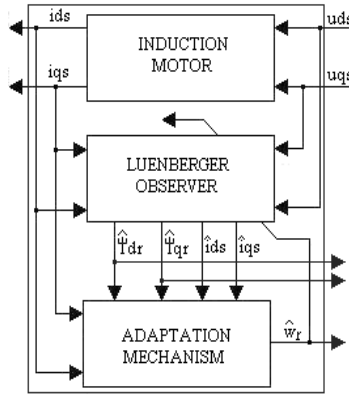
Fig. 3. The Principle Schematic of the ELO

where: $e_f = e_{yd} \cdot \widehat{\psi}_{qr} - e_{yq} \cdot \widehat{\psi}_{dr}$;

$e_{yd} = i_{ds} - \hat{i}_{ds} \; ; e_{yq} = i_{qs} - \hat{i}_{qs}$

The automatic controller of the component by the control system is granted based on strategies presented in the paper [8].
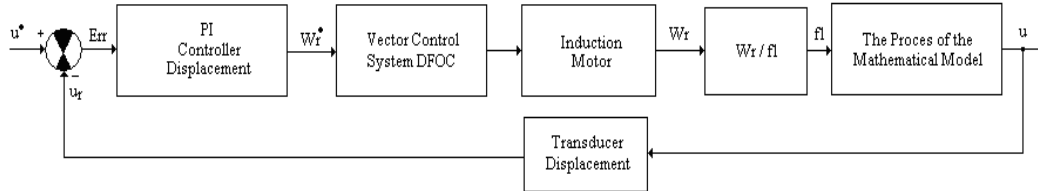
Fig. 4. The control system of the uniaxial deformation

4. THE SIMULATION OF THE CONTROL SYSTEM OF SMALL DEFORMATIONS IN THE ONE-DIMENSIONAL CASE

The advantage of the modeling the process to be automated, and simulation control system of the uniaxial deformation is that the designer can evaluate the dynamic performance of system simulation using Matlab – Simulink.

Thus, in the following, is presents a test carried out with a bar of length L = 40 cm. The bar is of the steel DP 600 and has the following characteristics: $b = 27,5[-]$; $\gamma = 125,9[-]$; $E = 182.000[\text{MPa}]$; $\sigma_Y = 349,4[\text{MPa}]$; $Q = 50,1[\text{MPa}]$; $C = 17.400[\text{MPa}]$.

On the based of the mathematical model of process, in the next figure is presented the imposed displacement and the actual displacement obtained in the bar at the point of traction.

The tests are conducted on the based of the automatic control system described above, using press INSTROM 5900. After the test, results the following graphs.
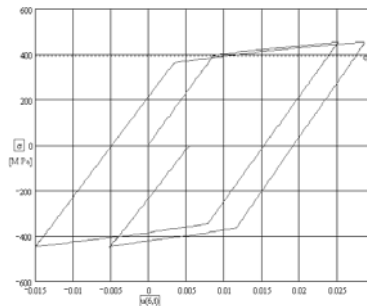
Fig. 5. The tension [MPa] in function by the displacement [m]

The induction motor used in the control system on the speed is one with the squirrel cage, and the electrical and the mechanical parameters are presented in the relations below: $P_N = 15[\text{kW}]$; $U_N = 400[\text{V}]$; $n_N = 1460[\text{rpm}]$; $f_N = 50[\text{Hz}]$; $z_p = 2$; $R_s = 0.2147[\Omega]$; $R_r = 0.2205[\Omega]$; $L_s = 0.06518[\text{H}]$; $L_r = 0.06518[\text{H}]$; $L_m = 0.06419[\text{H}]$; $J = 0.102[\text{kg} \cdot \text{m}^2]$; $F = 0.009541[\text{N} \cdot \text{m} \cdot \text{s/rad}]$.
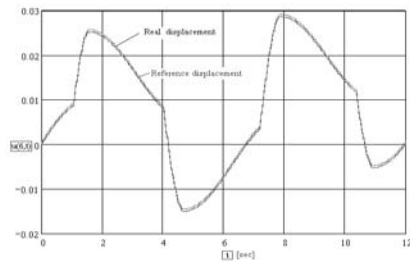
Fig. 6. The displacement [m] in time [sec]   **Fig. 7.** The forces [N] in time [sec]
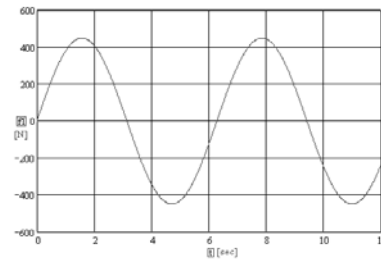
In the graphs presented in figure 5 to 7 is seen as for a displacement imposed by the form shown in this graphic, the automatically control system has a good dynamics, and the force of the compression that traction is a sinusoid which has maximum amplitude 450 N.

5. CONCLUSION

The control system proposed can be very useful in the traction-compression tests carried out for different industrial applications. Using the automatic control system of induction motor speed with help of the extended Luenberger observer makes this control system of the one- dimensional deformations to be one very precise. The very good dynamic of the response of the control system of one-dimensional deformations, makes us believe that its use in the context of industrial applications to be one very useful.

REFERENCES

[1] Armstrong P., Frederick C., *A mathematical representation of the multiaxial Bauschinger effect,* G.E.G.B. Report RD-B-N 731, 1996.
[2] Belytschko T., et al., *Nonlinear Finite Elements for Continua and Structures,* British Library Cataloguing in Publication Data, Toronto, 2006.
[3] Bathe J., *Finite element procedure,* Prentice Hall, Englewood Cliffs, New Jersey, 1996.
[4] Carabineanu A., Cleja-Țigoiu S., *Curent topics in continuum mechanics,* Ed. Academiei Române, București, 2002.
[5] Glowinski R., et al., *Analise numerique des inequations variationnelles,* Publie avec le Concours du Centre National de la Recherche Schientifique, Paris, 1976.
[6] Johnson C., *Numerical solution of partial diferential equation by the finite element method,* Cambridge University Press, Cambridge, 2005.
[7] Pana T., Stoicuta O., *Small speed asymptotic stability study of induction motor sensorless vector control systems with extended Luenberger estimator,* Proc. Int. IEEE AQTR, Cluj-Napoca, Romania, 2008.
[8] Pana T., Stoicuta O., *Controllers tuning for the speed vector control of induction motor drive systems,* Proc. Int. IEEE AQTR, Cluj-Napoca, Romania, 2010.
[9] Paraschiv M., et al., *Plasticitate cu aplicații în geomecanică,* Ed. Universității din București, 2004.
[10] Simo J.C., *Numerical analysis and simulation of plasticity,* Handbook of Numerical Analysis, volume VI, Elesevier, Amsterdam, 1998.
[11] Stoicuta O., Mandrescu C., *Real-time simulation of the extended Luenberger estimator using the eZdps 2812 development kit,* Proc. Int. AQTR, Cluj-Napoca, Romania, 2006
[12] * *, *www.instron.com*

E-LEARNING TECHNIQUE IN HUMAN RESOURCE

ROXANA BUBATU[1], EMIL POP[2], CAMELIA BARBU[3], PETRE VAMVU[4]

Abstract: In this paper the trainings ways based on e-Learning for institutions and companies are introduced.

At the beginning of the paper the concepts of these types of education, the methods and possibilities, the advantages and disadvantages are analyzed. In the following, types of e-Learning for training and education, like: synchronous and asynchronous training, the structure of e-Learning courses etc. are presented. Further is treated the support elements of entrepreneurship, the comportment and competence entrepreneurship and is analyzed necessity integration education entrepreneurship in school curricula through the demand and integration of entrepreneurship spirit in education.

At the end, the paper presents the curriculum components on an e-Learning application, which shows the advantages of this type of education especially for institutions and companies which invest in human resources.

Keywords: e-Learning, the e-Learning principles, asynchronous and synchronous training.

1. E-LEARNING, CONCEPTS, METHODS AND MEANS

E-Learning is the type of training where trainers use IT and Web technologies which considerably reduce the distance and the period of time allowing the trainee to prepare on their own pace using convenient stress free methods.

The benefit of using on-line courses to other methods of information providers, such as Word and PowerPoint online documents, is that e-Learning has been created as a dedicated software based on training concepts, presenting the information in several ways, allowing the access to explanations understood by everyone, eliminating redundant elements and replacing them with those understood, self-evaluation, self-correction, and teacher in education [1], [5].

Considering that an e-Learning course fully uses the internet and Web pages, these include all the basic characteristics of a Web site and are based on them for the realization of an easy access to information. Consequently e-Learning resembles to the Web sites with an ergonomic and simple user interface, while e-Learning courses need to be simple but informative. Basic elements may be found on the starting page, such

as: the name of the course, the summary, the objectives and the navigation menu of the course. From the access to information point of view, it is ideal that any 4 level course architecture to be accessed by only three clicks. Such course architecture usually contains 4 hierarchical levels [1].

Level 1: Called Course;
Level 2: Called Chapter;
Level 3: Called Pages;
Level 4: Called Subpages.

There are two ways of using e-Learning: the *synchronous* and the *asynchronous*.

- *Synchronous e-Learning* means that teachers and students meet at a pre-convened hour for the course.
- *Asynchronous e-Learning* means that students use the material they have at their disposal on the Web site, which is sufficient enough and may be used at any given time in any place, the relation with the teachers and colleagues being made on-line.

Synchronous e-Learning

Synchronous e-Learning resembles classroom training but there still are a lot of differences between them. Usually the teacher and the students are together in an open conference where PowerPoint may be the most known presentation instrument but it also requires a web format delivery mechanism. For the courses taught in the classroom, probably, the most known transmission system is the shared board which may be used to see the content of the presentations and to allow the trainer to share the desktop with the students, by using a projector. Therefore the trainers control what is shown, heard and on the projected slides on the board, and through the question table made by the student, he can give answers, realizing therefore the best communication by instant messages.

Asynchronous e-Learning

Asynchronous e-Learning represents a guided student. The content is available on-line for the students, and it has to be full so that the reference study may be possible. Therefore, PowerPoint presentations are the poorest choices, a software content presenter and a lot of other instruments being necessary for understanding the course, for self-examinations, communication with the teacher and the colleagues, applications, etc.

The following is a presentation of the characteristics of the two e-Learning types from the point of view of their advantages and disadvantages.

2. THE SUPPORT OF ENTREPRENEURSHIP

Entrepreneurship is an attitude characterized by personal or group generate a process of decisions and choices based on innovation and change, induced by the contractor. Entrepreneurship can support, promote, stimulate and educate. In Figure 1 presents the block diagram of entrepreneurship support.

Distinguish four groups of elements of entrepreneurship support. The first 3 are groups for improving the entrepreneurial activity, the 4th is entrepreneurship education that prepares medium and long term development.

Improving the entrepreneurial activity depends on the following: access to finance, facilitate entry/ exit market and government support schemes.
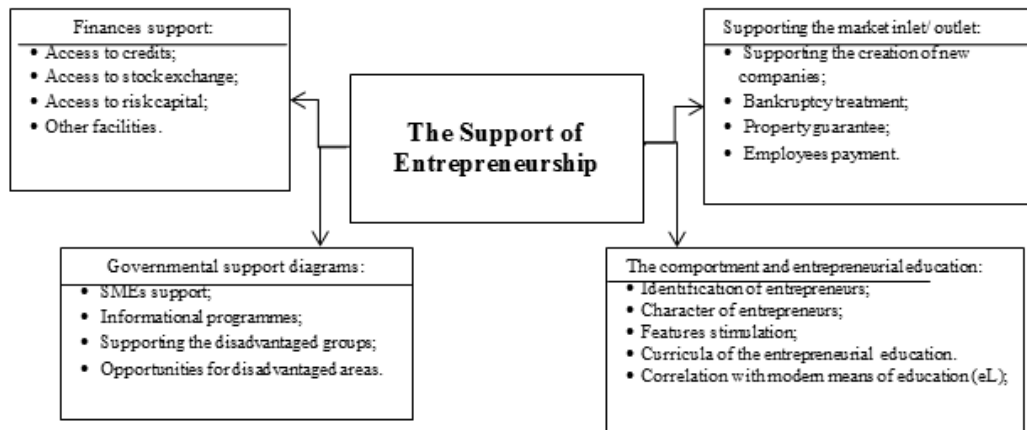
Fig. 1 The elements supporting of Entrepreneurship

In a recent study shows that lack of funding is the primary barrier to entrepreneurship. SMEs do not qualify for bank credit access and then governments can facilitate access to loans for start-up companies, bringing credit guarantee schemes.

Entrepreneurial activities are shaped or even determined by start-ups and access to markets. Avoid discouraging entrepreneurial activities as a result of start-up difficulties can be done by simplifying bureaucratic barriers to starting and developing businesses in carefully balance the public interest, environmental protection and health and safety standards.

The schemes of government support can't replace proper functioning of markets, but can complement and support other strategies to create an environment for entrepreneurship and eliminating barriers to entrepreneurial behavior. Development of entrepreneurship education programs or support, review existing and promote the exchange of good practice can be a solution.

3. STRUCTURE OF E-LEARNING COURSES

Web type Courses, also called Web 2.0 have been lately developed for e-Learning professional formation combining the best Web design and design training techniques [2].

The characteristics of the course are the following:
- Ensure the training in the pre-established time;
- They are used a long term resource;
- The duration of the course is of 15 or 20 minutes;

Duration of a course

Here are a series of solutions regarding the minimization of the duration of courses:

- The basic rule says that: a trainee needs 1 minute for each page.
- A chapter of the course needn't comprise more than 15-20 pages, therefore 15-20 pages per chapter.
- In order to create a functional course for a busy person, a first step is to divide the course in segments of 15-20 minutes each.
- Dividing a course in 5 chapters, each of 15-20 pages, allows the trainee to study a chapter per day and finish the course in one week. These have a feeling of fulfillment if they are able to finalize learning a course in a relatively short period of time.
- Longer courses are created in separate modules.

Courses Architecture

A simple and efficient method for designing a course is to divide the structure material on 4 levels:

Level 1: The course

The first page presents the name of the course and a short summary. The summary may also be the training objective of the course or a high level general view composed of several phrases. The summary is very important because:

- Asynchronous learning does not have a trainer in front of the class to confirm if what is learned is the correct thing.
- The trainers are interested in training when they have a reference framework which may be composed of the objectives and a summary of the material to be studied.
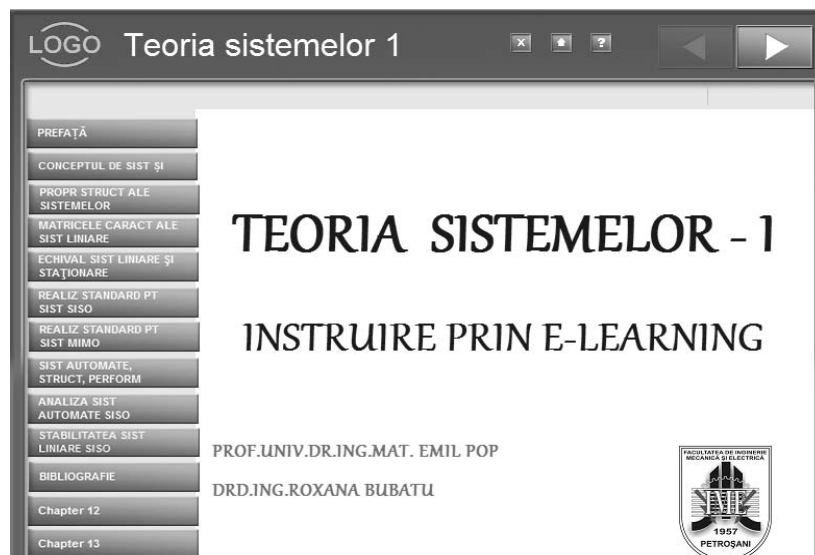
Fig. 2 The e-Learning Course

Level 2: Chapters

Each chapter has a title and a summary or a list of learning objectives. Also, optionally, a list of the pages in the chapter may be given, for reaching more objectives:

- The books are divided on chapters and sub-chapters in order to help readers understand the material to be studied. The same reasoning is also applied to e-Learning.
- For the future, the trainees who have studied the course may also use a chapter and a direct information access guideline.

Level 3: Pages

A content page should provide:

- A summary, because an easy way of beginning a new subject is provided to the course creators.
- The basic material also contains bookmarks helping the trainees to read attached journals making therefore a difference. The best thing is the journalistic style written material and which needs to be followed considering a series of details.
- Optional information is on the fourth level, and they are also called as drill-down elements. The detailed content should be provided only if the trainee wants to, the provision of optional information drill-down made by the page.

Fig. 3 The page content of e-Learning Course

The screen should comprise approximately 400 words or 30 text lines, in order to be easily displayed.

- Avid using edit on multiple columns. It happens that the trainers forget to read the second column.

Level 4: Sub-pages

Level 4 subpages or drill-down page may be used to consolidate learning. These pages amend the marked element on the contents pages. Often, a course creator may use

extra materials to create a course which contains more information accessed using the drill-down, figure 4.

Drill-down pages may be: an article, a link for a web resource, an exercise; a simulation, a movie and a test.
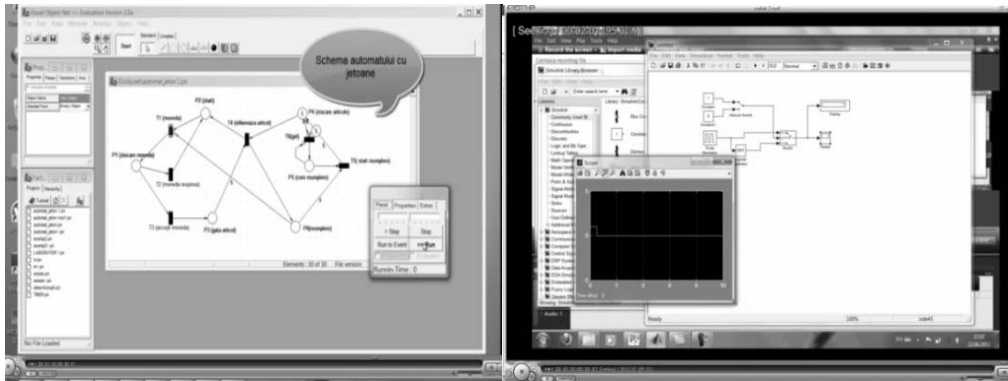
Fig. 4 A capture

Drill-down pages should be optionally accessed by the trainer. The display experience level of the trainees is different, and need to wait for each simulation series, even if they are not interested in order for them to continue the course.

4. CONCLUSIONS

E-Learning has already become a new learning system, the characteristics of which are the following:

- It is appropriate for initial training of trainers as well as for continuous formation in institutions and commercial companies;
- This learning system ensures the most efficient professional formation considering the cost/quality ratio;
- Asynchronous e-Learning allows the formation and development of the human resource, launching or designing new projects.
- As a major disadvantage we may appreciate the hardware-software cost of the system and the difficulty in realizing specific on-line courses.

REFERENCES

[1]. **Rosen A.**, *E-learning 2.0 Proven Practices and Emerging Technologies to Achieve Results.*
[2]. **Kay Lehman, Lisa Chamberlin**, *Making the Move to e-Learning. Putting Your Course On-line.*
[3]. **Allen, I.E., &Seaman, J.**(2007). *On-line nation: Five years of growth in on-line learning.*Nehjedham, MA: Sloan-C.
[4]. **Pop E., Bubatu R.,** *Teoria sistemelor I - Instruire prin e-Learning,* Editura Universitas, ISBN: 978-973-741-299-7, Petrosani 2012.

VIRTUAL INSTRUMENTATION USED TO BUILD AN ELECTRIC MOTOR SIMULATOR

NICOLAE PĂTRĂŞCOIU[1] , CAMELIA BARBU [2], CECILIA ROŞULESCU[3]

Abstract: In this paper we propose a state – space model for the DC motor build for constant flux and considering two inputs: supply voltage and load torque. The three states of the resulted model are represented by angular speed, angular displacement and current supply and either of these states can be an output variable for simulation model. Consequently, the system's model has two inputs and three outputs. Using this model, LabVIEW functions and programming structure is build a virtual instrument through which is possible to observe the dynamic characteristics of the DC motor in different operating conditions

1. INTRODUCTION

One of the most used actuator in control systems is direct current (D.C.) motor. It is the means by which electrical energy is converted to mechanical energy. D.C. motors have a high ratio of starting torque to inertia and therefore they have a faster dynamic response**.**

In some application D.C. motors are used with magnetic flux produced by field windings. The speed of D.C. motors can be controlled by applying variable armature voltage. These are called armature voltage controlled D.C. motors. Wound field D.C. motors can be controlled by either controlling the armature voltage or controlling the field current. In this paper we consider modelling and simulation of an armature controlled D.C. motor [2].

There are many types of D.C. motor and their detailed construction is quite complex but it is possible to derive the equations for a satisfactory dynamic model from basic electromagnetic relationships.

[1] *Assoc.Prof., PhD., University of Petrosani*
[2] *Lecturer**, PhD., University of Petrosani*
[3] *Prof. "Grigore Geamănu" School*

[2] *Ph.D Prof Eng. at University of Petrosani*
[3] *Ph.D Prof Eng. at University of Petrosani*

The general output variable of this actuator can be angular speed or angular displacement motion, but coupling the motor axle with wheels or drums and cables it can obtain the translational motion.

2. BUILDING THE SIMULATION MODEL

The physical model of an armature controlled D.C. servo motor is given in Fig. 1, where [2]:

e_a, i_a – armature supply voltage and current;
e_f, i_f – field voltage and current;
R_a, L_a – armature winding resistance and inductance;
e – back electromotive force (e.m.f.);
$\omega(t)$ – angular speed;
$T_m(t)$ – electromagnetic torque;
$T_L(t)$ – load torque
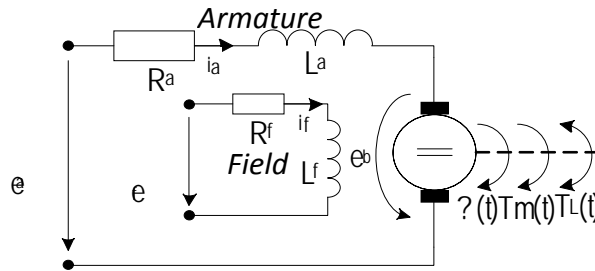
Fig.1. Armature controlled D.C. motor

Applying the second theorem of Kirchhoff on supply circuit, applying the equilibrium equation of torques on the axis of motor, known that the electromagnetic torque is dependent on the excitation flux and also on the supply current in armature circuit, and if the excitation flux is considering constant, it can be obtained the complete model for the armature controlled D.C. motor [3]:

$$\frac{di_a(t)}{dt} = \frac{1}{L_a} \cdot e_a(t) - \frac{R_a}{L_a} \cdot i_a(t) - \frac{k}{L} \cdot \omega(t)$$

$$\frac{d\omega(t)}{dt} = -\frac{F}{J} \cdot \omega(t) + \frac{k}{J} \cdot i_a(t) - \frac{1}{J} \cdot T_L(t)$$

(1)

Considering the angular displacement $\alpha(t)$ instead of angular speed $\omega(t)$ like output variable is necessary to include the relationship between these:

$$\omega(t) = \frac{d\alpha(t)}{dt}$$

(2)

So based on equations (1) and (2) it can build the mathematical MIMO model in state-space form so that is possible to use it into a program simulation.

To build the state-space MIMO model, are defined the input, state and output vectors [5], [8] i.e.:

- input vector $u(t)$ whose 2 components is represented by armature voltage $e_a(t)$ and load torque $T_L(t)$, i.e.:

$$u(t) = \begin{bmatrix} e_a(t) \\ T_L(t) \end{bmatrix} \qquad (3)$$

- state vector $x(t)$ whose 3 components is represented by armature current $i_a(t)$, angular displacement $\alpha(t)$ and angular speed $\omega(t)$, i.e.:

$$x(t) = \begin{bmatrix} i_a(t) \\ \alpha(t) \\ \omega(t) \end{bmatrix} \qquad (4)$$

- output vector $y(t)$ whose 3 components we consider that is the same with state vector components (relation (4)) so that is possible to simulate these three physical variables.

Having these vectors is possible to write equations (1) in the matrix form [6], [8]:

$$\begin{vmatrix} \dot{i}_S(t) \\ \dot{\alpha}(t) \\ \dot{\omega}(t) \end{vmatrix} = \begin{vmatrix} -\dfrac{R_a}{L_a} & 0 & -\dfrac{k}{L_a} \\ 0 & 0 & 1 \\ \dfrac{k}{J} & 0 & -\dfrac{F}{J} \end{vmatrix} \cdot \begin{vmatrix} i_S(t) \\ \alpha(t) \\ \omega(t) \end{vmatrix} + \begin{vmatrix} \dfrac{1}{L_a} & 0 \\ 0 & 0 \\ 0 & -\dfrac{1}{J} \end{vmatrix} \cdot \begin{vmatrix} e_a(t) \\ T_L(t) \end{vmatrix} \qquad (5)$$

Bring on output vector definition the input-output equation can write in matrix form:

$$y(t) = \begin{vmatrix} 1 & 0 & 0 \\ 0 & 1 & 0 \\ 0 & 0 & 1 \end{vmatrix} \cdot \begin{vmatrix} i_S(t) \\ \alpha(t) \\ \omega(t) \end{vmatrix} + \begin{vmatrix} 0 & 0 \\ 0 & 0 \\ 0 & 0 \end{vmatrix} \cdot \begin{vmatrix} e_a(t) \\ T_L(t) \end{vmatrix} \qquad (6)$$

Having now the mathematical model, described by matrices A, B, C, D is possible to simulate the D.C. motor.

To realize the simulation of the DC motor are considered the shapes for armature voltage and load torque variation shown in Fig.2
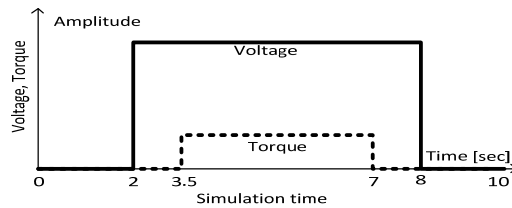
Fig.2. Inputs shapes

Using these shapes for the input variables that are applied to the motor, i.e.: armature voltage and its load torque and the following Matlab sequence program, can be obtained the graphs of variation for considered output variables, i.e.: current, displacement and speed.

```
tfinal=10;
t=0:tfinal/1000:tfinal;
R=0.7; L=0.05; Km=0.05;
J=0.0001; F=0.005;
A=[-R/L 0 -Km/L;0 0 1;Km/J 0 -F/J];
B=[1/L 0;0 0;0 -1/J];
C=[1 0 0;0 1 0;0 0 1];
D=[0 0;0 0;0 0];
motor=ss(A,B,C,D)
u1=zeros(200,1);
u2=20*ones(601,1);
u3=zeros(200,1);
u=cat(1,u1,u2,u3);
T1=zeros(350,1);
T2=2*ones(301,1);
T3=zeros(350,1);
TO=cat(1,T1,T2,T3);
U=cat(2,u,TO)
lsim(motor,U,t)
```

Graphs obtained are shown in Fig.3
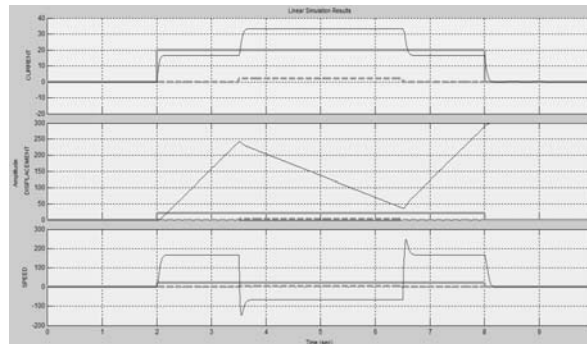
Fig.3. Outputs obtained by Matlab simulation

By using this simulation method can achieve remarkable results in terms of accuracy of determining the values of the output variables [5]. This method has the disadvantage of not allowing a dynamic change of the model by modifying the parameters of the motor (like R_a, L_a, k, J, F) or changing shapes and parameters of input variables.

This disadvantage can be eliminated by integration of the mathematical model into a virtual instrument created in LabVIEW that allow the users the dynamically settings of the parameters and choice of shapes and values of the input variables [1].

3. CONSTRUCTION OF THE VIRTUAL SIMULATION TOOL

A program developed in LabVIEW is called a virtual instrument (VI) and it has two components: the block diagram that represents program itself and the front panel that is the user interface [9].

The front panel is the user interface of the virtual instrument and is built with controls and indicators, which are the interactive input and output terminals [7].

The front panel has two components, one used to set the parameters of the simulation and another used to collect the results obtained from simulation. Switching between the two components is accomplished by the user via the Tab Control button.

The first component, called Simulation Process, contains elements (Control type) through which the user can:

- sets the motor parameters (DC Motor Parameters): R_a [Ω], L_a [H], k [N·m/A], J [kg·m^2], F [(N·m)/(rad·sec)];

- sets simulation time:
- choose, from the list, the shapes for the input variables and sets their parameters (amplitude and duration);
- choose simulation previews for current and/or displacement and/or speed

This part of the front panel also contains, elements of graph indicator type through which it can display, on the user request, a preview to the input and output variables, in other words the preview of the simulation [7], [8].
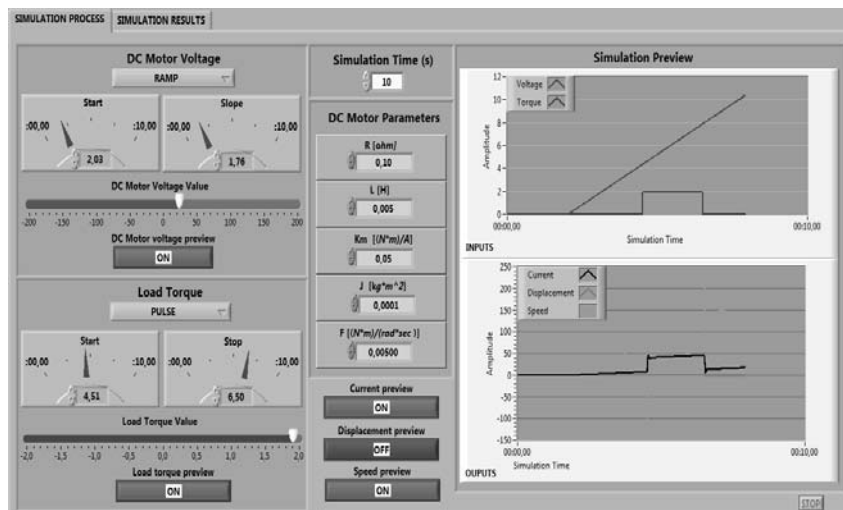
Fig.4. First component of the front panel of the simulator

The entire first component of the front panel is shown in Fig.4.

The second component, called Simulation Results, of the front panel of the simulator allows the user, acquisition of the information about the dynamic behaviour of DC motor.

This contains elements (Control type) through which the user can:
- select of display state - space equations form and select the transfer function, both models are represented by coefficients calculated based on the DC motor parameters set on the front panel;
- select and display the graphical results of the simulation, i.e. the graphical responses for the imposed outputs, Fig.5
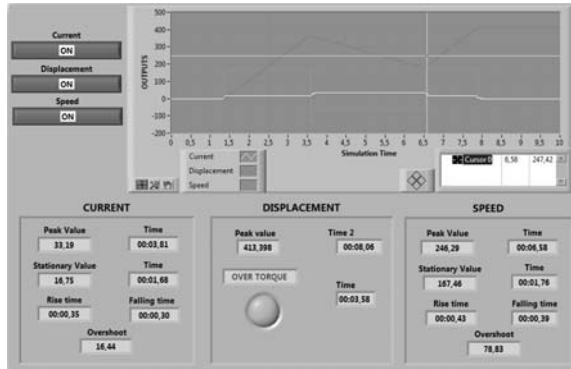
Fig.6. DC Motor simulation results
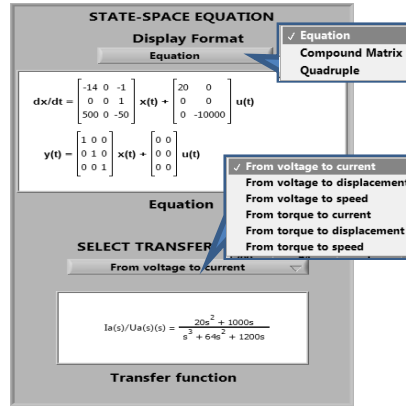
Fig.5. DC Motor models

For each selected output variable is open a window which display parameters that are relevant to this dynamic system, such as: the peak value (maximum value) and time of its occurrence, the steady state value and its determining time, rise time, falling time, overshoot. For displacement, in case if, the load torque is greater than the active torque occurs motor reversing and this situation is signalled by a flashing message (OVER TORQUE) and a proper light indicator with displaying the time of its occurrence, Fig.6.

Fig.7. Second component of the front panel of the simulator

The entire second component of the front panel is shown in Fig.7.

After is built the front panel, is add code using graphical representations of functions to control the front panel objects. The block diagram represents the program under which the simulator run, and contains the graphical source code. Front panel objects appear as terminals, on the block diagram. Block diagram objects include terminals, subVIs, functions, constants, structures, and wires, which transfer data among other block diagram objects.

Fig.8. Main program algorithm

The basic structure in realizing virtual instrument is While Loop that continues to run the program until the Stop button on the front panel is pressed by the user.

The program is running in two sequences according to the main algorithm shown in fig.8
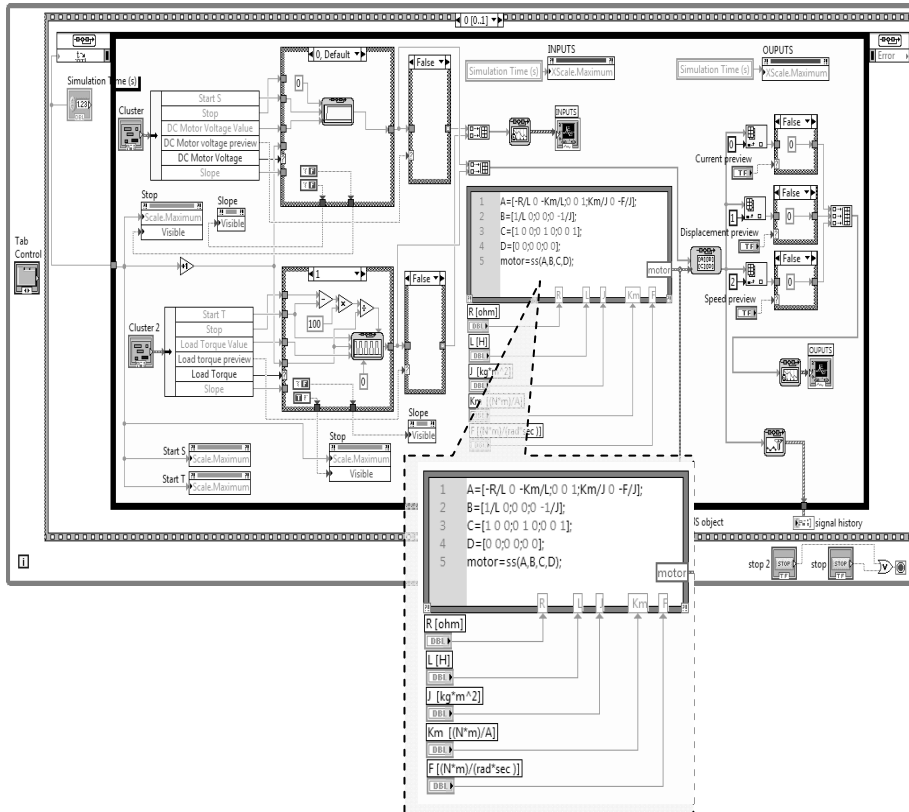
Fig.9. The first sequence and the MathScript Node

User selects one of the shape (step, pulse or ramp) and the values for the two variables input u_a and T_L and depending on constructive parameters of the DC motor, with all values set also by the user on the front panel, is generates the state – space model. By numerical simulation, based on this model, output variables are determined, and also, are displayed state-space and transfer functions models of the DC motor. For output variables defined dynamic system parameters are calculated, namely: maximum value, steady state value, rise time, falling time, overshoot

The main element of the first sequence is the Control and Simulation Loop in conjunction with MathScript Node [4].

Control and Simulation Loop is one of the components of the LabVIEW Control Design and Simulation Module. With this module it can construct plant and control models using transfer function, state-space model, or zero-pole-gain model, also it can

analyse system performance with tools such as step response, pole-zero maps, and Bode plots. This module allows simulating linear, nonlinear, and discrete systems with a wide option of solvers. With the LabVIEW Control Design and Simulation Module, it can analyse open – loop model behaviour, design closed-loop controllers, simulate online and offline systems, and conduct physical implementations. Simulation time is set from corresponding control on the front panel and this is the only parameter of the loop.

The state – space model of the DC motor is placed into Control and Simulation Loop through a MathScript. MathScript is a high – level, text – based programming language. MathScript includes more than 800 built – in functions and the syntax is similar to MATLAB, it can also create custom – made m-file like in MATLAB. To process scripts in LabVIEW it can use LabVIEW MathScript Window or a MathScript Node. If is necessary to integrate MathScript functions (built – in or custom – made m-files) as part of a LabVIEW application and combine graphical and textual programming, like this application, it used MathScript Node.

The first sequence of the program and the MathScript Node used to introduce the DC motor model into program is shown in Fig.9

DC motor parameters are introduced into the model and these can be changed interactively via the corresponding buttons on the front panel. The output from the MathScript Node, is SS (state-space) object called *motor*, and is a 2D matrix which is a representation of the state-space system dynamic equations that corresponding to the general forms (9) and (12). It can extract from this output, the matrices A, B, C and D but also other information, such as: properties, state names, transport delay. This object, together with the input vector, is used to generate the output vector $y^T = [i_a,\ \alpha,\ \omega]$ through LabVIEW simulation function State – Space. Each of the three components of the output vector can be identified using the Index Array function that returns the element or subarray of n-dimensional array corresponding to the index value. After identifying any of these three components can be visualized on the front panel, through a graphic indicator. The obtained vector is also processed through the Collector function. This function collects a signal at each time step of the simulation and returns a history of the signal value and the time at which this function recorded each value in the history. Based on the signal history can be identified, in the next sequence, the values of dynamic regime.

4. CONCLUSIONS

It is known that computer simulation is an experimental method based on a set of techniques by which operating with virtual things, the functioning of a real system or process is understood. To understand the functioning of systems dynamics, simulation environments such as Matlab or Simulink are used, and these simulations can be made based on corresponding mathematical models. These simulation environments are very powerful in terms of numerical calculation, but offer few facilities for interactive modification of model parameters and/or the simulation conditions.

The simulator that we propose combines the computing power of the Matlab-Simulink environment with interfacing facilities provided by the LabVIEW programming environment. In this way, it can possible to understand the dynamics of a system such as a DC motor, following its chart of response to different stimuli or different operating conditions. On the other hand, by obtaining the mathematical model expressed by transfer function in various operating conditions of the DC motor, this one can be used in modelling of complex systems in which the DC motor represents a subsystem.

REFERENCES

[1]. **Faraco G., Gabriele L**.Using LabVIEW for applying mathematical models in representing phenomena, Computers & Education Vol. 49, Issue 3, 2007, pp 856-872

[2] **Fransua, A**. - Masini si actionari electrice. Ed. Tehnica, Bucuresti 1986

[3] **Golnaraghi F., Kuo C. B**., Automatic Control Systems, 9th Edition**,** John Wiley & Sons, Inc. (2010)

[4] **Halvorsen H.P**.- LabVIEW MathScript. Tutorial, Telemark University College, Department of Electrical Engineering, Information Technology and Cybernetics, 2011

[5] **Jagan, N.C.** -Control Systems, 2th Edition, Modelling of Elements of Control Systems, BS Publications, (2008).

[6] **Matko, D., Karba, R**.-Simulation and Modelling of Continous Systems Prentice Hall, New York, 1992

[7] **Pătrăşcoiu N**.-Sisteme de achizitie si prelucrare a datelor. Instrumentatie virtuala Ed. Didactica si Pedagogica, Bucuresti, 2004

[8] **Pătrăşcoiu N**.- Modeling and Simulation of the DC Motor Using Matlab and LabVIEW, International Journal of Engineering Education, Vol. 21, No. 1, 2005, pp. 49-54

[9] *** * ***   LabVIEW. User Manual, National Instruments, April 2003 Edition Part Number 320999E-01

AUTOMATIC MONITORING SYSTEM OF A WAREHOUSE BY GSM

ARON POANTA[1], BOGDAN SOCHIRCA[2]

Abstract: Along with Ethernet data transmission, the GSM data transmission is widely spread all over the world. The evolution of cellular telephony makes that the GSM devices is a part of our life. If a system has a GSM capability that system can be interrogated or commanded from every part of the world. In this paper we integrate a GSM transceiver with a microcontroller system in order to obtain a surveillance system with GSM capability, system that can be monitored from everywhere.

Keyword: monitoring system, GSM, surveillance, AT commands, microcontroller, SMS, surveillance system.

1. INTRODUCTION

The GSM system history begins in 1982 when the European Conference of Postal and Telecommunications Administrations (CEPT), consisting then by telecommunication administrations of twenty-six nations took two important decisions.

The first was to establish a team named "Group Special Mobile" (from here we have the term "GSM" that exists today for Global System for Mobile Communications) to develop a set of common standards for future pan-European cellular network. The second was to recommend that two bands of 900 MHz for the system to be set aside.

CEPT has taken these decisions in an attempt to solve the problems created by uncoordinated development of individual national mobile communication systems using incompatible standards. Failure to use the same terminal in different countries while traveling in Europe was one of these problems, another problem was the difficulty to establish a mobile communications industry across Europe that could be competitive on world markets due to lack of larger markets with common standards. By 1986 it was clear that some of these cellular networks without quality would remain similar to the early 90s.

As a result, a directive was given for two frequency bands of 900 MHz, although in a somewhat less than those recommended by CEPT to be kept exclusively for a pan-

---

[1] *Ph.D Prof Eng. at University of Petrosani*
[2] *Ph.D Lecturer Eng. at University of Petrosani*

European service to be opened in 1991. At the same time members make progress GSM excellent produces appropriate standards. A major decision was to adopt a digital rather than an analogue.

GSM was taken over in 1989 by ETSI (European Telecommunications Standards Institute) and they finalized the GSM standard in 1990. GSM service started in 1991. Also this year was renamed the Global System for Mobile Communications (GSM).

2. GSM ENCRYPTION [2]

The GSM encryption is one of the best available encryption. Along with the Ethernet transmission, the GSM transmission data is an affordable system, very suitable for fast and cheap transmission data.

GSM network utilizes an algorithm called A3 authentication algorithm in order to authenticate mobile users and protect the network from unauthorized service access. Figure 1 shows the stages of the authentication process between MS (Mobile Station) and a GSM network represented by a BS (Base Station).
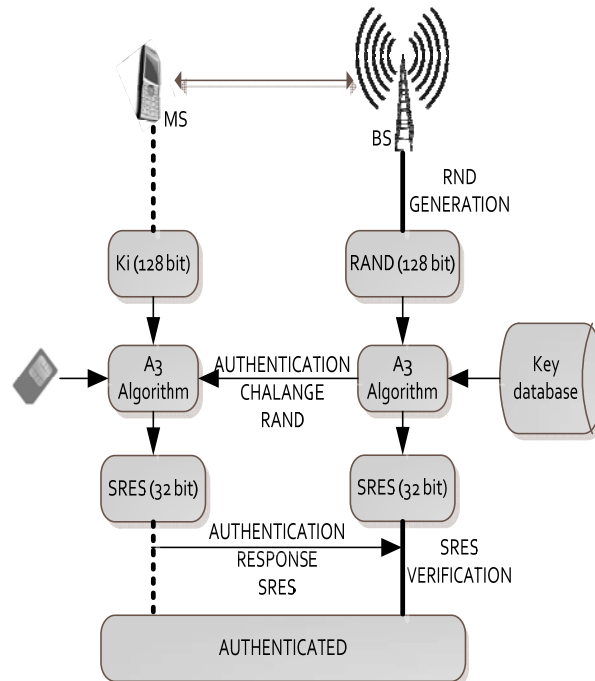
Fig.1. GSM authentication process

First, the AuC generates a random 128-bit token (RAND), which is sent to the Mobile Switching Centre (MSC).

The MSC sends RAND through BS to the MS as an authentication challenge.

The MS uses RAND and the secret subscriber key Ki, which is stored in the SIM card, as input arguments for the A3 algorithm in order to produce a 32-bit response (SRES).

The AuC retrieves the MS's shared secret key from the key database, and uses the same algorithm to produce the SRES, which is sent to the MSC.

Finally, the MS sends SRES as an authentication response back to the MSC through BS.

The MSC verifies that the SRES received from MS is identical to the SRES generated in AuC and authenticates the MS

In order to protect signaling and user data, the GSM uses 2 algorithms. The A8 algorithm generates the encryption key, whereas the A5 algorithm performs the actual data encryption.

The figure 2 shows the encryption key generation. Both the MS and the AuC utilize the Ki and RAND, which are already known from the authentication process, as input arguments for the A8 algorithm. The output is the 64-bit encryption key Kc, which is sent from the AuC to MSC. MSC then sends Kc to the MS, to which the BS is connected.
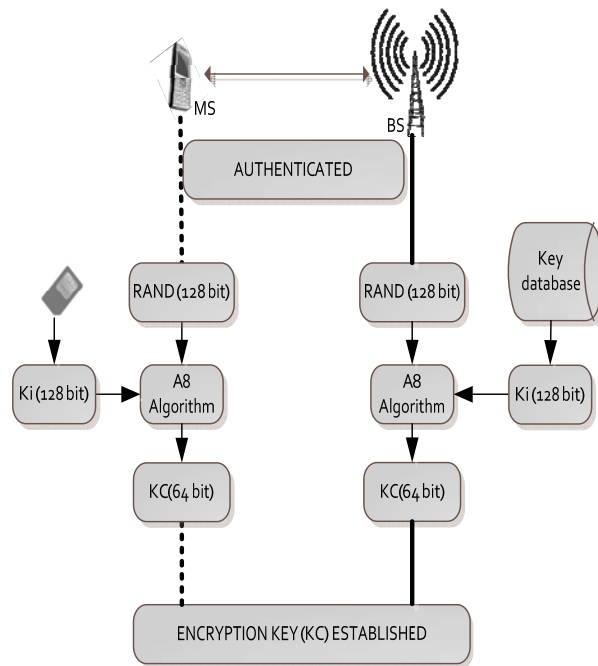
Fig.2. GSM encryption key generation process

Figure 3 shows the GSM encryption process. A5 is a symmetric encryption algorithm and thus the same input arguments are used for both encryption and decryption. The A5 algorithm receives Kc and a 22 bit frame dependent input (COUNT) and produces ciphered data-streams using a 114-bit key-stream
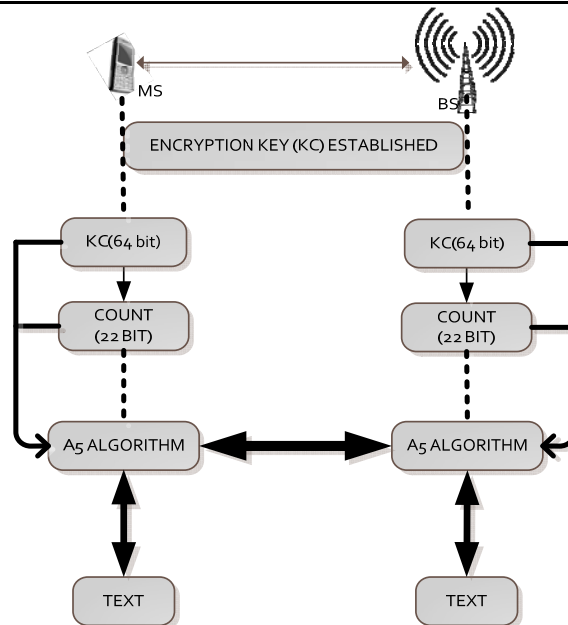
Fig.3. GSM encryption process

3. THE HARDWARE DESCRIPTION [1] [4]

The development board which is used for test and debugging is a development board from MikroElektronika called PICPLC16 V6, [5] [6] [7] generally used to develop industrial, home and office control devices. The system features GSM/GPRS communication, 16 relays, 16 opt coupled inputs, RS485, RS232, serial Ethernet, etc. (Fig.4)
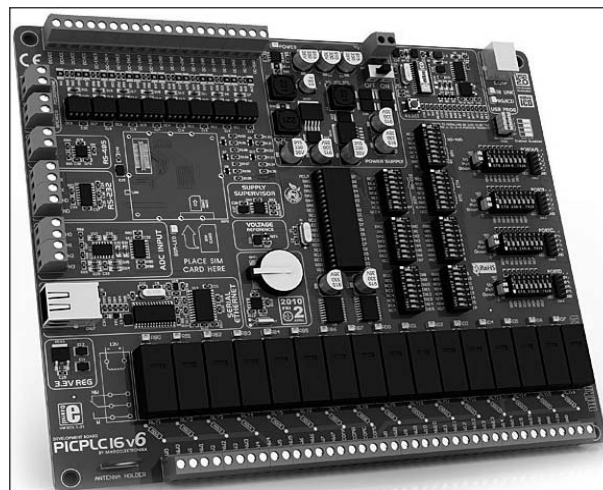
Fig.4. The development board

It uses a Microchip microcontroller PIC18F4520 (Figure 5.) witch have fallowing characteristics:

- C compiler optimized architecture.
- 75 instructions (83 with extended instruction set enabled).
- 4x phase lock loop (PLL) frequency multiplier allows clock speeds up to 40MHz.
- Up to 10 MIPS performance.
- Internal oscillator block.
- 20 interrupt sources.
- Priority levels for interrupts.
- 8 x 8 single-cycle hardware multiplier.
- Power management features.
- 32K bytes (16384 x 16-bit words) of Flash program memory.
- 1536 bytes of SRAM data memory.
- 256 bytes of EEPROM data memory.
- 36 I/O pins with individual direction control.
- High current 25mA source/sink for direct LED drive.
- 13 channels of 10-bit A/D.
- Two analog comparators.
- Four timer/counters (one 8-bit and three 16-bit).
- Enhanced USART module.
- Master synchronous serial port (MSSP) module supporting I2C and SPI.
- Parallel slave port (PSP).
- Programmable brown-out reset.
- Programmable high/low-voltage detect.
- In-circuit serial programming (ICSP) and in-circuit debug (ICD) via two pins.
- 5V operation.
- Operating temperature range of-40°C to +85°C.
- 40-pin DIP package.
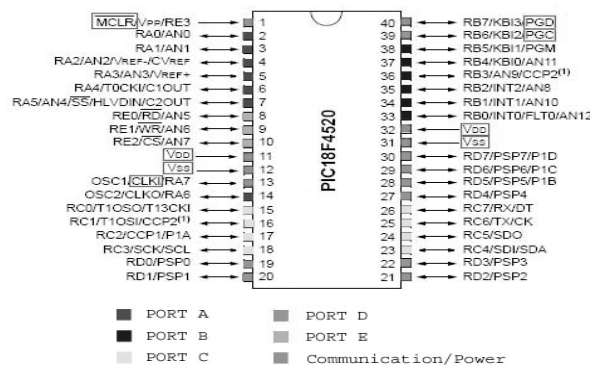
Fig.5 PIC 18F4520 pin out

The communication between microcontroller and the GSM module is realized with AT command. AT is the abbreviation of ATtention. Every command line starts with "AT" or "at". That's why modem commands are called AT commands. Many of the commands that are used to control wired dial-up modems, such as ATD (Dial), ATA (Answer), ATH (Hook control) and ATO (Return to online data state), are also supported by GSM/GPRS modems and mobile phones. Besides this common AT command set, GSM/GPRS modems and mobile phones support an AT command set that is specific to the GSM technology, which includes SMS-related commands. [8] [9] [10] [11]

Next are presented some of the tasks that can be done using AT commands with a GSM/GPRS modem or mobile phone:

* Get basic information about the mobile phone or GSM/GPRS modem. For example, name of manufacturer (AT+CGMI), model number (AT+CGMM), IMEI number (International Mobile Equipment Identity) (AT+CGSN) and software version (AT+CGMR).

* Get basic information about the subscriber. For example, MSISDN (AT+CNUM) and IMSI number (International Mobile Subscriber Identity) (AT+CIMI).

* Get the current status of the mobile phone or GSM/GPRS modem. For example, mobile phone activity status (AT+CPAS), mobile network registration status (AT+CREG), radio signal strength (AT+CSQ), battery charge level and battery charging status (AT+CBC).   * Establish a data connection or voice connection to a remote modem (ATD, ATA, etc).

* Send and receive fax (ATD, ATA, AT+F*).

* Send (AT+CMGS, AT+CMSS), read (AT+CMGR, AT+CMGL), write (AT+CMGW) or delete (AT+CMGD) SMS messages and obtain notifications of newly received SMS messages (AT+CNMI).

* Read (AT+CPBR), write (AT+CPBW) or search (AT+CPBF) phonebook entries.

* Perform security-related tasks, such as opening or closing facility locks (AT+CLCK), checking whether a facility is locked (AT+CLCK) and changing passwords (AT+CPWD).(Facility lock examples: SIM lock [a password must be given to the SIM card every time the mobile phone is switched on] and PH-SIM lock [a certain SIM card is associated with the mobile phone. To use other SIM cards with the mobile phone, a password must be entered.])

* Control the presentation of result codes / error messages of AT commands. For example, you can control whether to enable certain error messages (AT+CMEE) and whether error messages should be displayed in numeric format or verbose format (AT+CMEE=1 or AT+CMEE=2).

* Get or change the configurations of the mobile phone or GSM/GPRS modem. For example, change the GSM network (AT+COPS), bearer service type (AT+CBST), radio link protocol parameters (AT+CRLP), SMS center address (AT+CSCA) and storage of SMS messages (AT+CPMS).

    * Save and restore configurations of the mobile phone or GSM/GPRS modem. For example, save (AT+CSAS) and restore (AT+CRES) settings related to SMS messaging such as the SMS center address.

4. THE SYSTEM DESCRIPTION

    In this paper we propose to implement an automated alert system with GSM alerts. Surveillance system has 8 rooms to be supervised by our system (we considered that in the warehouse are offices); in every room is a motion sensor [3] that will be the trigger system, but the sensors can be modified with other types like: fire sensors, some special gas sensor (depending on what parameter we want to supervise) or other type of devices that can trigger our system. The number of rooms monitored can be changed, the model is made for 8 rooms (Fig.6), but it can be increase the number of rooms, which is limited only by the number of digital inputs of the microcontroller used. In the fallowing figure we imagine a scenario for placing sensor, motion sensors, in front of every door. Sensors are draw with yellow color.
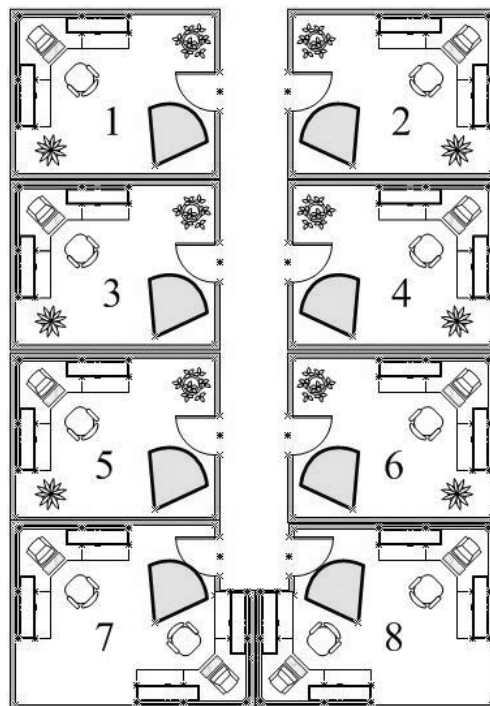
Fig.6 Example of warehouse monitored

    In phone's memory card is stored a predefined number of messages (SMS), one message for each room. The message is stored as "deposit" followed by the deposit number. Can be stored as many SMS that the telephone support, in some cases for a particular combination of events to be sent a proper SMS. The system can also send

SMS not only to a number but to several numbers. All this numbers are set by program with AT command, command specific for the GSM module.

At apparition of an intruder in the secured perimeter, the present sensor will signal that and through the development board, the microcontroller will send alert through SMS.

The system has a refresh rate of 25 seconds. If the intruder does not leave in 25 seconds, the system will send back a message that will warn the intruder presence in the area again.

Also the system can take some preventive measure, like in this case can switch the light in the room, or other measure.

The code is written in MikroC, and the fallowing code is set the GSM number where the message will be sent, and the select of the third SMS stored on the SIM card. (fig.7)

```
if (BUTTON(&PORTD,0,1,1)) {
delay_ms(500);
    UART1_Write_Text("AT+CMGS=");                Delay_ms(1000);
UART1_Write(0x22);
UART1_Write_Text("0762293453");
UART1_Write(0x22);
UART1_Write(0x0D);
Delay_ms(1000);
if (BUTTON(&PORTD,2,1,1)) {
delay_ms(500);
UART1_Write_Text("AT+CMSS=3");
UART1_Write(0x0D);
delay_ms(25000);
```

Fig.7 Example of code

REFERENCES

[1] Sochirca B., Poanta A., - Proiectarea şi dezvoltarea aplicaţiilor cu microcontroler, Editura Universitas, 2012.

[2] http://wireless.arcada.fi/MOBWI/material/CN_1_6.html

[3] Pătrăşcoiu N. -Senzori şi traductoare, curs, 2010

[4] Pop E., Leba M., Microcontrollere si automate programabile, Editura Didactica si Pedagogica, Bucuresti, 2003

[5] http://mikroe.com

[6] PICPLC16V6 user manual

[7] MikroICD Quick Guide

[8] http://www.developershome.com/sms/atCommandsIntro.asp

[9] PIC18F4520 datasheet

[10]   http://en.wikipedia.org/wik/Hayes_command_set

[11]   http://www.developershome.com/sms/atCommandsIntro.asp

ELEARNING, MODERN EDUCATION ALTERNATIVE BASED ON INFORMATION TECHNOLOGY. INDICATIV GUIDE

EMIL POP[1], ROXANA BUBATU[2], CAMELIA BARBU[3], MARIA POP[4]

Abstract: This paper analyzes how to use of alternative education eLearning. This is a type of learning, education or training, in which teachers, instructors use information technology for teaching, learning and assessment in combination with the internet that reduce distance, time and eliminate classroom allowing the students to access learning resources (courses problems, laboratories, processes, tests, examples of best practices, communication and social networks, access to their results, etc.) without limits, constraints and stress.

The first part of the paper presents the concepts used in eLearning, the types of training and learning through eLearning goals.

Continue are treated eLearning principles and methods, and in the last part of the work is done eLearning a guide in which is evidenced every step to achieve a successful course in format eLearning.

Keyword: eLearning, the eLearning principles, methods, eLearning guide.

1. INTRODUCTION

The Internet has come to confirm and strengthen the advantages that it provides experts about distance learning, openness, flexibility, efficiency and especially interactivity. Education based on "support of electronic" is called eLearning, which means using information and communication technologies in education.

ELearning is a type of learning, education or training, in which teachers and instructors use information technology for teaching, learning and assessment in combination with the Internet that reduce distance, time and eliminate classroom allows students to access resources educational training (courses, problems, labs, processes, tests, examples of best practices, communication and social networks, access to their results, etc.) in at their own pace and convenient ways for them without limits, constraints and stress [1], [3].

---

[1] Ph.D Prof Eng. at University of Petrosani
[2] Ph.D Student at University of Petrosani
[3] Ph.D Lecturer Eng. at University of Petrosani
[4] Ph.D Prof Eng. at University of Petrosani

Training institutions are now very receptive to the formation of eLearning, as investors spend millions of dollars teaching solutions for eLearning in different areas. We can say that investors can accurately decide the transition from one technology to another or from one methodology to another, but this cannot be without employee involvement and without measuring of their effectiveness, because every institution needs clear ideas and goals concentrates and the best goals are those that can be recovered and measured.

1.1. E-Learning Objectives

In the last 10 years, hundreds organizations have trying incorporation of eLearning in their development plan, but not all have succeeded because they have failed to reach expectations demanded by investors. For example, it is possible that a department staff can attain a much higher level of education, if they receive support from managers who need to come up with ideas and new objectives in terms of training, even if they have not experienced practice. But, instructors are expected to employees achieve in the future a development plan by which to modernize the institution. In case of a company is used for eLearning training of the staff. The executive staff can go in parallel with suppliers because they can present new solutions that put into practice leading to achievement goal. This arrangement of training can lead to improved productivity depending on the priority list.

In terms of retention, no need to achieve a high level of knowledge in the classroom, because the eLearning format can be accessed at any time. An effective system of eLearning is the model support at any time, by which students can refresh their knowledge when they need to perform a procedure, or when they are an unexpected situation. Through eLearning they can find keywords and anytime to access a unit course, but that means that they learn how to find and access the information they need [1], [2].

The benefit of using online courses in comparison with other methods for providing information, such as online documents in Word or PowerPoint, is that the eLearning has been created to explain concepts by presenting the same information in different ways, what is easier for students to understand new information and follow new procedures.

2. PRINCIPLES AND METHODS ELEARNING

From the classic way to higher education by correspondence on the Web has changed the way content of storing and means of communication between teachers and students, keeping a few principles [4]:
• The principle of openness, because of this principle the offer of courses is diversified and can cover many training needs. This allows the same institution to offer several courses simultaneously without problems linked to the number of students who participate;

- Principle of flexibility. The flexibility of space, time and pace of learning means that each student may consult printed materials, audiovisual resources, online materials, etc., under all conditions of time and space;
- Democratization of education;
- The socialization and interactivity. New technologies enable the sharing of timely, easily and frequency between students and teachers;
- The importance of motivation.

Focusing on formative eLearning as a method shall we say firstly, that it allows a complete the remote training where students and teachers meet in physical space during the course or the training activity or during the course blende learning when there are physical meetings between trainees and students.

A clear classification in terms of pedagogical education, the eLearning is synchronous and asynchronous type:

- Synchronous is the process to learning that is taking place simultaneously. The Communication between teacher and student takes place in real time, using technology to classroom, chat room, video installations, computers etc.;
- Asynchronous is the process in which there is no simultaneity, quite the contrary. Students accessing material created by trainers, but the tools used can be different but anyway they must use the Internet.

Once taken the decision to organize a training eLearning, the first thing to do is training action planning. Correct planning should include the following phases:

- The analysis system of description of objectives and goals to achieve;
- The design of a model for to obtain these goals and objectives of educational development;
- The development model, including the creation of training materials;
- Implementation of the model, which involves the implementation and distribution of training materials;
- Evaluation, which allows analysis results and objectives in order to improve future model.

The organization of entire online course requires the answer to three fundamental questions such as the:

- Identification of problematic cores, that is the response to the training needs detected, taking into account the socio-institutional context, goals and objectives of the training;
- Once identified those cores will be fixed priorities between them, namely the determination a hierarchy of importance of their approach.
- Finally, the most important is to formulate goals, must be understood as goals, results that need to be achieved through formative action. In this sense, we must not lose sight of that although the objectives are formulated to be focused on the learner, they can also function as key point of reference for the institution providing training with a view to assess what is appropriate to the plan parties.

3. PREPARATION COURSES IN ELEARNING FORMAT

Content disciplines will need to have some basic characteristics:
- Have a logical structure;
- Have the appropriate objective reality;
- To be current and relevant with training needs;
- Be exemplary and representative;
- Be transferable and applied in other fields of knowledge;
- Sustainable and not obsolete;
- Be appropriate for the cognitive development of students;
- Significant for student;
- Functional and usable;

Once it was established course content in accordance with rules outlined above, must be thought of and defined presentation and virtual organization, so that access to it and understand it to be as quick and simple as possible.

The instruments pedagogical specific to online courses are:
- Teaching materials;
- Assessment tests;
- Practical cases;
- Forum;
- Virtual communities.

The structure of materials teaching for a course in format eLearning, made a so-called eLearning Guide, which is divided into 3 stages:

A. *Course format*

COURSE TITLE

Course Objectives: (recommended is 1 paragraph), will explain what the teacher wants that pedagogical objectives for student to the end of course.

1. *Chapter Title*

Presentation: (recommended are 3 rows) short description of contents.

    1.1.   Title Section

        1.1.1. Subsection

        1.1.2. Subsection.

Glossary

Recommended bibliography

Web pages

Indexes

B. *The drafting*

a.   Clarity, basic rules of politeness to facilitate learning;

b.   Communication should be direct and concise;

c.   Using enumeration, followed by developing the above description of the main ideas and important concepts, etc.;

d.   The basic rule says that a student he needed one minute per page;

e.   A section of a course shall not contain more than 15-20 pages, so 15-20 minutes;

f. To create a course that works well, begin by dividing the course into segments of 15-20 minutes;

g.   Breaking a course in 5 chapters, each of 15-20 pages allow the student to study a chapter a day and so the ends in a week. They have a sense of accomplishment when they see that they can complete the course in a relatively short time;

h.   Longer courses are created in modules of 5-15-20 chapters.

A chapter should provide:

- A summary as this provides an easy way for course designers start a new topic.
- The material should contain marking points: that students read the material attached with a different medium and thus make the difference, for example, an article, an exercise or simulation;
- Optional information occupies the third level, hyperlink;
- Detailed content should be given only if the student wishes.

C. Presentation

The technicians and teachers can collaborate effectively, and to achieve the desired objectives will be able to use materials such as: graphics, photos, icons, animations, movies and any other instrument for obtaining a friendly and attractive material.

4. EVALUATION THROUGH ELEARNING

Depending on the pedagogical strategy that was adopted by the trainer, the assessment or test self will have or not impact on the course.

The possibility most widely used and convenient is that the test is a simple tool to verify that the student has assimilated content of the course. The IT system has to enable that once finished the test, the student may know the number of correct and incorrect answers. The test should not exceed 15 questions.

The assessment of students

To evaluation is assigned a very important part in the process, so in most cases trainers and managers at human resources tend to concentrate heavily on testing desiring to highlight [3]:

1. Identification the theoretical knowledge of courses;
2. Identifying the practical knowledge of courses;
3. Identifying the level of skill and understanding;
4. Reflects toward the future thinking of the students;
5. Expressing their new ideas of students help trainers in the development of new methods.

Assessment methods:

• Realization of online exams;

• The questionnaires with open questions, such as: "Define the term or list of tools to ..."

• The questionnaires with closed questions so-called "test grill", which have the advantage that they have been developed and programmed the platform, with correct answers and standard feedback.

Evaluating the trainers

It's about trying to determine far as possible if we are running the program adapted to the needs and objectives, so will be subject to review following elements: awareness of the problems, working, reporting how learners competence in and technical knowledge, organizational skills, facilitation skills, skills assessment, minimal technical skills, evaluating the trainers can be on several levels:

External evaluation - by other trainers or external trainers;

Inter-evaluation - by other trainers during a training program in which they work as a team or delivering a training program with a trainer and co-trainer [4];

5. CONCLUSIONS

In this paper, a study was conducted on e-Learnig education, methods, principles and the drafting and passage rates of classical format of the format online. Knowing these principles and openness to e-Learning, is improving and developing teaching skills, attracting students and resources, increase the prestige and institutional development.

REFERENCES

[1] **Bela Markus**, Hungary, *Learning Piramyds*, From Pharaohs to Geoinformatics FIG Working Week 2005 and GSDI-8 Cairo, Egypt April 16-21, 2005
[2] **Bubatu R., Barbu C**., *The e-Learning education impact in human resource training*, 5th International Symposium Occupational Health and Safety – SESAM 2011
[3] ROSEN A., E-learning 2.0 Proven Practices and Emerging Technologies to Achieve Results
[4] **Vasista K., Srini Tatapudi, N. Vasista, N. Sarma, S. Sarma**, *Knoledge management strategy for NGOS Towards Contributing to Corporate Social Responsability*: A View from Tatapudi Trust, International Jurnal Of Marketing, Financial Services & Management Research, Vol. 1 No.4, April2012, ISSN 2277 3622

INFRARED MEASUREMENT OF THERMOELASTIC STRESS ON MECHANICAL COMPONENTS

Zvonko DAMNJANOVIĆ[1], Dragan MANČIĆ[2], Dragoljub LAZAREVIĆ[3], Radoje PANTOVIĆ[4]

Abstract: Combining thermal imaging techniques measurements tension and Thermal imaging analysis gives a general picture of the distribution of tension. In this work presented visual and virtual instrumentation based on infrared analysis of thermoelastic stress. A simple test The parts of the construction where the highest tension occur are determined by the thermal analysis. The TSA also helps to make a faster and in a predictable manner, without need for extensive iterative investigations, what reduces both time and costs.

Key words: TSA Software, Thermoelastic stress analysis, Infrared thermography, Structural health monitoring, Thermoelasticity.

1. INTRODUCTION

Thermoelastic stress analysis is based on the principle of thermoelastic measurements. This principle is well known in gases: adiabatic compression or expansion caused by temperature variations. This effect exists in solid and liquid, and the temperature difference but they are very small compared to gas.

Usually compression solid element causes temperature rise and cause traction state temperature reduction, as illustrated in Figure 1.

The theory of thermoelastic effect was initiated by Weber [1] and Kelvin[2] isotropic homogeneous material under adiabatic conditions, then proceed Blot [3] and Rocca&Bever[4] in the modern mechanical and thermodynamic theory. Within the elastic range, material submitted to stretching or compression stresses experienced reversible negative or positive temperature ("~ 1 milli Kelvin for 1 MPa stress in mild steel) Thermoelastic stress analysis using radiometry consists of measurements with
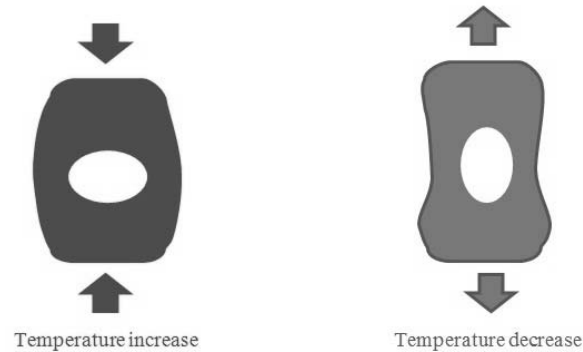
---

[1] Technical Faculty in Bor, University of Belgrade, Serbia, zdamnjanovic@tf.bor.ac.rs
[2] Faculty of Electronic Engineering, University of Niš, Serbia, dragan.mancic@elfak.ni.ac.rs
[3] Faculty of Mechanical Engineering, University of Niš, Serbia, dlazarevic@masfak.ni.ac.rs
[4] Technical Faculty in Bor, University of Belgrade, Serbia, pan@tf.bor.ac.rs

Fig.1. Temperature and volume variation in solids

scanning infrared radiometer, these very small temperature variations of the sample under mechanical loading, then calculate the stress map with adequate model thermoelastic coupling. [5]. First studies that using a standard infrared camera completed in early 1980. [6-8]. To achieve adequate solutions in terms of stress measurement, statistical noise rejection method was previously proposed to improve the resolution of standard thermal infrared thermography ekuipments[9-10]. Statistical advantage of our procedure is that no synchronization necessary link between the testing machine and IR equipment. Thermal resolution of about 2 mK, responds to stress resolution of about 2 MPa for steel, will take less than 5 minutes in industrial tests, [11]   operating procedure can be easily adapted to any infrared thermography camera. Usually in thermoelastic stress analysis, hypothesis adiabaticiti applied, ignoring the heat conductivity of the sample. If this is the case at high frequencies or low loading conducting material, it is much more uncertain in most current tests. In the case of academic sample, the influence of heat diffusion is quantified by means of the finite element model of thermoelastic coupling, according to the experimental results. Moreover, adiabaticiti criterion is rigorously established. Finally, several techniques have been proposed inverse to restore attenuated thermal contrasts under nonadiabatic conditions, and the results obtained by the successor model of thermal diffusion are presented. [12]

Concept of thermoelastic stress analysis based on infrared thermografy and stress-pattern analysis by thermal emission is presented. This technique uses computer enhancement of infrared detection of very small temperature changes in order to produce digital output related to stress at a point on the surface of a structure, a stress graph along a line on the surface, or a full-field isopachic stress map of the surface. Under cyclic loading, at a frequency high enough to assure that any heat transfer due to stress gradients is insignificant, the thermoelastic effect produces a temperature change proportional to the change in the sum of the principal stresses. Although calibration corrections must be made for use at widely differing ambient temperatures, the technique works over a wide range of temperatures and on a variety of structural materials including metals, wood, concrete, and plain and reinforced plastics[13], [14].

2. THERMOELASTIC STRESS ANALYSIS (TSA) MEASUREMENT PRINCIPLE

Explanation of the thermoelastic effect, measurement principle, history and applications can be found in [3]. Thermoelasticity is based on the thermoelastic effect, i.e. every substance (solid, liquid or gas) changes its temperature if volume changes due to external loading. For an homogeneous solid material, if no heat exchange take places (i.e. the loading is sufficiently quick) the temperature change ΔT can be related to the stress by the following equation (1) [15], proposed the first time by Lord Kelvin in *Encyclopaedia Britannica 9th edn. In 1878*:

$$\Delta T = \frac{T\,\alpha\left(\Delta\sigma_1 + \Delta\sigma_2\right)}{C_p\rho} \tag{1}$$

where $\Delta\sigma_1 + \Delta\sigma_2$ represents the sum of the stress time fluctuation in two perpendicular directions on the specimen surface (i.e. the first stress invariant time fluctuations), α is thermal expansion coefficient, T is absolute temperature of the component, ρ denotes density and C_P corresponds to specific heat at constant pressure.
In order to apply this measurement principle to detect stress maps, it is therefore necessary to measure a spatial distribution of temperature changes. In order to have a non contact stress measurement technique temperature changes can be measured without contact on the surface on a loaded mechanical component by a differential thermocamera. Typically temperature fluctuations are measured synchronous with a reference signal, related to the loading cycle of the mechanical component. The data processing is performed by the lock-in technique, that mix the output signal from the infrared detector with a reference signal related to the dynamic loading.

The new idea proposed here is that the measurement of heat movie with high speed and high resolution thermocamera. Here DeltaTherm 1560 system produced by the Stressphotonics benefits. At each dinamic random time signal recorded at each pixel thermal film evaluation power spectrum is performed. Map amplitude spectrum of each peak detected represent the map of the first stress invariant at that frequency or operating mode forms in terms of stress, according to equation (1).
This measurement technique could appreciate the obvious benefits of intrusive techniques, using acceleration sensors as a contact for example, but it is also important to respect the benefits not contact other optical techniques.

A possible approach for thermal processing film in order to obtain operational mode shapes described by many newspapers, possibly useful technique for thermal film processing. Brincker R., Zhang, L., Andersen, P. (2000). - Brincker, R. and Andersen P. (1999) - R Brincker., Zhang, L., Andersen, P. (2000) - H. Herlufsen and N. Moller, Bruel & Kjaer, Denmark (2002) - Aoki, M. 1987 - Viberg, J. (2007). [16].

3. EXPERIMENTAL PART
3.1. Used equipment for testing

For recording and analysis was used infrared camera Varioscan 3021ST, JENOPTIK Laser, Optik, Systeme GmbH producer (Fig. 2). The basic characteristics are: Measuring temperature range from -40°C do +1200°C and Thermal sensitivity ±0.03ºC at 25°C. Spectral range 8–12μm, Detector type MCT (HgCdTe), Detector cooling- Liquid nitrogen, 360 x 240 pixels.

Fig.2. Varioscan 3021ST, JENOPTIK Laser, Optik, Systeme GmbH used in this research

Varioscan high resolution is a high-quality optical measuring slow-scan thermographic system, which scanning the object field in a raster using a single element detector. Varioscan high resolution (model 3021ST) is a thermographic system for the wavelength range of 8–12μm, width temperature resolution of ±0.03ºC and temperature measuring range of -40 to 1200°C. The camera operates on the principle of object scanning. The object is scanned through a two-dimensional reflecting scanner.
The horizontal scanner scans in lines with 360 pixels each, and recording at a frequency of 135Hz. This scanner operates as a resonance oscillator driven by a DC motor. The vertical scanner builds up the complete image from the individual lines. At an image refresh rate of 1Hz up to 240 lines can be captured. VARIOSCAN *high resolution* can also operated with the following resolutions (pixel x lines): 360x200, 360x100 and 360x50, with image refresh rates 1s, 0.4s and 0.2s (depending on number of lines).

On the Model 3021 are used MCT (HgCdTe) detectors and having an edge length of 50x50μm. The Model 3021-ST works with an integrated Stirling cooler. The output signal of the detector is amplified, digitized width 16bits, visualized with an 8bit resolution (256 colors) and transferred for further processing to the PC-104 module. Every color of the displayed thermogram represents a defined temperature. The implemented control software Irbis controls all camera functions.

The implemented control software Irbis controls all camera functions.

InfraTec's state-of-the art IRBIS $^{®}$ 3 software package is the ideal tool for fast thermographic image data analysis and comfortably creating reports in Microsoft Word. Several lens packages with application specific expansion modules are available. IRBIS $^{®}$ 3 is compatible with all infrared camera systems of InfraTec's product range.

Basic functions

- Support for infrared camera file formats of InfraTec's product range
- Multi-lingual user interface
- Visualisation of thermal images with screen/printer-optimized colour palettes
- Manual and automatic temperature range selection
- Temperature profiles along any lines and across any measured areas
- Automatic indication of maximum and minimum temperature mean value
- Print and export of thermal images or tables of measured values
- Display of up to 10 coloured isotherms
- Image improvement through digital filtering
- Integrated Word-based report function Highlights
- Additional graphic and image-editing functions
- Freely definable colour wedges and enlargement factors
- Accumulation of recorded thermographic images
- Visualisation of images in differential image mode
- Various models for emissivity correction (also by pixel)
- Establishement of temperature values differences of thermal images
- Multi-window option
- Various statistics functions
- Set up of video sequences

3.2. Results and discussion

Tests were performed on the testing machine of 100 kN (10 /91 ZDM type, accuracy class 1, "WPM Industriewerk Leipzig" VEB Thürengen Industriewerk Rauenstein, Masch. Nr. 2214/22- 1963) at the Laboratory of Mechanical Materials Faculty of Mechanical Engineering in Niš (Fig. 3).

Fig.3. Test in Laboratory
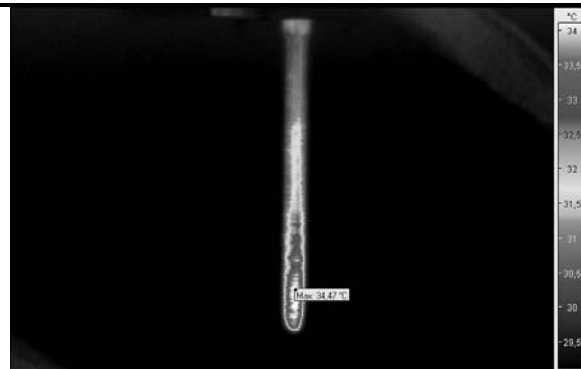
Fig.4. Thermogram

Table 1. Temperature values for some parts
of the temperature changes vs. time diagram

Figure	Time	Tmax
No:	t (hh:mm:ss)	(ºC)
101000	13:22:08	30,50
101000	13:22:12	30,48
101001	13:22:12	30,50
101002	13:22:16	30,69
101003	13:22:20	30,36
101004	13:22:24	30,29
101005	13:22:28	30,30
101006	13:22:32	30,23
101007	13:22:36	30,30
⋮	⋮	⋮
101098	13:36:38	34,57
101099	13:36:32	34,47
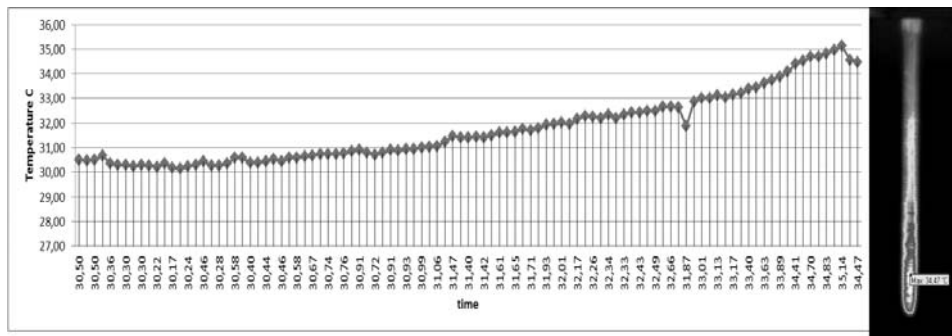
Fig. 5. Diagrams temperature changes vs. time with thermograms in specific points

4. CONCLUSION

The experimental results for steel specimens, considered in this paper, indicate the fact that the testing of metal structures requires new contactless methods. A joint measurement concept Thermoelastic Stress measurement system from an extended infrared and digital image correlation technique has been presented. One of the advantages of the presented procedure, in addition to the greatly simplified

experimental test set-up, is the fact that the relevant thermo-mechanical fields are directly evaluated into a finite element mesh, and hence the interface with numerical simulations aiming at identification does not involve any unwanted loss of accuracy in unnecessary projection steps for the comparison. Combining thermal imaging techniques with measurements using a measuring tape tension can lead to great benefit in maintaining these structures. The proposed procedure of non-destructive analysis provides good basis for a wide range of investigations and eliminates, or reduces, the need of expensive destructive tests. The TSA also helps to make a numerical analysis faster and predictable, without need for extensive iterative investigations, what reduces both time and costs.

REFERENCES

[1] **Weber W.,** *Über die spezifische Wärme fester Körper insbesondere der Metalle*, Annalen der Physik and Chemie, 96, 177-213 (1830).

[2] **Thomson W.,** *On the Dynamical Theory of Heat*, Trans. Royal Soc. Edinburgh, 20, 261-283 (1853).

[3] **Biot M.A.,** *Thermoelasticity and Irreversible Thermodynamics*, J.Appl. Phys., 27(3), 240-253 (March 1956).

[4] **Rocca R., Bever M.B.,** *The Thermoelastic Effect in Iron and Nickel as a Function of Temperature*, Trans.Am.Inst.Mech.Eng., 188, 327-333 (Febr. 1950).

[5] **Belgen M.E.,** *Infrared Radiometric Stress Instrumentation Application Study*, NASA CR-1067 (1968).

[6] **Henneke E.G., et al.,** *Thermography - An NDI Method for Damage Detection*, J. Metals, 31,11-15 (1979).

[7] **Blanc R.H., Giacometti E.,** *Infrared Radiometry Study of the Thermomechanical Behaviour of Materials andS tructures*, First International Conference of Stress Analysis by ThermoelasticTechnics, Sira Ltd, London (November 1984).

[8] **Nayroles B., et al.,** *TEl~thermograph & infrarouge etmEcanique des structures*, Int. J. Eng.Sci., 19, 929-947 (1981).

[9] *Evaluate the Amplitude of Cyclical Noisy Signal in IR Thermography*, NATO ASI Series, Series E: Applied Sciences, 262 (1993).

[10] Offermann S., **et al.,** *Thermoelastic Stress Analysb with Standard Infrared Equipments by Means of Statistical Noise Rejection*, Res. Nondestruct. EvaL, 7(4), 239-251 (1996).

[11] **Offermann S., Beaudoin J.L.,** *Mechanical Stress Pattern Analysis with a Standard Infrared Camera and Statistical Treatment*, lnt. Conf.MAT-TEC 96, Marne la VallEe, 25-27 (1996).

[12] **Offermann S., et al.,** *Thermoelastic Stress Analysis Under Nonadiabatic Conditions* , Experimental Mechanics, Vol. 37 (4).

[13] **Marendić P., et al.,** *Uvod u termoelastičnu analizu naprezanja*, P. Marović, M. Galić, L. Krstulović - Opara, Drugi susreti Hrvatskoga društva za mehaniku, pages 43-48. Split, 2008.

[14]   **Di Renzo A., et al.,** *Non contact measurements of stress fields on rotating mechanical components by thermoelasticity*, http://sem-proceedings.com/26i/sem.org-IMAC-XXVI-Conf-s13p06-Non-Contact-Measurements-Stress-Fields-Rotating-Mechanical-Components.pdf

[15]   **Harwood N., et al.,** *An introduction to thermoelastic stress analysis*, Adam Hilger Publishing, 1991.

[16]   **Flori R., et al.,** *Operational modal analysis by thermoelasticity*, http://www-b.unipg.it/misure/data/articles/Operational%20modal%20analysis%20by%20thermoelasticity.pdf

HCI: INTERACTIVE 3D WEB APPLICATIONS

LORAND BOGDANFFY[1], EMIL POP [2]

Abstract: The paper analyses the possibility of using a new type of user interface, stepping up from the standard 2-dimensional into 3-dimensional. The reason is to create a more immersive, natural environment, easier user interaction, offering extended accessibility features, as well as being more entertaining.

Key words: 3D, interface, Silverlight, head tracking, stereoscopy.

1. INTRODUCTION

Technological advances are always pushing high end technology into consumer markets, anything that is in a concept state or used only by developers and scientists, might as well be on our desktops in a few years. A good example for that are the advances made in 3D monitors. It seems like one of our priorities in entertainment (mainstream consumer) and some parts of high end research in different domains like medicine for example, is bringing the world, real or virtual, as realistically as possible in front of our eyes, ears, maybe even touch sometime in the not so distant future. Viewing 3D is perfectly natural; we just didn't have the technology to bring it in our homes yet. More and more, 3D monitors and consumer cameras are becoming available, but this is only to record and watch later. In this paper, different approaches are analyzed to see how a real time 3D user interface could be designed as to increase accessibility, have its usage as natural as possible, and be accessible to the mainstream consumer, from anywhere, requiring as little hardware as possible.

2. 3D VIEWING TECHNOLOGIES

The purpose is simulating human vision. Like most species, humans have stereoscopic vision, meaning we have two eyes, two light sensitive sensors, placed adjacent to each other, about 6-7 cm apart. This is the most important and basic thing to consider and it means that any artificial imaging device we use must have this stereoscopic feature and capture two separate images to be able to recreate a scene.

[1] Ph D. Student at the University of Petrosani, *lorandbo85@yahoo.com*
[2] Ph D. Professor at the University of Petrosani, *emilpop@upet.ro*

Having this source, now we need a way to display it. No matter what, each image must be seen by one eye. There are several methods:

-    **Anaglyph**: this technology dates back to the beginning of the twentieth century, and the way it works is by eliminating color components from each of the two images (red from one image, green and blue from the other) so that after overlaying the 2 images obtained simultaneously and using glasses with red and cyan filters, most of the green-blue (cyan) image is seen using the red filter, and most of the red image is seen using the cyan filter. This is the simplest form of 3D vision, accessible to anyone, even printable on paper, the downside being the low quality of the formed image, ghosting, resulting in eye strain.

-    **Passive glasses**: a more modern approach that we see in many 3D cinemas is the use of polarized passive glasses. The two frames that form the stereoscopic image are presented one after the other, fast enough that the viewer is unaware of it, and by using light polarization, one frame is seen by just one eye, and the next by the other and so on. This technology is available for the general consumer, but is being used mainly in cinemas and one of its downsides is, because of how polarization works, any tilt applied to the glasses will let light through the wrong side of the glasses creating a ghosting effect.

-    **Active glasses**: this is the technology that entered in the mainstream user homes allowing watching of 3D images and videos using a 3D capable monitor, and active glasses. The Left & Right images are presented one after each other at a high frame rate (60 frames / source), and using an infrared communication system the monitor sends a synchronization signal to the glasses witch use LCD filters to alternately block light from one eye and the other. This technology is mature, only small improvements are still made, the image is almost perfect.

-    **Lenticular and Parallax Barrier**: it's a "no glasses" technology, the two images are interleaved vertically, and vertical strips are used to block the images form each eye so that left sees only the left components and the right just the right, downsides are that the user has a limited range of movement, the image resolution is reduced to half. This technology is used for mobile devices, and it's difficult to implement on large screens [4].

-    **Other technologies**: the 3D evolution is trying to go towards "no glasses" 3D using special monitors still in development, but one thing in common these viewing methods have is that the source is the same: stereoscopic.

-    **Viewer Tracking** (or head tracking). This comes to play only in interactive sources, in generated virtual environments. It means the viewed scene is changed according to user location, even if the image is presented on a planar monitor; this gives a good impression of a 3D world. The methods above, except Parallax barrier or technologies that require you to remain still, could benefit from head tracking, as long as the source isn't recorded visually, rather recreated as a 3D environment.

3. WHY 3D INTERFACE

It's not just about the way the virtual world is displayed, 2D or 3D, but also about the user interaction [1]. These days, most of us use a 2D desktop; web pages are

2D, the 20+ year old "mouse" works on 2 axes, what if we could have a 3-axis pointer? How about no pointer at all? Just gesture recognition [2]. Well these things are not far from entering our homes, the only problem is there is no standard yet, different technologies are being developed [1], and they are being used on game consoles for different games, practical use is limited to high end users in domains like engineering, etc.

In the following I will present an idea that could be basis for future development of human computer interfaces. The project has 2 components, one that handles user location and indicator position, and one that provides the visual feedback.

The tracking side of the project uses two simple cameras, capable of a high resolution of 1280x720 and about 20 frames a second. The cameras chosen are off the shelf available to the end-user "webcams", connected via two USB ports.

4. THE APPLICATION

The program is developed in C# using Silverlight 4. Silverlight is a plug-in developed by Microsoft compatible with standard web browsers like IE, Firefox, Chrome, etc. It is capable of accessing video and audio inputs available on a computer. The great thing about Silverlight is the capability of creating fast, responsive interfaces, but this is just 2D, with some perspective tricks, so no shading, lights or cameras.

The main goal is to design a user interface that will have depth. Objects can be placed outside the monitors XY plane, at a depth of Z. This is actually just an illusion, there's no way to draw an object off-screen, but instead, its projection will be drawn. Unifying the planes should be the first thing to consider, to have a common measure unit of placement in space, whether real or virtual space.

Placing an object on the interface will always have an XYZ coordinate in millimeters, an algorithm will calculate the location in pixels the objects projection has to be placed so it appears to the user to be in the respective XYZ position. For this some things have to be considered. In a plane, we can place objects on screen at X-pixels horizontally and Y-pixels vertically. So placing an object in the middle of the screen means placing it in half Screen Pixel Width and half Screen Pixel Height.

Resolution of the monitor is read by the application, physical size reading is not possible, so the user is required to input the physical screen width in millimeters. A constant will store the pixels/distance ratio.

In the first part, the user location determination method is presented. The paper doesn't focus on an advanced face recognition algorithm [3], because the difficulties that changing light on the users face due to changing image on the screen, or even no light on the user, and of course extra processor time. So rather than complicate it, a simple marker, backlit marker will be used for tracking the user. Also, a marker will be used as an indicator used to interact with the interface.

Placement of the cameras: the cameras will use a simple stereoscopic view setup, placed one by the other at a measured distance that we will name CM_{offset}. The setup is important for getting the most accurate distance determination. A guideline for the CM_{offset} value: if the user will be usually close, viewing a regular 20-24" monitor,

value should be smaller, if the user is farther away, value should be greater. If possible the cameras should be in the same plane as the monitor.

One of the challenges is to make this application flexible, so no matter what brand or type of imaging device is used, the program should work in the same way for everyone. To achieve that, we must consider that different cameras will have different view angles. To accurately measure distance with this setup, a camera calibration procedure is needed. The acquired image resolutions are known, defined, in this case, the high definition camera records a stream of images with a reduced resolution of 640x360, width/height ratio of 16:9 (or 1.77), still the cameras view angle has nothing to do with its resolution, so an easy way to find out is when placing the cameras side by side, parallel, measuring the distance between them (CM_{offset}) and measuring the closest distance an object can be placed so that it shows in both images ($Obj_{minDist}$). If we know these values, a simple formula is used to determine the viewing angle:

$$CM_{viewAngleX} = \frac{360\left(\tan^{-1}\frac{\frac{CM_{offset}}{2}}{Obj_{minDist}}\right)}{\pi} \tag{1}$$
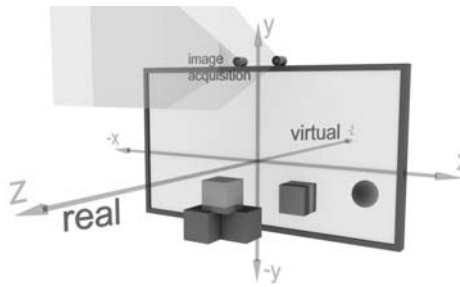
Fig 1: Representation of real versus virtual world
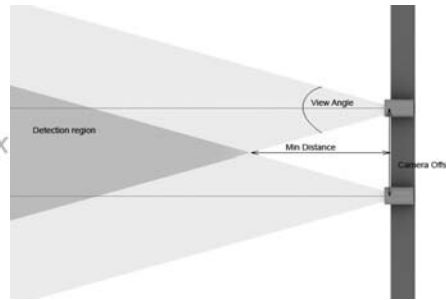
Fig 2: Top view of the cameras view angles

5. CONFIGURATION

Knowing $CM_{viewAngleX}$ it's just a matter of multiplying with our frame ratio to find $CM_{viewAngleY}$. The application will automatically determine the viewing angle of the cameras when provided with the CM_{offset} and $Obj_{minDist}$ values.

$$CM_{viewAngleY} = \frac{CM_{viewAngleX} * frame_{height}}{frame_{width}} \tag{2}$$

Having this angle enables us to determine also the vertical view angle (because we already know the image w/h ratio) and most importantly to determine an interest point's location from the two images. Silverlight can connect to the imaging devices,

and provide a succession of image vectors. Two sources are supported images are taken from both of them. The first step in locating any objects of interest is eliminating any background interference, by looking only at movement. This is fine, because we are only interested to change the interface in the event of real world actions occurring. So, by eliminating the static environment by subtracting 2 sequential images, only parts of the image with motion remain. In the remaining image, made up only by motion components, the algorithm looks for a pattern or something specific to the indicator/marker used, like color or brightness.

Search Algorithm: Some optimizations in recognizing the same pattern in both images are implemented. Because of acquiring stereoscopic images, contents in one image will likely be found in the other image as well, with minor differences, depending on the similarity of the image acquisition devices, . So after isolating motion, a check for similarities is done, objects with different distances will be easier to locate. The location in space of the found objects of interest (user, indicator) will be determined on all axes (XYZ) starting with the distance from the image acquiring devices, the Z-axis. To determine this axis, the object (in this case the indicator or user) will eventually be represented in the acquired frames by only 1 pixel in each. Having this location on the X axis (the Y should be the same in both) determining Z is simple:

$$Obj1_Z = \frac{pixels_N}{\left|Obj_{leftX} - Obj_{rightX}\right| * Obj_{minDist}} \tag{3}$$

Obj1z is measured in millimeters and everything on the right of the equation is pixels. After getting the distance to our, user or indicator, represented on the Z axis, the real world location X and Y coordinates have to be determined, and this is done using:

$$Obj1_Y = \tan\frac{\frac{pixels_y}{2} - Obj_{leftY}}{\frac{CM_{viewAngle}}{2} * \frac{pixels_y}{2}} * Obj1_Z + CM_{offset} \tag{4}$$

$$Obj1_N = \tan\frac{\frac{pixels_y - Obj_{leftX} + Obj_{rightX}}{2}}{\frac{CM_{viewAngle} * pixels_y}{2}} * Obj1_Z \tag{5}$$

Now we have the real world coordinates of the objects (user and an indicator) we seek, we will focus on the applications user interface.
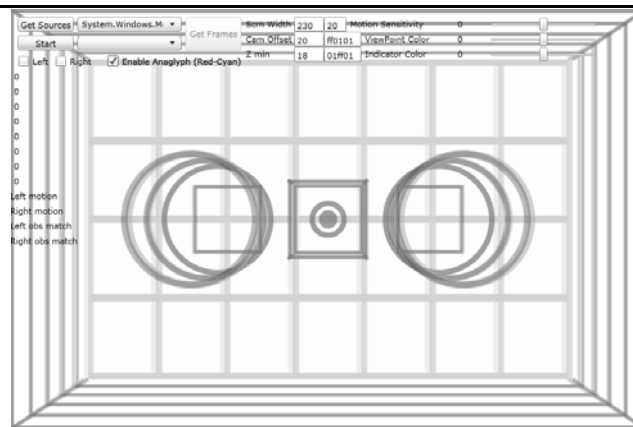
Figure 3: Application interface

6. THE INTERFACE

The built interface is a demo / concept, witch for now only display's basic shapes, but these shapes are visible in a 3 dimensional environment. An option to display the interface in anaglyph mode is added, but this option and the glasses are not a requirement to actually perceive the 2 dimensional objects as being at different depths because of the user tracking feature, that rearranges the objects projections on the 2D monitor according to observer location. This of course is only visible live, not on paper unfortunately. The user has the possibility to look around objects, and to eliminate occlusion if it's possible, just like real-world objects set in space. The interface is drawn taking into account the objects depth, object that are closer are scaled.

7. CONCLUSIONS

Considering what we have seen and the exponential rate at which technology is developing, it is clear that at some point in the near future we will have some sort of virtual interactive environment at the touch of our fingertips, in our homes. It's still unknown what method of displaying this environment will be used, maybe holographic, or something similar to what was presented in this paper. This is just a concept but could easily be built on, adding other functionality like interactions using gestures, using an actual 3D accelerated environment that will be available for use in modern web browsers that will support it natively, or by using an external plug-in like Silverlight.

REFERENCES

[1] R. Kjeldsen, J. Kender, Toward the use of gesture in traditional user interfaces, in: International Conference on Automatic Face and Gesture Recognition, 1996
[2] C. Maggioni, K.B., Gesture computer — history, design and applications, in: R. Cipolla, A. Pentland (Eds.), Computer Vision for Human-Machine Interaction, Cambridge, 1998
[3] P.A. Viola, M.J. Jones, Rapid object detection using a boosted cascade of simple features, in: IEEE Computer Society Conference on Computer Vision and Pattern Recognition, 2001
[4] *** - Wikipedia.org

FLEXIBLE MEASURING SYSTEM FOR DISTANCE BASED ON OMRON PROGRAMMABLE LOGIC CONTROLLER

ROXANA BUBATU[1] PETRE VAMVU [2] CAMELIA BARBU [3] EMIL POP[4]

Abstract: This paper present an automated system for measuring distances with improved flexibility. The system is based on a PLC device coupled with a number of encoders and performs multi axes measurement. The measuring parameters and the functionality of the system can be modified in real time by operator using a HMI (Human Machine Interface). This real time modification of the measuring system parameters leads to a great degree of flexibility of the system and improved efficiency.

The advantages of the designed system and the functional value where tested through an implementation on a pole driving machine. Through this implementation we succeeded to improve quality and speed of pole driving task proving the system worth, reliability and improved efficiency of an automated system including this measuring system.

Keywords: Measuring system, programmable logic controller, distance

1. INTRODUCTION

One of the most sought-after goals in mechanical industry and automation of civil construction nowadays is performing a fast and accurate measurement in an automated fashion [1].

One solution for enhancing existing automation solution is to integrate an automated measuring system to the production process. Compare with conventional techniques the automated measuring process is faster, more reliable and as an advantage is free from human operator influence. The flexible measuring system for distances is design with regards to a certain application.

_____

[1] Ph.D. Student, University of Petrosani
[2] Ph.D Assistant Professor, University of Petrosani
[3] Ph.D. Lecturer, University of Petrosani
[4] Ph.D. Professor Eng.Mat., University of Petrosani

2. PROBLEM FORMULATION

The application was designed regarding the automation process of a pole driving machine. This machine is a self-driven piece of equipment that uses two caterpillar tracks for movement as depicted in figure 1. The machine has a mobile arm used to load the pole and driving that pole into the ground. The arm can be moved in a direction parallel with the machines caterpillar tracks. The mobile arm can perform a fine tune of the position where the pole will be inserted.

The coarse positioning is realized by moving the entire piece of equipment on the vicinity of the place where a new pole will be inserted. The pole insertion into the surface is realized with the help of a hydraulic system which use the hydraulic pressure to perform a rapid and powerful knock on the top of the pole.

Taking into account that for most of the applications where this machine is intended to be used, the distance between the poles is fixed the process of measuring and marking the positions where the pole should be inserted is very time consuming. Also this manual measuring and marking of the positions for the poles necessitate few others crew members.

This type of machine described before is usually used for installing poles for road safety barriers. The density of poles for the road safety barriers is high and the introduction of an automated solution for measuring and positioning the equipment will increase efficiency and speed.

In order to introduce an automated measuring system on this machine we have taken into account that the total distance is a sum between the distance drove by the machine and the distance travelled by the mobile arm. Also the flexible measuring system has to be able to be scaled to for different type of equipments, to be able to accept modifications of the measuring parameters, to display the travelled distance and different type of alarms related to travelled distance and to be programmed to activate an alarm or a signal when the distance travelled match the programmed distance.

Fig.1 Pole inserting machine

3. PROBLEM SOLUTION

For determining the distance very precise we have used a measuring system that include two precise rotary encoders, a display panel and a high speed PLC [2]. The encoders used are high resolution encoders so the result delivered by those two encoders is very accurate.

One encoder is placed near the caterpillar track. A specific diameter wheel was mounted on the encoder shaft, and the wheel is in permanent contact with the surface. This encoder placed near the caterpillar track measure the distance travelled by the machine on the ground.

A second encoder is positioned on the mobile arm and the measuring wheel fitted on the encoder shaft is in close contact with a part fixed on the machine itself.

The two encoders deliver their signals to the PLC unit. The PLC is able two register the pulses from the encoders and store them into special internal counters. Also on the PLC unit is connected a 2 line multifunctional display. On this multifunctional display we can observe the distance travelled by the machine, the distance travelled by the mobile arm, the total distance travelled by the entire system. Also using this multifunctional display unit we can modify the encoders parameters, the parameters specific to the dimensions of the measuring wheels fitted on the encoders' shafts. The system is able to emit alarms when the machine has travelled close enough to the next position where the pole will be inserted.

The designed system allows the operator and engineer to modify many parameters like:
- Distance between the poles
- Distance set off alarm
- Encoder parameters
- View of distance using pulse encoder coordinates
- View of the distance recorded by each encoder

Fig.2 High speed encoder mounted on the mobile arm

The system allows the user to modify the set distance between the poles in order to view on the display the remaining distance to be travelled to the next position. The system also allows the user to modify the distance threshold at which the proximity alarm will trigger. Do to wear on the measuring wheel fitted on the encoder shaft the parameters of encoders have to modifiable through this display in order to realize the calibration of the device.

The measuring system uses high speed rotary encoders which delivers up to 2000 pulses for each rotation. The encoders are very small pieces of equipments, the whole package weighing just 100 grams.

This is a multifunctional display which can be connected to virtually any PLC that uses a Com Link Protocol.

Setting and displaying the parameters is done through the NT2S display (figure 2). This is a multifunctional 2 lines by 16 characters which includes 6 functional buttons.

By altering the parameters through the display, they are immediately modified in the program implemented on the PLC.

The multifunctional display can be programmed to display up to 30 different screens of which design and content are set through the specialized NTXS software.

Surfing the screens is done by special buttons on the display or the PLC can send a command to the display of which screen to become active.

Fig.3 NT2S Multifunctional display

The brain of the system is the CP1E PLC (figure 4). This PLC has the ability to accept encoder pulses on two especially included channels from high speed encoders. This ability makes this PLC one of the best tools for intelligent electric drive applications. Also this characteristic allows us to use this PLC to create a flexible measurement system for distances.

The functions implemented by the PLC are presented in the following section. After the self testing realized on the boot up process the internal counters are incremented or decremented by the movement on the encoder's shafts. The internal counters store theirs values in 2 sixteen bits variables.

Fig.4 CP1E PLC

Parallel with these two others mathematical functions are running. Those functions take the counters values and multiply them with the parameters so the output of those mathematical functions represents the travelled distance in millimeters.

Those functions take into account the number of pulses register by the internal counter, the diameters of the measuring wheels fitted on the encoder's shafts and the characteristic of the encoder, the number of pulses for each rotation.

The mathematical function implemented has the following expression:

$$Output = \frac{N_P}{4 \cdot E_C} \cdot \pi \cdot D \qquad (1)$$

Where:

N_P - represent the number of pulses registered by the encoder.

E_C - represent the encoder constant (number of pulses for each rotation).

D - represent the diameter in millimeters of the measuring wheel fitted on the encoder shaft.

The results are stored in 2 variables which are used to express the distance travelled by the mobile arm and by the machine itself using the caterpillar tracks.

Also parallel with the functions described before the PLC is performing others tasks like: control of the display unit, transmitting and receiving the parameters to and from multifunctional display, calculating the remaining distance to the target point, triggering the proximity alarm, resetting the counters when a new measuring task is initiated. The mathematical functions are implemented through a number of ladder blocks as we can see in figure 5.
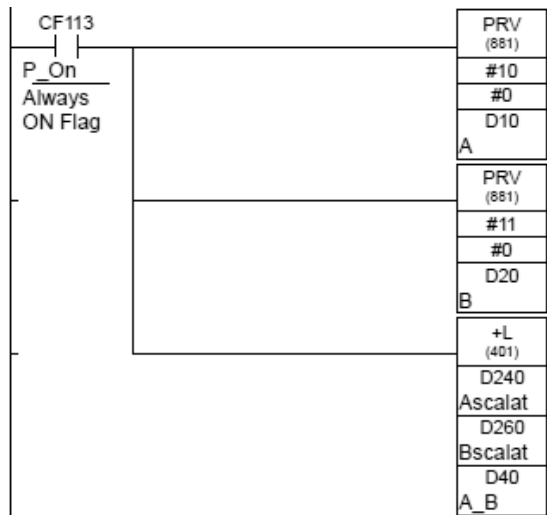
Fig.5 Ladder blocks for implementing mathematical functions

The design of the screens and the parameters used were created using the versatile menu of the NTSX software. Also using the software mention above I created the Tag list used to reference the name of the variables with the parameters stored in the common address space DM.

The common address space is used as a distributed environment between al the units of a system. The parameters from the common address space can be modified by any unit which is part of the system and has access right to the common address space.

First screen of the application displays the distance travelled by the machine from the position where the last pole was inserted.

The number displayed represents the distance travelled by machine on caterpillar tracks summed with the distance travelled by the mobile arm. Also on the first screen is depicted the remained distance to the target position.

Also using the functional buttons on the multifunctional display on screen number one we can set the value for the distance between two consecutive poles used to calculate the target position.

The screen number two display the distance recorded by each encoder. The screen number 3 allows us to set the trigger distance for the alarm proximity. By using this proximity alarm the operators can maneuver rapidly the machine and using the mobile arm can do a fine adjustment to the target position.

The screen number 4 allows the user to introduce the parameters for the encoders and measuring wheels in order to calibrate the machine. This set up of the values assure the correct transforming of the encoder pulses in millimeters units, assuring the calibration of the machine. On the screen number 5 the number of pulses registered by each encoder is depicted.

4. CONCLUSIONS

By introducing the measuring system for distances described before on the pole insertion machine the necessity of a second crew used to mark the insertion positions of the poles was no longer needed. Also this system brings more accuracy and faster speed on the process of insertion of the poles.

The benefits of this system were not resuming to just increasing of the speed and accuracy but also the hole procedure of operating the machine was changed in order to increase productivity. By introducing the flexible measuring system for distances on the pole driving machine the operator of the machine drive along and introduce the poles where the system tell him to. A day or two later a team of workers come and mount the road safety barriers. The flexible measuring system conducted to a reduction of the number of workers with 40 percents and an improvement of productivity with 35%.

REFERENCES

[1]. Paziani F.,Giacomo B., Tsunaki R.H - *Robot measuring form errors*, Elsevier Robotics and Computer Integrated Manufacturing 25, 2009
[2]. Fawaz K., Merzouki R., Ould-Bouamama B. - *Model based real time monitoring for collision detection of an industrial robot*, Elsevier Mechatronics journal, Vol. 19, 2009
[3]. Pătrăşcoiu N., Tomuş A.M. - *Events Acquisition and Sorting Technique Using Virtual Instrumentation*, 9th International Carpathian Control Conference ICCC´2008, Sinaia, 2008

POSITION CONTROL OF ABB ROBOT

ANGELA EGRI[1], VALI-CHIVUTA SIRB[2], OLIMPIU STOICUTA [3]

ABSTRACT: *Our goal was to developed, implemented and practical experimented an XYZ position control system for a ABB industrial robot. The electrical motors used are induction squirrel cage motors. The position adjustment system is based on a vectorial control, sensor-less, of the mechanical speed of the induction motor. The speed estimation and components of the rotor flux is made using the Luenberger Extended Estimator. The design of the adaptation component is based on V.M. Popov hypersensitivity. In the final the position adjustment of the ABB robot is analyzed using Matlab - Simulink.*

KEY WORDS: *Luenberger observer, induction motor, sensor-less, vectorial control, Matlab – Simulink.*

1. INTRODUCTION

In this paragraph we will present a possibility for the deduction of the estimation law of one or more parameters, when the first solution of the problem is used in order to simultaneously identify the states and the parameters. In order to realise the adaptive mechanism we presume that the equations of the two models are linear equations in which we suppose that only the A matrix contains the parameters that we need to estimate. This is the case of the induction motor regardless whether we identify speed or rotor resistance. For calcules we will consider the most general case in which the reference model is really the induction machine and the adjustable motor is a Luenberger [1] observer, whose outputs are the estimated values of the stator currents and rotor fluxes. In order to deduce the adaptive law we need to consider as outputs of the observer only the estimated stator currents. Now we can write the equations of the two models like this:

$$\begin{cases} \dfrac{d}{dt}x = A \cdot x + B \cdot u \\ y = C \cdot x \end{cases} \tag{1}$$

---

[1] *Assoc. prof. eng., phd. at the University of Petroşani;*
[2] *Lecturer eng. ,phd. at the University of Petroşani;*
[3] *Lecturer eng. ,phd. at the University of Petroşani*

$$\begin{cases} \frac{d}{dt}\hat{x} = \tilde{A} \cdot \hat{x} + B \cdot u + L \cdot (y - \hat{y}) \\ \hat{y} = C \cdot \hat{x} \end{cases} \tag{2}$$

in which the A,B and C are the matrixes of the stator currents model – rotor fluxes, and the gain matrix of the observer, L, is built according to the construction algorithm of the estimator presented in the preceding paragraph. In the case of the adjustable model the A matrix is noted with tilde (~) because is built on the estimated parameters.The generality of this case compared to the one in which both models are observers results from the existence of the L and C matrixes. In order to build the adaptive mechanism, for start we will calculate the estimation error given by the diference:

$$e_x = x - \hat{x} \tag{3}$$

Derivating the relation (3) in relation with time and by using the relations (1) and (2) the relation (3) becomes:

$$\frac{d}{dt}e_x = A \cdot x - \tilde{A} \cdot \hat{x} + L \cdot (C \cdot x - C \cdot \hat{x}) \tag{4}$$

Expression (4) can also be written as:

$$\frac{d}{dt}e_x = (A + L \cdot C) \cdot e_x + (A - \tilde{A}) \cdot \hat{x} \tag{5}$$

This equation describes a linear system in reversed connection with a non-linear system. The non-linear system receives at its entry the error between the outputs of the two models, and, as output, has the term $(A - \tilde{A}) \cdot \hat{x}$. If we consider the two systems connected in negative reaction we will note with:

$$\rho = -(A - \tilde{A}) \cdot \hat{x} \tag{6}$$

As one may notice, this problem is frequently treated in the literature of the non-linear systems, being exactly the configuration of the Lure problem [2], and of one of the problems treated by Popov [3] (fig.1). Considering, according to the Popov terminology [3], the non-linear block described by $\Phi(e_y)$ the integral input- output index associated to it is:

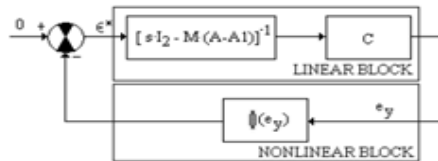$$\eta(t_0, t_1) = Re\left[\int_{t_0}^{t_1} e_y^T(t) \cdot \rho(t) dt \right] \tag{7}$$

Fig . 1. Control loop of Lure problem

In which we have introduced the following notation:

$$e_y^T = \begin{bmatrix} e_y^T & 0 & 0 \end{bmatrix} \tag{8}$$

in order to preserve the compatibility between the dimensions of the input and output. In order for block to be hyper-stable a necessary condition is:

$$\eta \left(0, t_1 \right) = \int_0^{t_1} e_y^T (t) \cdot \rho (t) dt \geq - \gamma^2 (0) \tag{9}$$

for any input-output combination and where $\gamma (0)$ is a positive constant. Under these circumstances, using the relation (6) the expression (9) becomes:

$$\eta \left(0, t_1 \right) = - \int_0^{t_1} e_y^T (t) \cdot \left(A - \tilde{A} \right) \cdot \hat{x} \cdot dt \geq - \gamma^2 (0) \tag{10}$$

In the following we will presume that the error $A - \tilde{A}$ is determined by only one of the parameters of the electrical equations of the induction machine. In this case we may write:

$$A - \tilde{A} = (p - \tilde{p}) \cdot A_{er} \tag{11}$$

where p is the respective parameter (speed or rotor resistance), and A_{er} is a constant matrix, with elements depending on the place where p appears in A matrix's coefficients. For any positive derivable f function we can demonstrate the following inequality:

$$K \cdot \int_0^{t_1} \frac{df}{dt} \cdot f \cdot dt \geq - \frac{K}{2} \cdot f^2 (0) \tag{12}$$

On the other hand, using the relation (11), the expression (10) becomes:

$$\eta \left(0, t_1 \right) = - \int_0^{t_1} e_y^T (t) \cdot (p - \tilde{p}) \cdot A_{er} \cdot \hat{x} \cdot dt \geq - \gamma^2 (0) \tag{13}$$

Using the relations (12) and (13) we can write the following relations:

$$f = p - \tilde{p} \tag{14}$$

$$- e_y^T \cdot A_{er} \cdot \hat{x} = K \cdot \frac{df}{dt} \tag{15}$$

From the relation (15) it immediately results that:

$$- k \cdot e_y^T \cdot A_{er} \cdot \hat{x} = \frac{d}{dt}(p - \tilde{p}) \tag{16}$$

Because K is a constant and then, in case of a slower p parameter variation related to the adaptive law, we can write:

$$\hat{p} = \tilde{p} = k \int e_y^T \cdot A_{er} \cdot \hat{x} \cdot dt \tag{17}$$

Relation (17) represents the general formula used to build an adaptive law. The "k" constant is chosen so that we get a good estimation regime.

2. EXTENDED LUENBERGER OBSERVER (ELO)

This observer is a solution based on the use of an adaptive mechanism, in which the reference model is the induction motor, and the adjustable one is a Luenberger-type linear state observer. The output being both components of the stator currents in the unitary system of the stator measured for the first and estimated for the second. More than that, estimated rotor fluxes are used to realise the direct orientation after the rotor flux (DFOC)command (fig. 2). The equations of the Luenberger observer are those given by the relations (2) in which the matrixes A, B, L and C are those obtained within the preceding paragraph. The adaptive mechanism is deduced from the general expression (17), considering that, in this case we have:

$$e_y = \begin{bmatrix} i_{ds} - \hat{i}_{ds} \\ i_{qs} - \hat{i}_{qs} \\ 0 \\ 0 \end{bmatrix} = \begin{bmatrix} e_{yds} \\ e_{yqs} \\ 0 \\ 0 \end{bmatrix} \; ; \quad \hat{x} = \begin{bmatrix} \hat{i}_{ds} \\ \hat{i}_{qs} \\ \hat{\psi}_{dr} \\ \hat{\psi}_{qr} \end{bmatrix} \tag{18}$$

and the A_{er} is:

$$A_{er} = \frac{1}{\omega - \hat{\omega}} \cdot (A - \hat{A}) = \begin{bmatrix} 0 & 0 & 0 & a_{14} \\ 0 & 0 & -a_{14} & 0 \\ 0 & 0 & 0 & -1 \\ 0 & 0 & 1 & 0 \end{bmatrix} \tag{19}$$

Under these circumstances we obtain:

$$\hat{\omega} = k \int e_y^T \cdot A_{er} \cdot \hat{x} \cdot dt \tag{20}$$

Introducing in (40) the relations given by (18) and (19) we obtain:

$$\hat{\omega} = k \int \left[e_{yds} \cdot \hat{\psi}_{qr} - e_{yqs} \cdot \hat{\psi}_{dr} \right] \cdot dt \tag{21}$$

in which we considered the arbitrary character of the k constant. Within numerical implementation of the ELO algorithm, the relation (21) is computed by using one of the methods for numerical evaluation of the integral. Sometimes, instead of the adaptive law (21) a more complex form is used:

$$\hat{\omega} = k_p \cdot \left[e_{yds} \cdot \hat{\psi}_{qr} - e_{yqs} \cdot \hat{\psi}_{dr} \right] + k_i \int \left[e_{yds} \cdot \hat{\psi}_{qr} - e_{yqs} \cdot \hat{\psi}_{dr} \right] \cdot dt \tag{22}$$

in which appears a proportional component of the same expression that is integrated, from the need to have two coefficients to control the dynamic of the speed estimation.
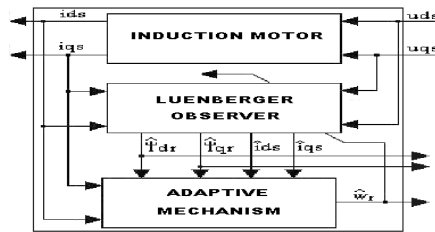
Fig . 2 . Extended Luenberger Observer

3. VECTORIAL SPEED CONTROLL SYSTEM

The block diagram of the control system of the mechanical angular speed ω_r of the induction motor [4] with a direct orientation after the rotor flux (dfoc) is presented in fig. 3. In figure 1 we marked with B2 the control block of the speed control system with direct orientation after the rotor flux (DFOC) and with B1 the extended Luenberger observer block (ELO). Some of the equations that define the vector control system are given by the elements which compose the field orientation block and consist of:

$$\begin{cases} u^*_{ds\lambda_r} = \dfrac{1}{b^*_{11}} \cdot \left[b^*_{11} \cdot v^*_{ds\lambda_r} - a^*_{13} \cdot |\psi_r| - a^*_{31} \cdot \dfrac{i^2_{qs\lambda_r}}{|\psi_r|} - z_p \cdot \omega_r \cdot i_{qs\lambda_r} \right] \\[2mm] u^*_{qs\lambda_r} = \dfrac{1}{b^*_{11}} \cdot \left[b^*_{11} \cdot v^*_{qs\lambda_r} + a^*_{14} \cdot z_p \cdot \omega_r \cdot |\psi_r| + a^*_{31} \cdot \dfrac{i_{ds\lambda_r} \cdot i_{qs\lambda_r}}{|\psi_r|} + z_p \cdot \omega_r \cdot i_{ds\lambda_r} \right] \end{cases} \tag{23}$$

PI flux regulator (PI_ψ) defined by the K_ψ proportionality constant and the T_ψ integration time:

$$\begin{cases} \dfrac{d x_6}{d t} = \psi^*_r - |\psi_r| \\[2mm] i^*_{ds\lambda_r} = \dfrac{K_\psi}{T_\psi} \cdot x_6 + K_\psi \cdot (\psi^*_r - |\psi_r|) \end{cases} \tag{24}$$

Couple PI regulator (PI_M_e) defined by the K_M proportionality constant and the T_M integration time:

$$\begin{cases} \dfrac{d x_7}{d t} = M^*_e - M_e \\[2mm] i^*_{qs\lambda_r} = \dfrac{K_M}{T_M} \cdot x_7 + K_M \cdot (M^*_e - M_e) \end{cases} \tag{25}$$

Mechanical angular speed PI regulator (PI_W) defined by the K_ω proportionality constant and the T_ω integration time:

$$\begin{cases} \dfrac{d x_8}{d t} = \omega^*_r - \omega_r \\[2mm] M^*_e = \dfrac{K_\omega}{T_\omega} \cdot x_8 + K_\omega \cdot (\omega^*_r - \omega_r) \end{cases} \tag{26}$$

Current PI regulator (PI_I) defined by the K_i proportionality constant and the T_i integration time:

$$\begin{cases} \dfrac{d x_9}{d t} = i^*_{ds\lambda_r} - i_{ds\lambda_r} \\[2mm] v^*_{ds\lambda_r} = \dfrac{K_i}{T_i} \cdot x_9 + K_i \cdot (i^*_{ds\lambda_r} - i_{ds\lambda_r}) \end{cases} \;;$$

$$\begin{cases} \dfrac{d x_{10}}{d t} = i^*_{qs\lambda_r} - i_{qs\lambda_r} \\[2mm] v^*_{qs\lambda_r} = \dfrac{K_i}{T_i} \cdot x_{10} + K_i \cdot (i^*_{qs\lambda_r} - i_{qs\lambda_r}) \end{cases} \tag{27}$$

The calcules of the couple block (C_1M_e):

$$M_e = K_a \cdot |\psi_r| \cdot i_{qs\lambda_r} \tag{28}$$

Flux analyser (AF):

$$\begin{cases} |\psi_r| = \sqrt{\widehat{\psi}^2_{dr} + \widehat{\psi}^2_{qr}} \\[2mm] \sin \lambda_r = \dfrac{\widehat{\psi}_{qr}}{|\psi_r|} \;;\; \cos \lambda_r = \dfrac{\widehat{\psi}_{dr}}{|\psi_r|} \end{cases} \tag{29}$$

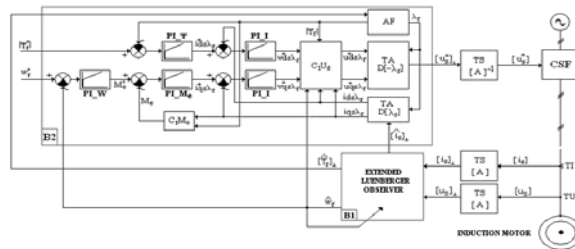Fig. 3. The block diagram of the DFCO

4. THE VECTORIAL CONTROL SYSTEM FOR ABB IRB 140 ROBOT

The vectorial control system of the ABB robot's position is based on the vectorial speed control to wich a position loop is added around a PD (**P**roportional **D**iferential) regulator wich has the following transfer function:

$$G_\theta(s) = K_\theta \cdot (1 + T_\theta \cdot s) \tag{30}$$

where: K_θ is the proportionality coefficien, T_θ is the time differentiating constant of the regulator. To show the role and performances of the tunig system shown above, we will present in the following part, the studied industrial robot. In figure 4 the ABB IRB 140 robot with 6 axis (Fig . 5) as part of Computer Integrated Manufacturing System from our Universty is presented. The extreme positions (Fig. 6) of the robot arm ABB IRB 140 define the maximum possible workspace [5].

Fig .4. ABB IRB 140 Robot   Fig. 5. ABB IRB 140 Axis
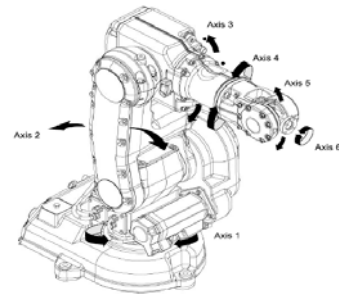
Positions at wrist center (mm) and Angle (degrees) for ABB IRB 140 robot is listed in table 1. For an in dept and clear analasys of the robot we used Matlab – Simulink [6] to create the mathematical model in dynamic mode of the robot presented above. So, in figure 7 the Simulink block that implements this type of robot is presented, together with it's mathematical model. The defining ecuations for the mathemathical model are:

$$T_1 = J_1 \cdot \frac{d^2\theta_1}{dt^2} + C_1 \cdot \frac{d\theta_1}{dt} + G_1 \cdot \theta_1 \tag{31}$$

$$T_2 = J_2 \cdot \frac{d^2\theta_2}{dt^2} + C_2 \cdot \frac{d\theta_2}{dt} + G_2 \cdot \theta_2 \tag{32}$$

where: J_1 and J_2 are the inertia moments of the joints one and two; C_1 and C_2 are the Coriolis coefficients of joints one and two, G_1 and G_2 are the gravitational coefficients of the two joints. In the mathematical model we considered joint 0 stationary so that $\theta_0 = 0\,[grade]$. Alfa$_1$ and alfa$_2$ are the accelerations of the two joints; w_1 and w_2 are the speeds of the two joints and teta$_1$, teta$_2$ the two joint's angles wich are shown in fig. 7. In the folowing we present the Simulink schemathic for the position's regulation system's analisis of the ABB industrial robot.
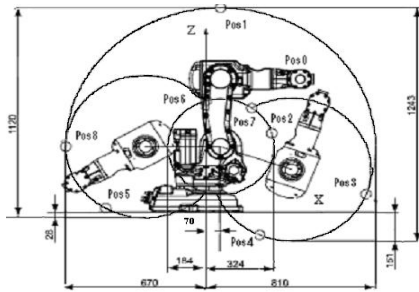
Pos. No . (Fig. 6.)	Pos.(mm) X	Pos.(mm) Z	Angle(deg- rees)Axis2	Angle(de g- rees)Axis 3
0	450	712	0	0
1	70	1092	0	-90
2	314	421	0	+50
3	765	99	110	-90
6	1	596	-90	+50
7	218	558	110	-230
8	-670	352	-90	-90

Fig. 6. ABB IRB 140 robot arms positions   Table 1. Positions and Angles for ABB IRB 140
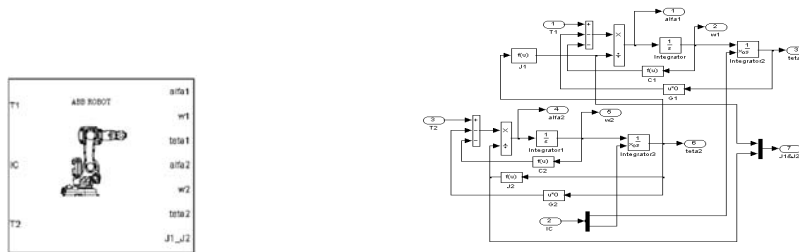
Fig. 7. Mathematical model in Matlab – Simulink

From the sismulation schemathic we notice that two systems of position regulation are used designed around the vectorial speed control systems, refered to as SRA1 si SRA2. The automated regulator type PD of the position presented in the simulation schematic in the previous figure was implemented outside of the block schematic of SRA1 and of SRA2. In the simulation, we took into consideration the mechanical speed reduction used by joints one and two of the ABB robot. The reduction coefficient for both of the joints is 1/130.
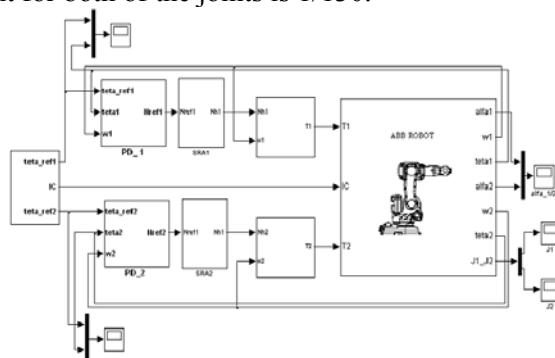
Fig. 8. Matlab – Simulink simulation schematic of the ABB IRB 140 robot

In the simulation we created a trajectory generating block, where we imposed a variation of the angle θ_1 between $\left(-\frac{\pi}{6} \quad \frac{\pi}{6} \right)$ and of the angle θ_2 between $\left(-\frac{\pi}{4} \quad \frac{\pi}{4} \right)$. After simulating we get the folowing results, presented in graphical form in the figures 9 and 10.
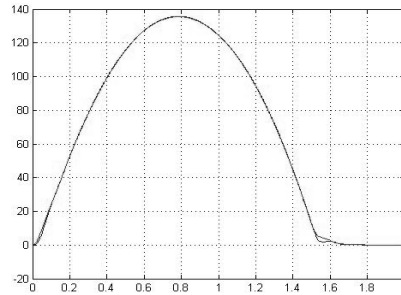
Fig. 9. Variation in time of the imposed speed and the estimated
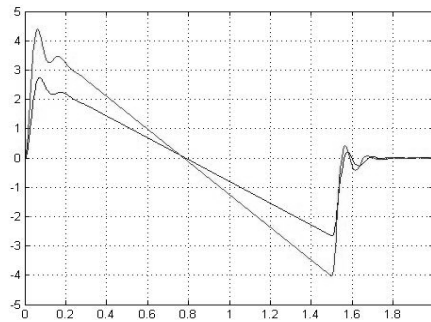
Fig. 10. Accelerations of joints

REFERENCES

[1]. **Luenberger, D.G**. : *An induction to observers*, IEEE Trans. On Automatic
     Control, vol.AC.-16, no.6, pp.596-602, December 1971.
[2]. **Cohen, G.,** *Théorie algébrique des systèmes à événiments discrets*, Centre
      Automatique et Système, École des Mines de Paris, Fontainbleau & INRI
      Rocquencourt, 1995.
[3]. **Popov, V.M**.: *L'hyperstabilite des système automatiques* , Dunod, Paris, 1973.
[4]. **Kubota, H., Matsuse, K., Nakano T**.: *DSP – based speed adaptive flux observer
      of induction motor*, IEEE Trans. of Industry Applications, vol.29, no2.,
       pp. 344-348, 1993.
[5]. **Murphy, R**.:*Introduction to AI Robotics,* MIT Press, 2000.
[6]. Pana, T.: *Matlab in sisteme de actionare electrica,* Ed.Mediamira,
      Cluj-Napoca, Romania, 1996.

WIND ENERGY - A SUSTAINABLE SOLUTION FOR THE ECONOMIC REHABILITATION OF THE TURCOAIA QUARRY AREA

ADRIAN NICOLAE DINOIU [1] EMIL POP [2]
IOANA CAMELIA BARBU [3] ILIE CIPRIAN JITEA [4]

Abstract: Renewable energy technologies are clean sources of energy that have a much lower environmental impact than conventional energy technologies. Renewable energy will not run out. Ever. So, with a good wind potential, Turcoaia area can have an economic rehabilitation through implementation of wind energy and transformation of negative impact on the environment in a positive impact.

Key words: renewable, wind, energy, Turcoaia, quarry, environment, modeling, simulation.

1. OVERVIEW OF TURCOAIA AREA [1] [2]

Turcoaia village is situated in the north-west of Tulcea county, on the right bank of the Danube. Distance from Tulcea is 64 km. Turcoaia village has a temperate continental climate with sub-Mediterranean influences, summers are hot with low precipitations and mild winters with strong winds. Its area is 56.51 km^2, with a population of 3695 inhabitants (census 2002), location 45 ° 07' N 28 ° 11'E. Area specific activities: agriculture, fisheries, quarries stone operation, transportation, forestry.

On the administrative territory of the commune Turcoaia, were two quarries: Quarry Iacob Deal, the largest in the country and Turcoaia quarry called Fantana lui Manole. Currently only Turcoaia quarry working anymore.

---

[1] *Ph.D. Student Eng., University of Petrosani*
[2] *Ph.D. Professor Eng., University of Petrosani*
[3] *Ph.D. Lecturer Eng., University of Petrosani*
[4] *Eng., INCD INSEMEX Petrosani*

Information about the role that quarries had in the developmental economic activity of Turcoaia and the negative impact it has on the environment are achieved through a series of geographical research methods and processes: *indirect geographic observation* by analyzing topographic and administrative territory map and *direct* through which we were informed of the danger it represents dumps for land and houses at the foot of Jacob Deal; *geographical description*, with which we saw the results of the observation and a picture of the activity of both quarries and their effects, analysis and synthesis used to highlight the evolution of them.

Macin Mountains are a mountain group belonging to the Dobrogea mountains. These mountains are the most obvious residual witness of the late Paleozoic orogenesis hercinic looking for Inselberg. Overall shape of a triangle with sharp, Macin Mountains are the largest width between the village Turcoaia and Lozova valley, which reach 24 km. They take place in the direction NW-SE direction in the form of parallel ridges, becoming more numerous and fragmented in the SW, with a main peak, starting in Bugeac and up on Carpelit Hill.

Fig. 1. Victoria Peak, view from Turcoaia

This main mountain chain culminates with Tutuiatu top height (467m). In its extension to the North West tip is Pietrosul Mare (426 m) and peak Pietrosu and heights decrease gradually, reaching 100-170 m near the town Văcăreni and Bugeac at 95m. Southeast of the tip Tutuiatu, Macin Mountains main ridge continues through a series of hilly peaks, as Costiag Hill (428m), Hill Negoiu with the top Piatra Mare (380 m), David Hill (354 m), Crapcea Hill (344 m), Carapcea Hill and Carpelit Hill (350 m).

The climate regime is temperate where summers are dry and winters are cold and lack of moisture. The average annual temperature varies between 10,5 °C and 11 °C. Summer, in July, average temperatures is 22 °C and in winter, in January, the average temperature value is -1,5 °C. Absolute maximum was recorded in 1968 at Jurilovca of 38 °C.

2. RENEWABLE ENERGY [3] [10]

Wind energy - both on the ground and at sea, the wind has the power to generate energy. Based on the evaluation and interpretation of data recorded, it follows that in Romania, we can set up wind turbines with a total power of up to 14,000 MW, which means a power input of about 23,000 GWh / year.

Solar Energy - It is an inexhaustible energy and therefore renewable. If we exploit the full potential of solar in our country, we can substitute in this form about 50% of domestic hot water or 15% share of heat for heating current.

Hydro Energy - Another renewable energy that Romania's hydropower potential is huge. Water is one of the most precious natural resources. Water is at the same time and the best source for green energy. At present, Romania's hydropower potential is exploited at a rate of 48%.

Biomass - fuel being used primarily for space and water heating and cooking. Fully exploiting the potential of biomass involves using a fully residues of forestry, sawdust and other wood waste, agricultural waste from grain or corn stalks, vine plant debris, waste and urban waste.

Geothermal energy is suitable for space heating and water. Due to its location, the main potential use is in rural areas - housing, greenhouses, aquaculture - at distances up to 35 km from the place of removal.
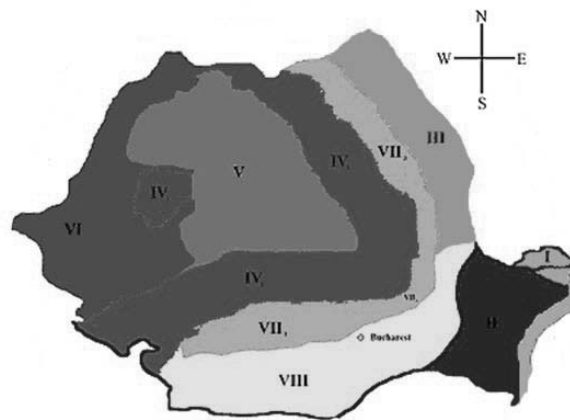
Fig. 2. Map of renewable resources (*Source: MEF*)

Legend:
I. Danube Delta (solar energy);
II. Dobrogea (solar and wind);
III. Moldova (plain and plateau - micro hydro, wind and biomass);
IV. Carpathian Mountains (biomass, micro hydro, wind);
V. Transylvanian Plateau (microhydro);
VI. Western Plain (geothermal energy);
VII. Subcarpathian (biomass, micro hydro);
VIII. South Plains (biomass, geothermal and solar energy).

2.1. Wind power [9] [11]

Wind power is the conversion of wind energy into a useful form, such as electricity, using wind turbines. In windmills, wind energy is directly used for milling grain and pumping water. At the end of 2011 globally are installed nearly 238 GW. Only in 2011 were installed 40.5 GW by wind turbines.

Wind energy is produced in large wind farms connected to the network, but also by individual turbines used for power generation in remote areas.

Advantages:
- The main advantage of wind energy is zero emission of pollutants and greenhouse gases, because no fuels are combusted;
- No waste is produced. Production of wind energy production does not involve any kind of a waste;
- Lower cost per unit of energy produced. The cost of electricity in modern wind power has decreased substantially in recent years.

Disadvantages:
- A practical disadvantage is the variation of the wind speed. Many places on Earth cannot produce enough electricity using wind power and because of this wind is not viable in any location;
- "Visual pollution" - an unpleasant appearance - and also produce "noise pollution" (too noisy). Others argue that the turbines affect the environment and surrounding ecosystems, killing birds and large vacant land for installation.

2.2. Wind power potential [4] [7] [8] [12]

To its geographic location, with wide open horizon to NE, E, SE, S, SW and W, in the studied area, characteristic of atmospheric dynamics is to be very active during the year.

As the origin of air masses, contributing to the winds in this area, we mention the following:
- in N winds are a result of the movement of polar air masses of continental origin, cold and wet;
- they are followed by NE and E winds that originate in dry continental air masses, moving from north-eastern Europe;
- S and SE winds generated by tropical continental air masses, usually hot and dry air with high prevalence in the late spring and early summer (29% and 13% respectively);
- SW and W winds will generated by air masses of tropical origin - Maritime (Azores anticyclone) that occur in the months of spring, summer and early autumn;
- NW winds generated by air masses of polar origin - sea, cold and wet, have lower frequency (7%) was significantly greater than the frequency in the summer months (32% in august), while contributing to increased producing rainfalls.

Prevailing winds are from the north, approx. 22%, plus those in the NE and NW. Winds from south, south east and west are rare frequency, but higher intensity.
The moderate winds have the highest frequency (speed between 3-6 m/s), approx. 57%, followed by weaknesses (speed below 3 m/s), approx. 18-35%.

Kinetic energy of wind intercepted by the blades of a turbine unit of time (P) depends on air density (ρ), the area covered by the rotor blades (πr^2), and the cube of wind speed (V^3), reduced by a factor of power efficiency (f_p) according to the formula:

$$P = 0,5*\rho*\pi*r^2 f_p*V^3 \qquad (1)$$

Proposed wind turbine type is Vestas V90-3.0 MW. Has a capacity of 3 MW and is designed to be low weight, making it easier to transport and install and reducing foundation costs thanks to its lower load.

Its innovative nacelle is lighter because its gearbox has an integrated main bearing that eliminates the need for a traditional main shaft. Blade weight is also kept to a minimum by using carbon together with glass fiber. The tower is lighter, too, as it uses magnets instead of welding to attach the tower internals to the tower wall.

This turbine delivers exceptional performance and a high yield, and can be supplied in a variety of hub heights (65-105m) to accommodate site-specific needs. Rotor diameter is 90 m and Swept area: 6362 m^2

If we know wind speeds at a height of 10 m, we can calculate wind speed at 80 meters height (2), average height at which you can install the nacelle.

$$V = V_0*(H/H_0)^\alpha \qquad (2)$$

where,
V – wind speed at 80m;
V_0 – wind speed at 10m;
H – proposed height (80m);
H_0 – original height (10m);
α – wind shear coefficient, equal with 0,14 for plan surface.
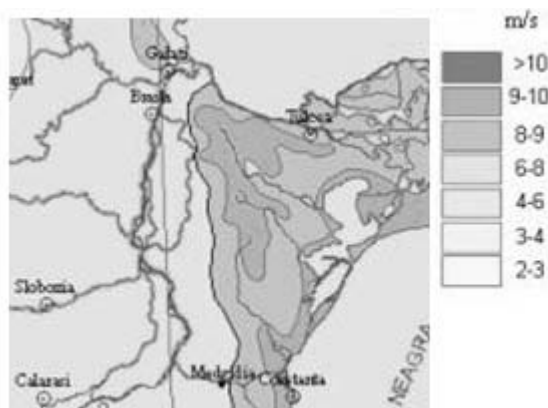

In the table 1 are average monthly values of temperature, relative humidity, solar radiation, atmospheric pressure, wind speed at 10m, calculated wind speed at 80m and available power at 80m considering the V90 turbine characteristics.

Fig. 3. Wind speed at 50m height

Month	Temperature	Relative humidity	Solar radiation	Atmospheric pressure	Wind speed (10m)	Wind speed (80m)	Produced power (80m)
	°C	%	kWh/m^2	kPa	m/s	m/s	kW
January	-0,6	76	1,45	100,9	5,5	7,4	760,8
February	0,4	73	2,24	100,7	5,4	7,2	720,1
March	5,1	66	3,21	100,6	5,9	7,9	939,2
April	11,6	58	4,33	100,2	5,0	6,7	571,6
May	17,5	53	5,56	100,3	4,3	5,8	363,6
June	21,4	54	5,92	100,1	4,2	5,6	338,8
July	24,0	51	5,96	100,1	3,8	5,1	250,9
August	23,6	50	5,27	100,2	3,8	5,1	250,9
September	18,8	54	3,96	100,4	4,2	5,6	338,8
October	12,9	60	2,54	100,8	5,4	7,2	720,1
November	5,7	72	1,49	100,8	5,3	7,1	680,8
December	0.6	75	1,15	100,9	5,6	7,5	803,1
Annually	11.8	62	3,59	100,5	4,9	6,6	538,0

Table 1. Atmospherically conditions

3. TRANSFORMATION OF NEGATIVE IMPACT ON THE ENVIRONMENT IN A POSITIVE IMPACT BY CREATING A WIND FARM [5] [6]

The current land use is tailings deposition. Potential failure to achieve future wind farms is under related natural resources.

Potential development is related of existing infrastructure: drinking water networks, sewage networks, the existing road communication paths in the area.

Without implementation, studied site will retain the current use being operated incorrectly and mismatch with actual intent regarding sustainable development and the needs of the village Turcoaia current economic recovery of resources in the area, namely the potential wind in the area.

Biodiversity:

- *Flora of the site* : Arrangement of vegetation in the area considered for the location of wind farm, varies depending on the action of climatic factors. Level of exposure to wind direction and consequently its dominant amount of moisture in the soil are the main factors that determined the qualitative composition of steppe vegetation on the site.

- *Fauna in the site* : Steppe and forest steppe fauna that characterize the locality Turcoaia is represented by specific rodent species: ground squirrel (Spermophilus citellus) orbetele (Spalax graecus), small hamsters (Mesocricetus newtons), steppe polecat (Mustela Eversmann) present only in Dobrogea, plus reptiles: Dobrogea lizard (Podarcis taurica), Guster (Lacerta viridis), horned viper (Vipera ammodytes Alpine), land turtle (Testudo graeca), insects (locusts, crickets).

Impact on biodiversity:

- *During construction works* : Impact on local biodiversity during construction objective is manifested mainly due to scraping for the construction of towers, foundations, access roads, the dust produced by construction work and noise due to machinery used. Construction of the wind farm will not affect the integrity of Macin Mountains National Park, being at its limit. Should also be noted that much of the effects on local biodiversity are temporary and reversible, manifesting only during construction.

Estimated impact of environmental factors air:

- *During the implementation plan*: Emission sources of air pollutants are ground sources, open (those that involve handling construction materials and soil tillage) and mobile (machinery and trucks).

For ground handling operations, ballast and cement materials and related disturbance on the embankment surface are sources of dust emission.

- *During operation*: the objective there sources of air pollution during operation objective.

Impact on the soil and subsoil

- *During construction works*: Regarding the impact it can have on soil and subsoil studied activity, it is recalled that the works will have a limited period of execution time. With topsoil stripping, with storage of part, remove the natural cycle, the amount of nutrients. A part of it will be restored, this circuit as ground vegetation layer deposited will be used to rehabilitate land, including soil cover, where it will lend. In this project is minimal scraping possible, with little impact on the ground.

- *During operation*: After construction, the wind turbine will not produce pollution on soil and subsoil.

Recommendations:

- Wind power blade tips will be painted in bright colors to avoid their hitting by birds.
- Towers will be indicated by flashing red light, with a long delay between two ignitions.
- It is forbidden to store equipment or motor vehicles on green spaces, except for the site organization.
- Fertile soil restoration of affected areas, from the tower, so that no non-integrated land remains in agricultural use outside the project provided.
- Placing turbines will be limited so the site perimeter, noise and vibration to the limits imposed by standards.
- Fire prevention activities must be supported by appropriate measures according to the legislation and manufacturers recommendations.
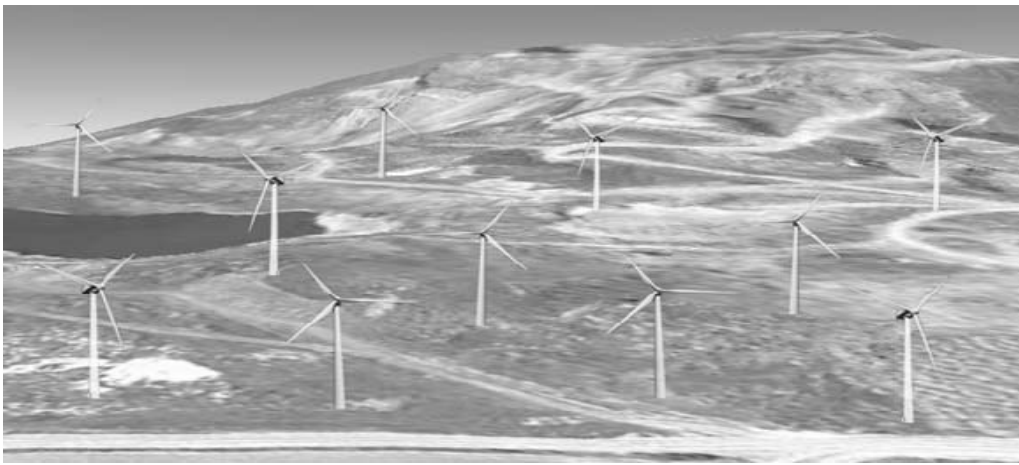
Fig. 4. An overview of proposed wind farm in Turcoaia

4. MODELING AND SIMULATION OF WIND TURBINE VESTAS V90 [7] [8]

We know from V90 product brochure that blade length (R) is 44 m, swept area (A_r) is 6362 m^2 and nominal revolutions (ω_T) 966 rad/s. Also we know the wind speed (W_s) at 80 m (Table 1) and air density (ρ) for the Turcoaia area equal with 1,225 kg/m^3. So we can calculate the blade tip speed ratio (λ):

$$\lambda = (\omega_T * R) / Ws \qquad (3)$$

Now, if we know λ, we can calculate the power coefficient (C_p) which depends of the blade tip speed ratio (λ) and the pitch angle (β). Usually, optimal, the pitch angle is 0,18 so, we will use with that value. The Betz's law, tell us that C_p maximum value is 0,59, but in practice is between 0,2 and 0,4.

$$C_p(\lambda,\beta)= (0{,}44-0{,}0167*\beta)*\sin\{[\pi*(-3+\lambda)]/(15-0{,}3*\beta)\}- $$
$$- 0{,}00184*(-3+\lambda)*\beta \qquad (4)$$

The mechanical power on the shaft of turbine is:

$$P = 0{,}5 * \rho * A_{r\,*} C_p * W_s^{3} \qquad (5)$$

The modeling of wind turbine V90 in MATLAB Simulink is presented in figure (5) and the simulation in figure (6).
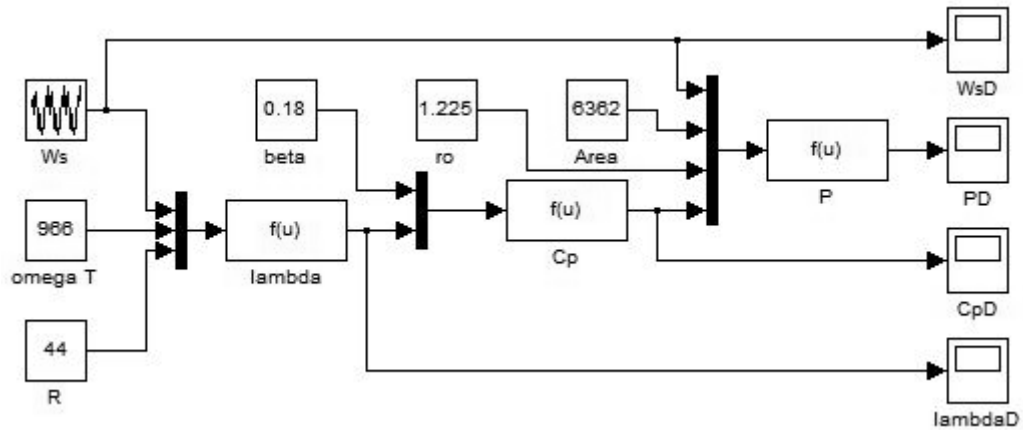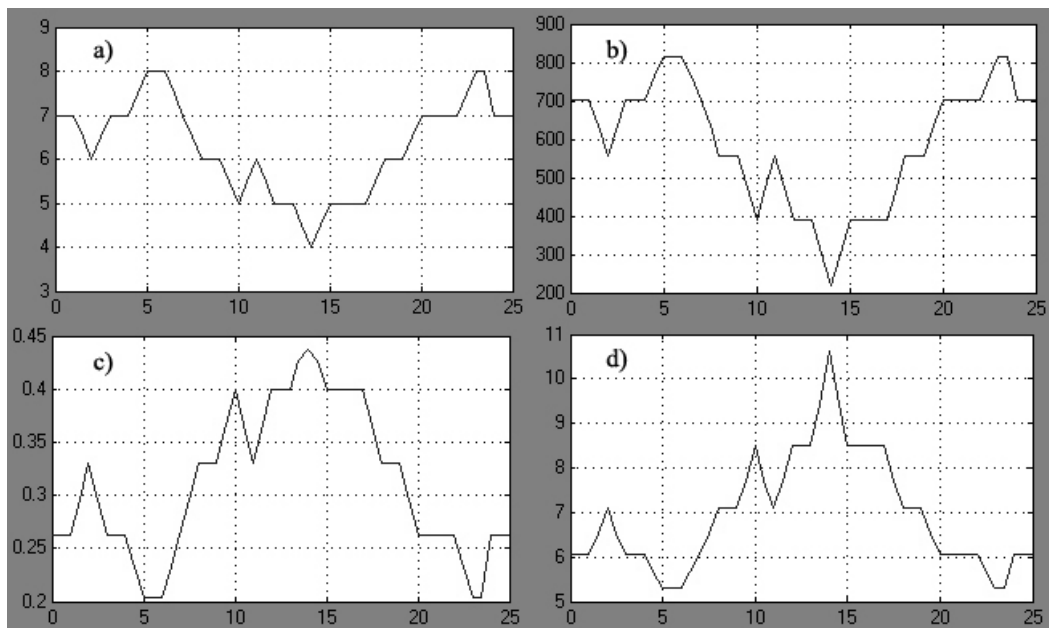
Fig. 5. V90's MATLAB Simulink model

Fig. 6. a) W_s – Wind speed; b) P – Mechanical power; c) Cp – Power coefficient; d) λ – Tip speed ratio.

5. CONCLUSIONS

The beneficial effect of producing electricity through clean methods cannot be disputed, because this method ensures energy production eliminating specific emissions of other methods.

Wind turbines do not produce any pollution on the environment during operation because wind energy is green energy.

Location area will not affect significantly flora and fauna in protected areas (parks, reserves and so on).

Sitting wind turbines in the vicinity of human settlements is recommended in the literature as migratory birds usually avoid this area and nesting and feeding areas are chosen outside inhabited areas.

Wind turbines have a positive landscape and contribute to the local economy.

REFERENCES

[1]. http://turcoaia-online.webs.com/

[2]. http://ro.wikipedia.org/wiki/Mun%C8%9Bii_M%C4%83cin

[3]. Barbu I. C, Pop E., Leba M. – Microsisteme energetice durabile regenerative, Editura Didactica si pedagogica, Bucuresti, 2009

[4]. http://eosweb.larc.nasa.gov/sse/RETScreen/

[5]. Petrescu T. - studiu de impact asupra mediului - Parc eolian comuna Cerna, Judetul Tulcea

[6]. Petrescu T. – Raport de mediu – Construire parc de centrale eoliene si retele electrice de racordare – sud II

[7]. Zobaa A., Bansal R. - Handbook of Renewable Energy technology, World Scientific Publishing Co. Pte. Ltd., 2011

[8]. http://www.vestas.com/en/media/brochures.aspx

[9]. http://en.wikipedia.org/wiki/Wind_power

[10]. http://en.wikipedia.org/wiki/Renewable_energy

[11]. REN21 - Renewables 2012 Global Status Report, 2012

[12]. S.C. IPROMIN S.A. Bucuresti - Studiul de evaluare adecvata deschidere carierei de piatra Valea lui Manole comuna Turcoaia, judetul Tulcea

ROMANIA'S ENERGY POLICY AND SUSTAINABLE DEVELOPMENT ALIGNED TO EU DIRECTIVES

SUSANA ARAD [1]

Abstract: *A safety increase in the energy supply and limiting the energy resources importation in the circumstances of an accelerated economic development can be insured through a strategy to develop Romania's energy development. This requirement can be achieved on the one hand, through the deployment of a policy supported by energy conservation, energetic efficieny increase which leads to disconnecting the economic development rythm and the evolution of energy consumption and on the other hand increase of the renewable energy resources efficiency. Developing the renewable energy resources potential gives real premisses to achieve strategical goals regarding the increase of safety in energy supply by varying the sources and decreasing the percentage of energy resources importation and developing on the long run the energetic department and protecting the environment. In this paper we present a study regarding the strategic goals on the short, medium and long run and the development level, the use and the potential of energy sources.*

Keywords: *energy, sustainable development, efficiency, renewable sources, CCS.*

1. INTRODUCTION

The Romanian energetic sector has to be a dynamic sector, which should actively support the economic development of the country and cutting down on the deviations towards the European Union. For that purpose, the main objective of the strategy of the energetic sector is complying with the required quantity of energy in the present as well as on the medium and long run at a price as low as possible, fit for a modern market economy and a civilized lifestyle standard, in quality conditions, safe supply and keeping the sustainable development principles.

According to New Energy Policy of the European Union (EU) [1] developed in 2007, energy is an essential element for the development of the Union. But equally, it is a challenge regarding the impact of the energy sector on climate changes, increasing dependence on imported energy resources and increasing energy prices.

---

[1] *PhD. Associate Professor Eng. University of Petrosani*

To overcome these challenges, the European Commission (EC) considers absolutely necessary for the EU to promote a common energy policy based on energy security, sustainable development and competitiveness.

The Commission recognizes the importance of fossil fuels and especially coal contribution to energy security. At the same time, the Commission emphasizes that future use of coal, especially, must be compatible with the objectives of sustainable development and climate change policy [6].

Total global energy demand in 2030 will be about 50% higher than in 2003, and oil is about 46% higher. Certain known oil reserves can sustain current levels of consumption only until 2040, and the gas until 2070, while global coal reserves provide for more than 200 years even an increase of operation.

Projections indicate growth, which will require increased energy consumption. In terms of the structure of primary energy consumption worldwide, evolution and prognosis of reference made by the International Energy Agency (IEA) shows the fastest growth over the next decade the share of renewable, and natural gas.

It is estimated that about a quarter of primary energy needs, globally, will be covered by the coal. While increasing energy and coal consumption will increase. Data from the World Energy Council (WEC) shows an increase of nearly 50% of global coal extraction in 2005 than in 1980. Figure 1 is highlighted developments in energy demand worldwide.

The Commission recognizes the importance of fossil fuels and especially coal contribution to energy security. At the same time, the Commission emphasizes that future use of coal, especially, must be compatible with the objectives of sustainable development and climate change policy.

Total global energy demand in 2030 will be about 50% higher than in 2003, and oil is about 46% higher. Certain known oil reserves can sustain current levels of consumption only until 2040, and the gas until 2070, while global coal reserves provide for more than 200 years even an increase of operation.

Projections indicate growth, which will require increased energy consumption. In terms of the structure of primary energy consumption worldwide, evolution and prognosis of reference made by the International Energy Agency (IEA) shows the fastest growth over the next decade the share of renewable, and natural gas.
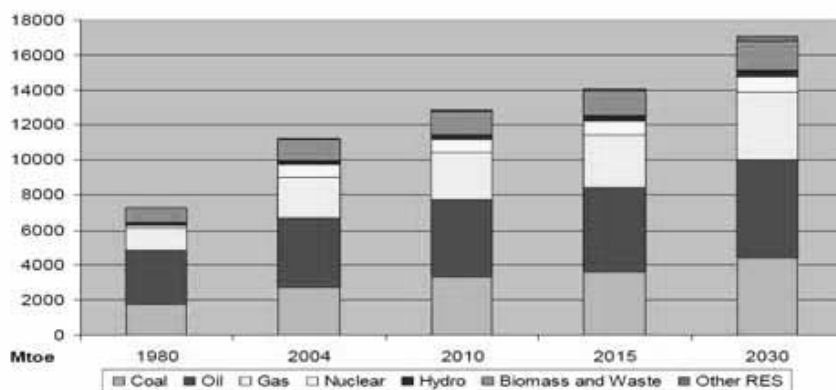

Fig. 1. The evolution of global energy demand (Source: *WEO 2006, OECD/IEA 2006)*

It is estimated that about a quarter of primary energy needs, globally, will be covered by the coal. While increasing energy and coal consumption will increase. Data from the World Energy Council (WEC) shows an increase of nearly 50% of global coal extraction in 2005 than in 1980. Figure 1 is highlighted developments in energy demand worldwide.

2. THE PRIORITY OBJECTIVES OF DEVELOPING THE ROMANIAN ENERGETIC SECTOR

Romania's energy strategy complies policy directions set out in the EU and contribute to achieving the targets set by the European Commission for all EU states.

Regarding the security of energy supply, the EU expects natural gas import dependency to increase from 57% currently to 84% in 2030 and oil from 82% to 93% for the same period [5].

One of the priority elements of the energy strategy is improving the energy efficiency. Increasing energy efficiency is a major contribution to achieving security of supply, sustainability and competitiveness, saving primary energy resources and reducing greenhouse gas emissions. Representative synthetic indicator regarding the efficiency of energy utilization at national level is energy intensity, or energy to produce a unit of GDP.

Improving energy efficiency is one of the most important strategic objectives for Romania, given that in the structure of the national economy and especially the industry there are still activities using energy resources as raw materials, mainly petrochemicals and fertilizers industry.

Energy intensity is a global indicator which allows the association of a country's energy consumption to the economic activities in the country. The report that expresses the energy intensity is directly proportional to the physical records (annual energy consumption) and inversely proportional to monetary records.

To measure the time variation of the energy intensity of a country the annual values of GDP expressed in constant national currency of the country (Gross Domestic Product at current prices and inflation corrected) can be used.

In terms of sustainable development, it should be noted that, in 2007, the energy sector is, in the EU, one of the main producers of greenhouse gases.

If drastic measures are not taken in the EU, with the current rate of energy consumption evolution and existing technologies in 2007, greenhouse gases emissions will increase in the EU by about 5% and about 55% globally by 2030. Nuclear power is currently one of Europe's largest renewable energy without CO_2 emissions. Nuclear power plants provide in 2007 a third of EU electricity production, thus having a real contribution to sustainable development.

In terms of competitiveness, the EU internal energy market ensures the establishment of fair and competitive prices for energy encourages energy savings and attracts investments in the sector [5].

The EU is becoming increasingly exposed to instability and rising prices on international energy markets and to the consequences of the oil reserves becoming

gradually monopolized by a small number of owners. Potential effects are significant: for example, if the oil price rises to 100 USD / barrel in 2030, energy imports in the EU-27 would cost about 170 billion EUR, which means a value of 350 EUR / year for each EU citizen.

European Commission proposes in the set of documents that are the New EU Energy Policy the following objectives:
- reduction of greenhouse gas emissions by 20% by 2020 compared to those in 1990;
- increasing the share of renewable energy in the total energy mix from less than 7% in 2006, to 20% of total EU energy consumption by 2020;
- increasing the share of bio-fuels to at least 10% of the energy content of transport fuels by 2020;
- reduction of global primary energy consumption by 20% by 2020.

On October 19th 2006, the EC adopted the Energy Efficiency Action Plan, afferent to the Directive 2006/32/EC on energy end-use efficiency and energy services, containing measures with which the EU could make measurable progress towards achieving its main objective, namely reducing its global primary energy consumption by 20% by 2020 [2].

Successful implementation of this plan would materialize in the EU as a reduction of energy consumption in 2020 to about 13% currently (2007).

3. THE IMPACT ON THE ENVIRONMENT

The energy sector is a major source of pollution as a result of extraction, processing and combustion of fossil fuels. In 2005, the burning fuel for energy production resulted in about 88% of total national emissions of NOx, 90% of SO2 and 72% of the particulate matter released into the atmosphere.

In the context of EU accession the Directive 2001/80/EC regarding large combustion plants has been transposed into the Romanian legislation and it's being implemented. Large combustion plants were inventoried, of which 78 must be in line with the requirements of environmental regulations, installments, until 2017.

Also Landfill Directive 1999/31/EC was transposed into Romanian legislation. Under these conditions, 20 landfill (ash and slag heaps in the energy industry that uses plant-based "hydro-transport") will be retrofitted to comply with environmental requirements until 2013.

It is known that all plants burning fossil fuels produce CO_2, which is the main cause of global warming. To maintain the important role of fossil fuels in the energy balance, solutions must be identified and implemented to reduce the impact of using these fuels on the environment. In this sense, the solution of capturing and storing the CO_2 (CCS) emissions will have to be considered when designing and building new power plants. At the same time, the current coal combustion technology will have to be replaced with clean technologies substantially mitigating pollution by significantly reducing emissions of SO_2 and NOx and particulate matter generated by coal-fired boilers [3].

Impact on the environment through the application of energy efficiency policies can be characterized by:

- emissions reduction in general and greenhouse gas emissions (CO_2), in particular; it is estimated, thus, the reduction by 4-7 million tones of CO_2 emissions per year by using fuel, harnessing this potential being an important source of funding;
- locally reducing environmental impact, both at the production and consumption of energy;
- pollution of surface and groundwater reduction by avoiding discharge of large quantities of wastewater from fuel production to the end user;
- soil pollution reduction by reducing large quantities of slag and ash deposited with electricity producers and/or heat energy.

A country's energy intensity is the ratio of the total energy consumption and GDP. Depending on the total considered consumption there can be determined:
- primary energy intensity by considering the total primary resources consumption;
- final energy intensity, by considering the total final consumption;
- electricity intensity by considering the final electricity consumption.

4. THE RENEWABLE ENERGY RESOURCES POTENTIAL

Theoretical potential of Renewable Energy (RES) in Romania is presented in Table 1 [4].

The available potential of these sources is much smaller due to technological limitations, economic efficiency and environmental restrictions [7].

Tabel 1. **Energy potential of renewable energy in Romania**

Source	Yearly energy potential	Economic equivalent energy (thousand toe)	Application
Solar energy	60x10^6 GJ 1.200 GWh	1.433,0 103,2	heat electricity
Wind energy (theoretical potential)	23.000 GWh	1.978,0	electricity
Hydro energy of which < 10 MW	40.000 GWh 6.000 GWh	516,0	electricity
Biomass and biogas	318x10^6 GJ	7.597,0	heat electricity
Geothermal energy	7x10^6 GJ	167,0	heat

Effective harnessed potential of wind energy and hydropower is significantly inferior to the technical harnessed one due to environmental restrictions (sites with prohibition of use).

It is necessary to devise studies on the impact of wind turbines on bird migration and defining a clear and unique map of areas where the construction of wind and hydropower units is not suitable for environmental reasons.

Use of renewable energy sources has a significant impact on the national power system and there is needed:

- Studies on the impact of taking over the power carried by wind turbines, micro hydro and cogeneration using biomass by the electricity transmission and distribution network (voltages $\geq$ to 110 kV) in different scenarios, in areas with high potential;
- The development of transport and distribution networks into a smart grid concept;
- Construction of new electricity generating capacity with high flexibility in operation and market development capabilities to counter and/or to limit the negative effects of uncontrollable variability of wind and micro hydro energy.

5. ZERO EMISSION SOLUTIONS TO THE GLOBAL CLIMATE CHALLENGE

Carbon Capture and Storage CCS is a process that consists of separating and recovering carbon dioxide (CO_2) from flue gases at large power or industry installations, then transporting it and injection it into a deep underground geological formation for storage. CO_2 is the major greenhouse gas contributing to global worming. All combustions of fossil fuels like gas, oil and coal generate CO_2 emissions that accumulate in the atmosphere and increase the greenhouse effect [8].

The first approach for reduction in CO_2 emissions focuses on the technology mix. No single form of power generation will address the dual challenge of securing the supply of reliable and affordable energy and affecting a rapid transformation to a low-carbon system of energy supply. It will take all types of generation technologies such as nuclear and renewable.

The second approach for CO2 reductions is that of production efficiency and energy management. In this field it must look to solutions for both new and existing plants. With 60% of the total of CO2 emissions in 2030 coming from plants that exist today, solutions must continue to be developed and implemented that increase their efficiency and enabled smart generation.

CO2 Capture and storage CCS describes a technological process by which at least of 90% CO2 is captured from large stationary sources transported to a suitable storage site then stored in geological formations deep underground. In the Figure 2 is shown the CCS process.

Founded in 2005 on the initiative of European Commission, the European Technology Platform for Zero Emission Fossil Fuel Power Plants (known as the Zero Emission Platform, or ZEP) represents a unique coalition of stakeholders united in their support for CO2 Capture and Storage (CCS) as a critical solution for combating climate change.
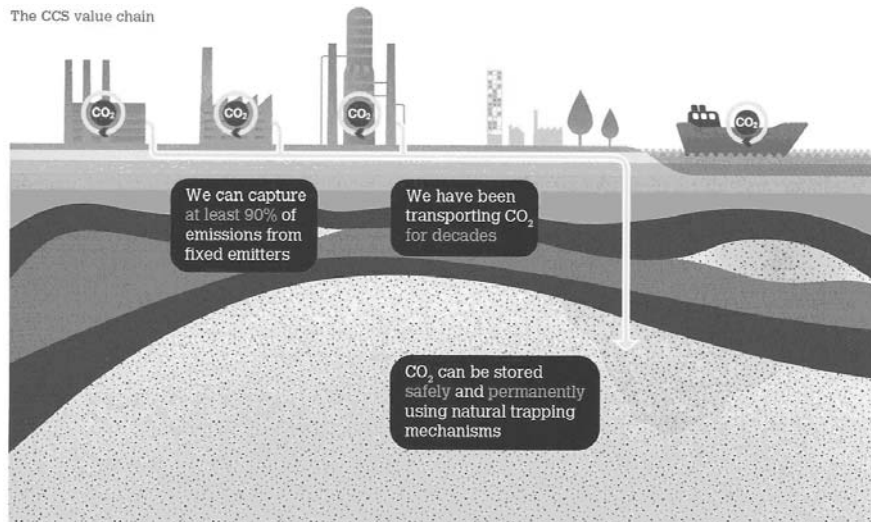
Fig.2. CCS value chain

Zero Emissions Platform (ZEP) works to reduce climate change through policy strategies and technology solutions that reduce greenhouse gas emissions. In order to make emission-free solutions prevail, ZEP takes an active, constructive part in the political climate debate to help politicians, industry and consumers choose climate friendly solutions.

ZEP believes that emission-free alternatives exist for all energy use.

Romanian energy policies will need to evolve to take into account EU climate change policies and legislation. To model the power generation of a specific country, predictions and forecast must be combined with reasonable assumptions made on likely outcomes. Approaching the electricity generation system in Romania presents many unique challenges in this regards. The Electricity Production Industry EPI in Romania is currently undergoing rapid change, with much of the present infrastructure to be replaced in the next decade. Existing fossil, nuclear, hydro and renewable capacities are modeled based on the projections from both the unpublished Draft Strategical Directions and Objectives for Romania Energy Sector for the period 2011-2035 and the Romanian National Renewable Action Plan (2010) [4], [5].

In 2007, the European Commission began to create an economic and legal framework to support flagship demonstration CCS power plant projects. This demonstration projects aim to show the potential of CO_2 capture and storage while testing the technology at scale, gaining valuable know how, reducing capital costs through gained experience. The Getica CCS project has been proposed as a flagship European demonstration project, demonstrating capture transport and the permanent storage of 1.5 million tones of CO_2 pro annum.

This first Romanian demonstration CCS facility is proposed to be retro-fitted to the 330MW lignite - fired power unit no. 6 owned by the Turceni from Oltenia Energy Complex.

CONCLUSIONS

Carbon Capture and Storage (CCS) will provide the chance for exploiting new technologies with application to all fossil fuels, first in terms of energy production based on natural gas.

All combustions of fossil fuels like gas, oil and coal generate CO_2 emissions that accumulate in the atmosphere and increase the greenhouse effect

The first approach for reduction in CO_2 emissions focuses on the technology mix. No single form of power generation will address the dual challenge of securing the supply of reliable and affordable energy and affecting a rapid transformation to a low-carbon system of energy supply. It will take all types of generation technologies such as nuclear and renewable.

In this respect focus areas are:
- Renewable energy production;
- Energy efficiency in buildings Carbon capture and storage (CCS);
- Electric power for the offshore petroleum sector;
- Emission reduction in industry;
- Carbon neutral transport;
- Climate friendly agriculture and forestry.

However, financial contributions from businesses will never affect our climate policy views, neither does it indicate approval of business practices.

REFERENCES

[1]. *Commission of the European Communities - Communication from the Commission to the European Council and the European Parliament - An Energy Policy For Europe {Sec (2007) 12}* Brussels, 10.1.2007 Com (2007) 1 Final.

[2]. *Commission of the European Communities - Communication from the Commission – Action Plan for Energy Efficiency: Realising the Potential {SEC (2006)1173} {SEC (2006)1174} {SEC(2006)1175}* - Brussels, 19.10.2006 COM(2006)545 Final.

[3]. *Guvernul Romaniei: National sustainable development strategy Romania 2013-2020-2030, Bucuresti,* 2008.

[4]. *Guvernul Romaniei: Planul Naţional de Acţiune în Domeniul Energiei din Surse Regenerabile (PNAER),* 2010.

[5]. *Monitorul Oficial al României, Partea I, Nr. 781/19.XI.2007. Strategia energetica a Romaniei pentru perioada 2007-2020,* Bucuresti 5.09. 2007.

[6]. Arad, S., Arad V., Julian C., *Tendinţe actuale în producerea şi utilizarea ca resursă energetică a cărbunelui din Valea Jiului* Revista Minelor, nr 9-10/2008, pp. 12-16, ISSN 1220–2053 cod CNCSIS 293, (C), Infomin Deva Publishing House, 2008.

[7]. Samoila, L. B., Marcu, M. , Vaida, M., *Guiding and Orientating System for Solar Panels,* Proceedings of 10-th International Conference on Environment and Electrical Engineering, Rome, Italy, 2011, http://ieeexplore.ieee.org/xpl/freeabs_all.jsp?arnumber=5874636.

[8]. Stepanescu I., Rehtanz C., Fotău I., Arad S. Marcu M., Popescu, F., *Implementation of small water power plants regarding future virtual power plants.* Proceedings of the IEEE International Conference on Environment and Electrical Engineering, Rome, Italia, 2011.

[9]. *www.alstom.com/power.*

MEASUREMENT OF THE HALF DECAY TIME FOR CHARACTERIZATION OF TEXTILES USED IN POTENTIALLY EXPLOSIVE ATMOSPHERES, REGARDING SAFETY AT ELECTROSTATIC DISCHARGES

MIHAELA PĂRĂIAN[1], EMILIAN GHICIOI[2], SORIN BURIAN[3], NICULINA VĂTAVU[4], ADRIAN JURCA[5], FLORIN PĂUN[6], LEONARD LUPU[7],

Abstract: *The static electricity is one of the potential ignition sources for the explosive atmospheres. In order to ensure an appropriate level of safety against explosions in Ex endangered areas, it is of a major importance to take adequate protective measures for preventing electrostatic discharges from persons.*

Preventing formation/discharging of static charges from persons suppose an assembly of measures and means to ensure appropriate paths for charges leak out (dissipation) to earth. This can be achieved by using dissipative clothing, appropriate electrically conductive footwear, appropriate flooring or other means for charge discharging to earth.

The requirements regarding PPE for use in explosive atmospheres are given in the ***European Directive PPE 89/686/EEC [Government Decision no. 115/2004 + Government Decision no.809/2005]****. The Directive stipulates that PPE intended for use in explosive atmospheres must be so designed and manufactured that it cannot be the source of an electric, electrostatic or impact-induced arc or spark likely to cause an explosive mixture to ignite.*

The test methods of textiles in general and the textile fabrics in particular, for assessment of protective performances against static electricity have been in a continuous development, together with development new materials, dissipative from an electrostatic point of view.

Within INSEMEX, a modern test stand had been carried out and experimented, for determination of the half decay time of charges on textile materials or the screening factor, for

---

[1] Ph.D.Eng. - *scientific researcher Ist degree at INCD-INSEMEX Petroşani*
[2] Ph.D.Eng. - *scientific researcher IInd degree at INCD-INSEMEX Petroşani*
[3] Ph.D.Eng. - *scientific researcher IInd degree at INCD-INSEMEX Petroşani*
[4] Ph.D.Eng. - *scientific researcher IIIrd degree at INCD-INSEMEX Petroşani*
[5] Ph.D.Eng. - *scientific researcher IIIrd degree at INCD-INSEMEX Petroşani*
[6] Ph.D.Eng. - *scientific researcher IIIrd degree at INCD-INSEMEX Petroşani*
[7] Ph.D.Eng. - *scientific researcher IIIrd degree at INCD-INSEMEX Petroşani*

the purpose of assessing the dissipative capacity of charges on textile materials used in manufacturing protective garment, according to the requirements defined at European level.

Keywords: electrostatics, explosive atmosphere, hazard, personal protective equipment, garment, fabrics

1. INTRODUCTION

The paperwork presents the development of laboratory tests for determination of electrostatic performance properties of the personal protective equipment (PPE) intended for use in potentially explosive atmospheres, according to the new European principles and practice in the labor safety and health field.

Romania, as a member state of the European Union, undertook in national legislation the European Directives. Thus the Government Decision no. 115/2004 was elaborated, regarding establishing of the essential safety requirements for the personal protective equipment and the conditions for placing them on the market, modified by HG 809/2005, which transposes the Council Directive no. 89/686/EEC of 21 December 1989 on the approximation of the laws of the Member States relating to personal protective equipment, *amended by Directives 93/68/EEC, 93/95/EEC and 96/58/EC.*

The PPE Directive **89/686/CEE (HG 115/2004+HG 809/2005)** provides that *PPE intended for use in explosive atmospheres must be so designed and manufactured that it cannot be the source of an electric, electrostatic or impact-induced arc or spark likely to cause an explosive mixture to ignite*

Preventing formation of electrostatic charges on person or on neighboring elements suppose an assembly of measures and means to ensure adequate paths to earth (dissipation) for the charges. This can be achieved by making use of dissipative clothing, footwear with a proper electric conductivity and adequate flooring or other means for discharging the charges to earth.

The main assessment criteria for the protective performances of materials and equipment is limitation of the electric resistance values, since it's a well known fact that as the resistance value decreases, the risk of dangerous electrization of materials decreases also. A safety limit of the electric resistivity is 5×10^{10} Ohms, usual for textiles used in manufacture for protective garments [2], [6], [7]. One of the most widely used material in clothing items is the 100% cotton. The textiles made of 100% cotton are adequate from the electrostatic point of view, respectively of electric resistivity, but only in conditions of a relative humidity higher than 65%. This implies a limited intended use for the garment items manufactured of 100% cotton, determined by the humidity conditions existing at workplaces. This is why new types of electrostatically dissipative materials had been developed, as well as new test methods for these, in order to assess conformity with the specific Ex requirements based on the half decay time criterion or screening factor. According to SR EN 1149-5, the electrostatic dissipative material shall meet at least one of the following requirements:

- $t_{50\%}$ < 4s or S > 0,2, tested according to the test method 2 (induction charging) of EN 1149-3:2004, where $t_{50\%}$ is the half decay time of charge and S is a protective coefficient;
- a surface resistance of less than or equal to $2,5 \times 10^9$ Ω, on at least one surface, when material is tested according to EN 1149-1.

For materials containing conductive threads in a stripe or grid pattern the spacing of the conductive threads in one direction shall not exceed 10 mm in any part of the garment. For testing of **personal protective clothing** regarding its protective performances from a point of view of dangerous electrostatic discharges in igniting flammable atmospheres, there is no recognized standardized method, and the fourth part of SR EN 1149 is yet work in progress.

Development of requirements for the PPE (personal protective equipment) used in environments with explosion danger is a frequently occurring topic on the work agenda of *CO-ORDINATION OF NOTIFIED BODIES PPE – Directive **89/686/CEE.***

Within INSEMEX Petroşani researches had been carried out, in the field of the explosion hazard of explosive atmospheres shown by static electricity, test stands had been executed, and a specific laboratory with test apparatus of last generation for testing of technical equipment exists, with high performance apparatus to ensure the required environmental conditions, since it's a well known fact that in order to model the maximum electrization conditions, a low relative humidity of 25-30 % is required [1],[3].

In the context of a general continuous development and perfecting the laboratory tests policy, up to the level of the newest achievements in the field, this year a new test stand had been carried out, for measurement of textile materials charge dissipation capacity according to method 2, **Induction charging**, in SR EN 1149-3 *Protective clothing. Electrostatic properties. Part 3:Test methods for measurement of charge decay.*

2. TEST STAND CARRYING OUT AND LABORATORY EXPERIMENTS FOR MEASURING THE CHARGE DISSIPATION CAPACITY - CHARGING BY INDUCTION

2.1 Test method principle

The test method principle: Charging of the test specimen is carried out by an induction effect. Immediately under the test specimen, which is horizontally arranged, a field-electrode is positioned, without contacting the specimen. A high voltage is rapidly applied to the field-electrode. If the specimen is conductive, or contains conducting elements, charge of opposite polarity to the field-electrode is induced on the specimen. Field from the field-electrode which impinges on the conducting elements does not pass through the test specimen and the net field is reduced in a way that is characteristic of the material under test. This effect is measured and registered behind the specimen with a suitable field-measuring probe.

As the amount of induced charge on the test specimen increases, the net field registered by the measuring probe decreases. It is this decrease in field that is used to determine the half decay time and the shielding factor.

2.2 Description of the test stand for measurement of the charge dissipation capacity
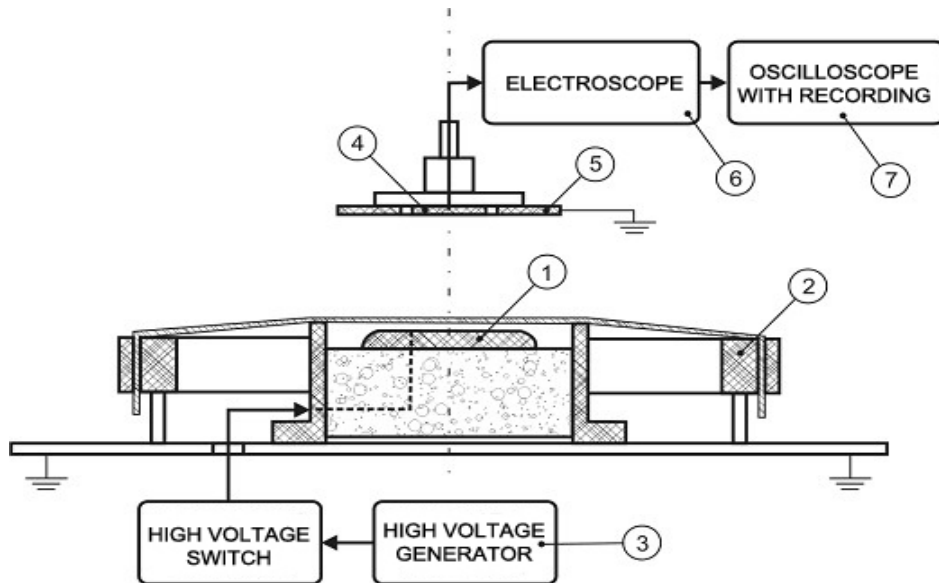
Fig. 1 Arrangement of equipment for measurement of the dissipative capacity of charges - induction charging

The principle graph of the test stand for measurement of the charge dissipation capacity - the induction charging method, for the purpose of laboratory testing of textiles used in manufacturing of garments used in environments with explosive atmospheres having in view conformity assessment with the essential safety requirements in the PPE Directive is shown in figure 1.

The test stand (fig. 1) consists in: *Field-electrode* (a polished stainless steel disc, (70±1) mm diameter, fixed to an insulating support) (1), *Support ring* (a metal ring, (100±1) mm internal diameter, connected to earth and positioned concentric to the field-electrode); *Specimen clamping rings* (2), *Voltage generator* capable of producing a (1200±50) V step voltage on the field electrode within 30 ms (direct current voltage supply of 5000 V and a HT fast switch) (3), *Field-measuring probe* (a metal disc, (30,0±0,1) mm diameter (4), surrounded by an earthed guard ring (5) and connected to an electronic electrometer (6) then to an oscilloscope (7) to record the time related data from the field-measuring probe output. The time resolution and response time of the recording device has to be 50 μs.

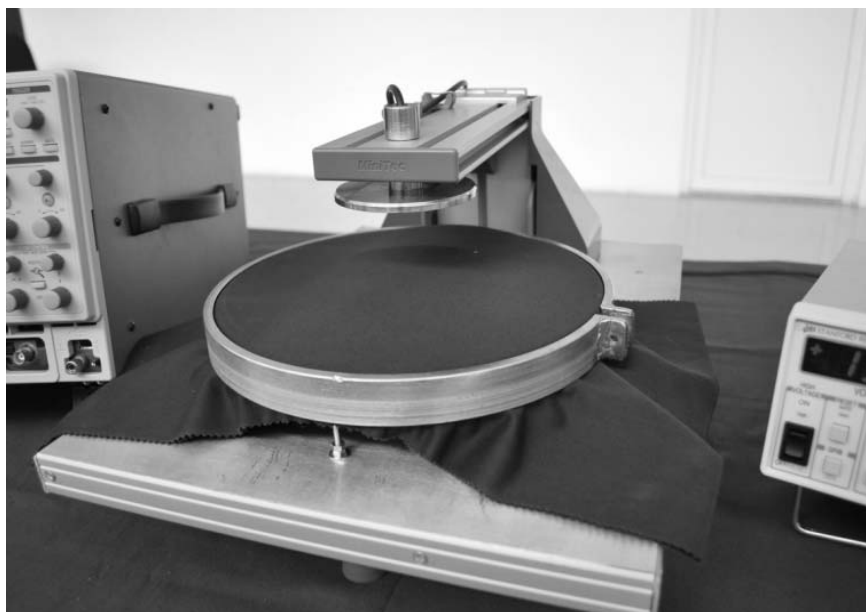In figures 2 and 3 the test stand is shown without and with the test sample.
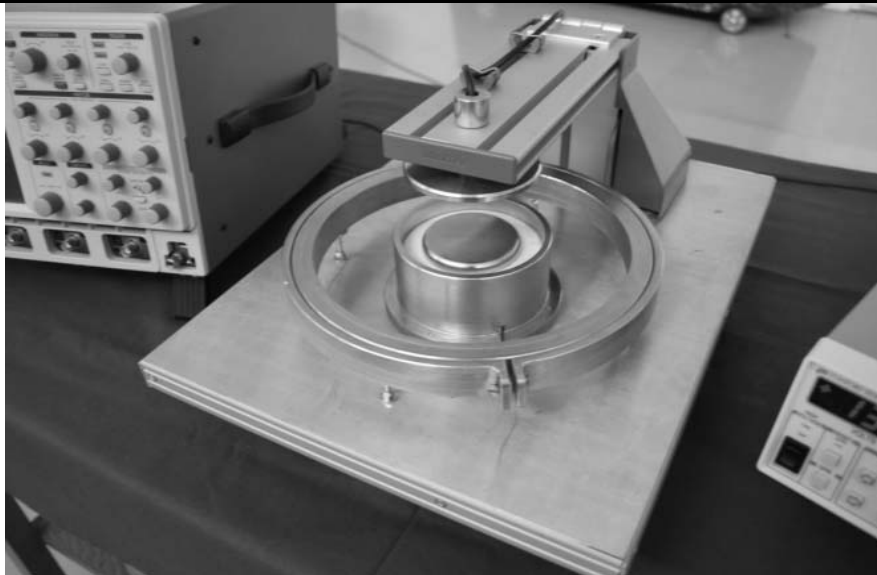
Fig. 2 Test stand without the test sample

Fig. 3 Test stand with the test sample

2.3. Laboratory tests

Laboratory tests had been carried out, on materials known as complying with the

SR EN 1149-5 requirements, having in view experimentation of the new test method and the new test stand carried out.

In figures.2 and 3 are shown the results obtained for two typed of materials tested.
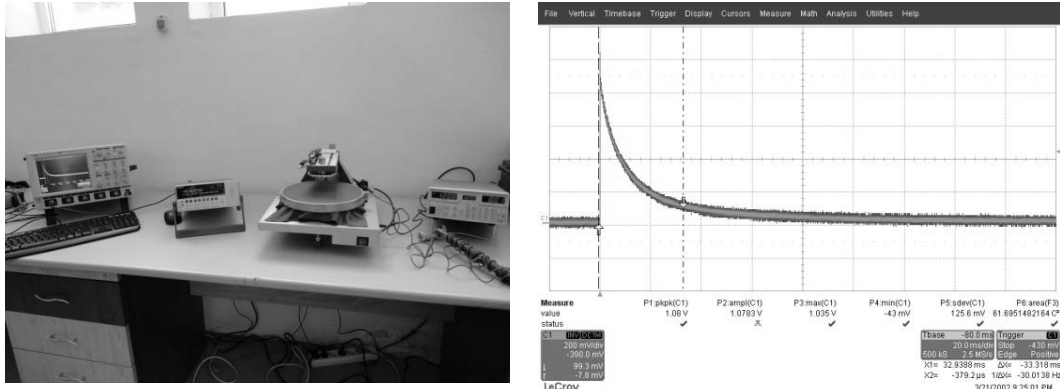
Fig. 4 Testing of sample no.1
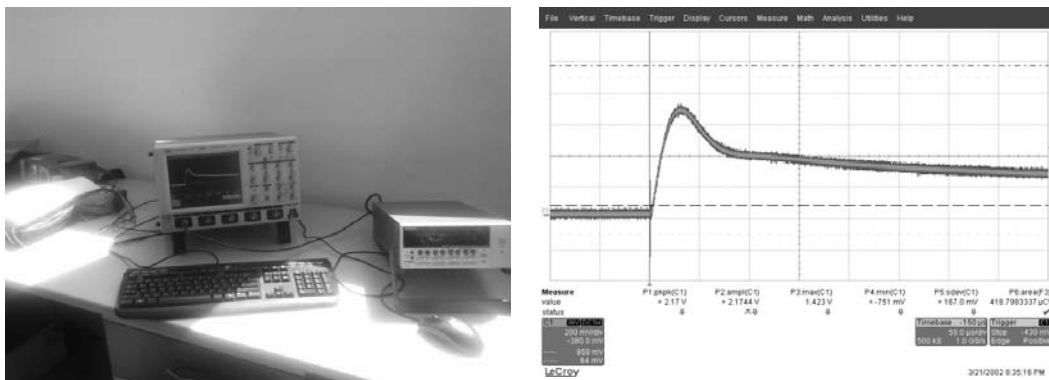
Fig. 5 Testing of sample no.2

RESULTS AND DISCUSSIONS

Experimentation in laboratory of the new method, had the purpose identifying the factors of influence for ensuring tests repeatability and reproducibility. Complying with the requirements of the SR EN 17025 [5] had been in view, in order to extend the laboratory competency field adding the method of determining the charge's half decay time.

As specified in the SR EN 1149-3 Annex, tribo-charging tests repeatability and reproducibility is never at the same level with the ones regarding resistance measurement, but in the EN 1149-3 method they are at a satisfactory level, and the charging capacity of various materials can be well compared through these tests.

Comparison between the results obtained by two laboratories showed differences of less than a factor of eight for test method 1. An inter-laboratory trial for method 2, using 5 different materials and 5 participating laboratories, in 3 different locations, showed a repeatability and reproducibility standard deviation as follows:

Parameter	S
Repeatability standard deviation, sr	0.004
Reproducibility standard deviation, sR	0.009
Half discharge time	t_{50}
Repeatability variance	30%
Reproducibility variance	40%

Thus, accuracy of the results obtained in the accredited test laboratory have to be also confirmed, in the future, by inter-laboratory tests.

3. CONCLUSIONS

The test stand carried out complies with the requirements in SR EN 1149-3. The implemented test complies with the requirements in SR EN 17025 in order to ensure the test laboratory competency.

By modernizing the testing / development capacity of the laboratory regarding PPE used in environments with explosion hazards, INCD-INSEMEX may become an important provider of specialized services for the PPE providers (manufacturers/distributors), users, the market inspection bodies or the control bodies in Romania and abroad.

REFERENCES

[1] Arad, S., Arad, V., Lupu, L., *The remote control of Electric Devices, Protection, Control and Monitoring Systems*. Industrial Electronics, 2006 IEEE International Symposium on, Proceedings of IEEE, vol I, pp 267-272, Montreal, Que, 2006, ISSN 0018-9219, ISBN 1-4244-0497-5. INSPEC Accession Number: 9132144, DOI 10.1109/ISIE.2006.295604,
[2] Haase J., Vogel C., *Testing and evaluation of electrostatic behaviour of electric inhomogeneous textiles with core-conductive fibers.*
[3] Lupu, L., Paraian, M., Ghicioi, E., Arad, S., Selection of technical equipment intended for use in underground firedamps mines, Proceedings of MPES2006, pp. 166-172, ISBN 88-901342-4-0, Edited by M. Cardu, R. Ciccu, E. Lovera, E. Michelotti printed in Italy by FIORDO srl-Galliate, Torino, Italy, 2006
[4] Paraian M., s.a., *Dezvoltarea metodelor de încercare pentru evaluarea performantelor de protecţie la electricitatea statică ale echipamentelor individuale de protecţie utilizate în industrie în locuri cu pericol de explozii – MELSTEIP, PN 07 45 02 13 – 2012.*
[5] *** *SR EN 1149-5: 2008 „Îmbrăcăminte de protecţie. Proprietăţi electrostatice. Partea 5. Cerinţe de performanţă pentru materiale si cerinte de proiectare”.*

[6] *** *SR EN 1149-3: 2004 „Îmbrăcăminte de protecţie. Proprietăţi electrostatice. Partea 3. Metodă de încercare pentru măsurarea capacităţii de disipare a sarcinilor”.*

[7] *** *SR EN ISO/CEI 17025 Cerinţe generale pentru competenţa laboratoarelor de încercări şi etalonări.*

[8] *** CLC/TR 50404 June 2003 Electrostatics - Code of practice for the avoidance of hazards due to static electricity (CENELEC TC 31 (sec)388, august 2002: prEN xxxxx Electrostatics. Code of Practice for the avoidance of hazards due to static electricity).

[9] *** *IEC TR 60079-32: Explosive atmospheres - Part 32: Electrostatics.*

[10]   *** *SR EN 61340-2-1:2004 ver.eng. Electrostatică. Partea 2-1: Metode de măsurare. Capabilitatea materialelor şi produselor de a disipa încărcările electrostatice.*

[11]   *** *SMT4-CT96-2079 “The evaluation of the electrostatic safety of personal protective clothing for use in flammable atmospheres”.*

[12]   *** *G6RD-CT-2001-00615 , ESTAT-Garments “Protective clothing for use in the manufacturing of electrostatic sensitive devices”, Duration March 1, 2002 – February 28, 2005.*

[13]   *** *Council Directive 89/686/EEC of 21 December 1989 on the approximation of the laws of the Member States relating to personal protective equipment.*

PERFORMANCE IMPROVEMENT OF AC ELECTRIC DRIVES USING FIELD ORIENTED CONTROL AND DIGITAL SPEED TRANSDUCERS

RAZVAN SLUSARIUC[1], FLORIN GABRIEL POPESCU [2], MARIUS DANIEL MARCU [3]

Abstract*: High performance drives, such as vector controlled drives, employ field oriented control and require current feedback as an integral part of their control loops. In these cases motor current is not simply limited at a pre-defined level. It is controlled to match a continuously changing torque demand. The vector components of the stator current in each phase are calculated, which requires current from all three phases. Using a digital position transducer can increase the accuracy of speed and torque response.*

Key words: torque, feedback, encoder, sensorless.

1. INTRODUCTION

Up to the end of the 1980s, high performance drive applications inevitably required the use of a DC drive. However, the high maintenance requirements of DC drives have encouraged the development of alternative solutions. Vector controlled AC drives have evolved to provide a level of dynamic performance that has now exceeded that of DC drives.

Closed-loop vector control is not required for every AC VSD application, in fact only on a minority of applications. But there are a number of applications that inherently require tight closed-loop control, with a speed regulation better than 0.01% and a dynamic response better than 50 radians/sec. This dynamic response is about 10 times better than that provided by standard V/f drives.

[1] *PhD. Student Eng. at University of Petrosani*
[2] *Ph.D. Assistant Eng. at University of Petrosani*
[3] *PhD. Associate Professor Eng. University of Petrosani*

2. A MATTER OF PERSPECTIVE

One way to understand how FOC (sometimes referred to as vector control) works is to form a mental image of the coordinate reference transformation process.

If you picture an AC motor operation from the perspective of the stator, you see a sinusoidal input current applied to the stator. This time variant signal generates a rotating magnetic flux. The speed of the rotor is a function of the rotating flux vector. From a stationary perspective, the stator currents and the rotating flux vector look like AC quantities.

Now, imagine being inside the motor and running alongside the spinning rotor at the same speed as the rotating flux vector generated by the stator currents. If you were to look at the motor from this perspective during steady state conditions, the stator currents look like constant values, and the rotating flux vector is stationary.

Ultimately, you want to control the stator currents to obtain the desired rotor currents (which cannot be measured directly). With coordinate reference transformation, the stator currents can be controlled like DC values using standard control loops.[1]

The control block diagram for a high performance vector control AC drive system is essentially a *cascaded closed-loop* type with speed and torque control loops: • There are two separate control loops, one for speed and the second for current. This control strategy is similar to that used for the control of a DC drive.

− **Speed loop** controls the output frequency, proportional to speed.
− **Torque loop** controls the motor in-phase current, proportional to torque.[3]

• The **speed reference** command from the user is first fed into a comparator, from where the error controls the speed regulator.
• The speed error signal becomes the set point for the torque (current) regulator.
This signal is compared to the calculated current feedback from the motor circuit and the error signal determines whether the motor is to be accelerated or decelerated.
• There is a separate control loop for the flux current (V/f regulator).
Finally, the signal passes to the PWM and switching logic section, that controls the IGBTs in such a way that the desired voltage and frequency are generated at the output according to the PWM algorithm (sine-coded, star modulation, VVC, etc.).

Although a shaft mounted incremental encoder can be used to measure speed in an AC drive, it is often considered to be an additional expense. In some cases it is difficult to mount on the motor, for example when motors have integral brakes.

Even when an encoder is not used, the cascaded closed loop control can still be implemented because speed can be calculated by the active motor model, but with a lower level of accuracy due to the difficulty of calculating slip, particularly at very low speeds. Vector controlled drives which do not use encoders are usually referred to as **sensorless vector drives**.
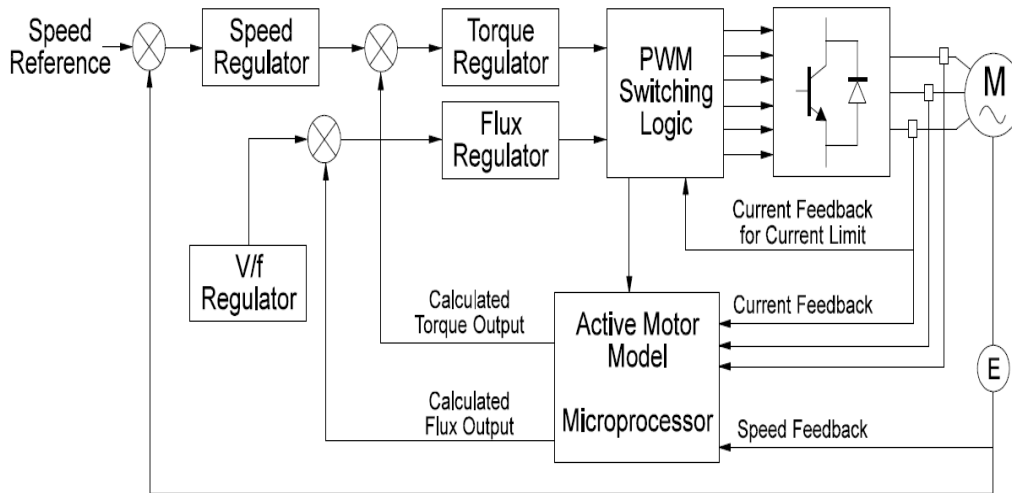
Fig.1. Block diagram of the flux-vector converter control circuit

The dynamic response of vector control drives, which do not use an encoder, is usually inferior to those that do.

Typical applications for this type of high performance VS drive are:
• Crane and hoist drives
• Re-winders on paper and steel-strip lines
• Paper machines
• Printing machines
• Positioning systems for automated manufacturing lines etc.

When setting up high performance VSD controllers, a modest *proportional gain* gives a good transient response, while the *integral gain* gives high steady state accuracy. PI controllers have the advantage that they can maintain a non-zero output to drive the converter although their input is zero. This is an advantage in closed-loop control because high accuracy should lead to zero error at the controller input.

Suitable values of *P* and *I* determine the step and ramp parts of the response respectively and have to be calculated for each inverter–motor–load combination. [2]

• The **values of *P* and *I* for the speed loop** are dependent on the motor flux, load friction and inertia as they influence the response of speed to current.

• The **values of *P* and *I* for the current loop** depend on the inverter gain, motor resistance and leakage inductance, since they influence the response of current to the motor frequency.

In modern digital drives, the *P* and *I* values for both current and speed loops can be set by keypad or, alternatively, most modern digital drives usually include an algorithm for *self-tuning*.

This removes the difficulties of 'tuning the loops', which was traditionally necessary with older analog DC drives. The *P* and *I* gains of the speed loop can be

setup during commissioning to meet application requirements and seldom need to be changed.

There are a number of disadvantages of the vector controlled AC drive, when compared to a DC drive:

The vector controller is far more complex and expensive when compared to the simple cascade controller of a DC drive.

Encoder speed feedback is usually necessary to obtain accurate feedback of the motor shaft speed. Fitting these encoders to a standard squirrel cage AC induction motor is often difficult and makes the motor more expensive.

In recent years, 'Sensorless' vector control has been developed where an encoder is not required. The approximate speed is calculated by the processor from the other available information, such as voltage and current. However, the speed accuracy and dynamic response of these drives is inferior to those using encoders.

The nature of the drive itself often requires the AC motor to operate at high torque loadings at low speeds. The standard squirrel cage AC induction motor then requires a separately powered cooling fan, installed at the ND end of the motor.

Regenerative braking is more difficult with a vector drive than with a DC drive. Resistive type **dynamic braking** systems are most often used with AC vector control drives.

3. CURRENT FEEDBACK IN AC VARIABLE SPEED DRIVES

Current feedback is required in AC variable speed drives for a number of purposes:
• **Protection**, short circuit, earth fault and thermal overload in motor circuits.
• **Metering,** for metering and indication for the process control system.
• **Control**, current limit control and current loop control. Several methods have been developed over the years to measure the current and convert it into an electronic form suitable for the drive controller. The method chosen depends on the required accuracy of measurement and the cost of implementation.

The main methods of measurement are as follows:
• **Current shunt**, where the current is passed through a link of pre-calibrated resistance. The voltage measured across the link is directly proportional to the current passing through it. This method was often used in drives with analog control circuits.
• **Hall effect sensor**, where the output is a DC voltage, which is directly proportional to the current flowing through the sensor. High accuracy and stability over a wide current and frequency range are amongst the main advantages of this device. This device is commonly used with modern digital control circuits.

The performance of a normal core type current transformer is usually not adequate for power electronic applications because its performance at low frequencies is poor and accuracy of measurement of non-sinusoidal waveforms is inadequate.

4. CURRENT FEEDBACK IN HIGH PERFORMANCE VECTOR DRIVES

High performance drives, such as vector controlled drives, employ field oriented control and require current feedback as an integral part of their control loops. In these cases motor current is not simply limited at a pre-defined level.

It is controlled to match a continuously changing torque demand. The vector components of the stator current in each phase are calculated, which requires current from all three phases. This can be achieved preferably with one hall effect CT in each output phase or alternatively two in the output phases and one on the DC bus. [5]

If only two-phase sensors are used, the third phase can be calculated from them, however the bus current sensor is still required for device protection.

High accuracy motor current feedback is also necessary to provide control of motor torque. Torque control is necessary in applications such as rewind/unwind systems, hoists, winches, elevators, positioning systems, etc.

5. SPEED FEEDBACK FROM THE MOTOR

In closed-loop speed control of electric motors and positioning systems, the speed and position feedback from the rotating system is provided by transducers, which convert mechanical speed or position into an electrical quantity, compatible with the control system.

The following techniques are commonly used today:

• **Analog speed transducer**, such as a tachometer generator (tacho-generator), which converts rotational speed to an electrical voltage, which is proportional to the speed, and transferred to the control system over a pair of screened wires.

• **Digital speed transducer**, such as a rotary incremental encoder, which converts speed into a series of pulses, whose frequency is proportional to speed. The pulses are transferred to the control system over one or more pairs of screened wires.

• **Digital position transducer**, such as a rotary absolute encoder, which converts position into a bit code, whose value represents angular position. The code is transferred digitally to the control system over a screened parallel or serial communications link.

Single-turn absolute rotary encoders generate a parallel digital output, which represents the angular position of the shaft over one revolution. Each angular position is represented by a code, comprising several digital bits (Table 1). The rotating optical disk has multiple tracks, one for each bit of the output code. Even if the power fails, once restored, the position of the shaft is accurately known without any resetting routine, as would be required for incremental encoders.

One revolution (360°) is divided into a specified number of positions. The number of possible positions (*position resolution*) depends on the number of tracks printed onto the disk.

Table 1. **The relationship between the number of tracks (bits) on the disk and the resolution of an absolute rotary encoder**

No. of tracks (bits in code)	Resolution (No. of positions)	Resolution (deg per position)	Resolution deg/min/sec
1	2	180.00^0	$180^000'00''$
2	4	90.00^0	$90^000'00''$
3	8	45.00^0	$45^000'00''$
4	16	22.50^0	$22^030'00''$
5	32	11.25^0	$11^015'00''$
6	64	5.63^0	$5^037'30''$
7	128	2.81^0	$2^048'45''$
8	256	1.41^0	$1^024'23''$
10	1024	0.35^0	$0^021'06''$
12	4096	0.088^0	$0^005'16''$
16	65 536	0.0055^0	$0^000'20''$

The **binary absolute encoder** uses a binary number (counting system to the base 2) to represent the position number of the shaft (Figure 2).
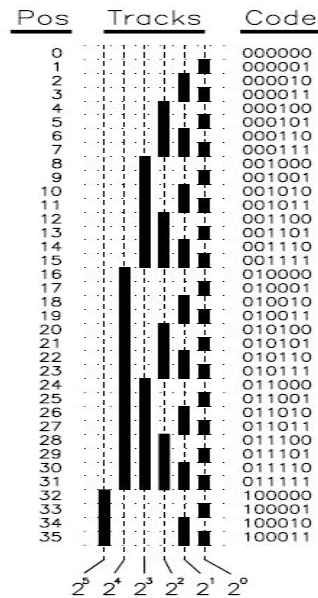
Fig.2. Binary code

Analog speed transducers are increasingly being replaced by digital devices, which are more compatible with modern digital control systems.

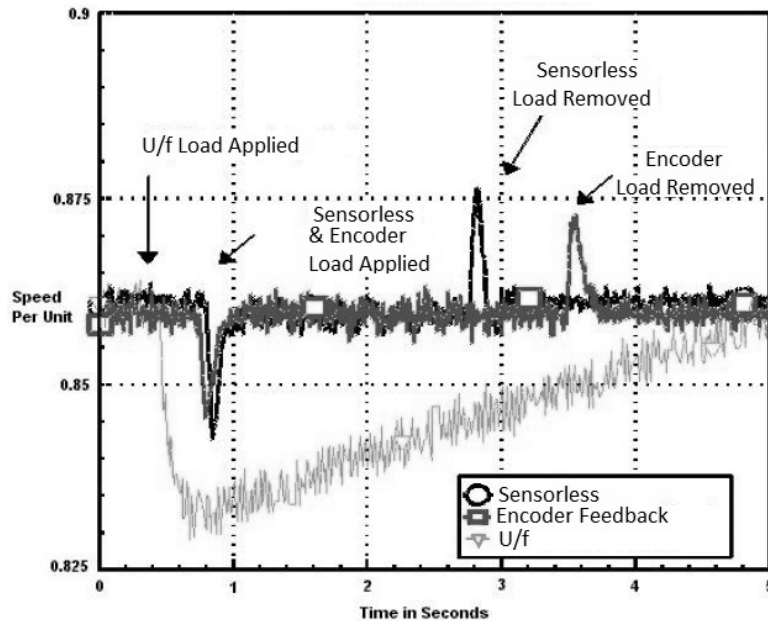The graph below shows a drive operating with and without an encoder, and a U/f drive. [4]

Fig.3. Load disturbance response

Notice the difference with and without an encoder. You can clearly see the response to the step load and the recovery time. The same can be seen when the load is removed.

Contrast that against the U/f response, which recovers much slower. The high bandwidth current regulators and high performance speed regulator ensure that the drive using a digital speed transducer delivers high dynamic performance.

In the following table can be observed that speed transducers used with field oriented control method increase the accuracy of speed from 0.5% to 0,001%.

Table 2. **Speed transducers used with field oriented control method**

	DC drive with encoder	**V/f flux vector sensorless**	**V/f flux vector with encoder**	**Field oriented sensorless**	**Field oriented with encoder**
Speed accuracy	0.01%	1%	0.1%	0.5%	0.001%
Torque response	10-20 msec	100 msec	10-20 msec	1-10 msec	1-10 msec

6. CONCLUSIONS

In this case o variable speed drive used with field oriented control method can be observed that when using a digital speed transducer it's a major improvement when the requirement of the system is a very accurate speed and torque response.

Experiments and simulations in typical operating conditions demonstrate high dynamic performance during speed and flux tracking including load torque rejection, which is of the same order as for standard field-oriented solutions with speed measurement.

Even though it may seem an added expense to the entire cost of the system, if the demand is a speed more accurate than 0,01% and 50 rad/sec then a digital transducer is a must.

REFERENCES

[1] Jorge Zambada, *Sensorless Field Oriented Control of PMSM Motors*, Microchip technology, Chandler, 2007.
[2] Malcom Barnes, *Practical Variable Speed Drives and Power Electronics*, Newnes, 2003.
[3] Marcu Marius Daniel, *Convertoare statice in actionari electrice,* Editura TOPOEXIM, Bucuresti, 1999.
[4] Rockwell Automation, *Publication DRIVES-WP002A-EN-P* , June 2000.
[5] http://machinedesign.com

SAFETY REQUIREMENTS FOR ELECTRICAL EQUIPMENT USED FOR COMMUNICATION IN AREAS WITH HAYARD OF EXPLOSIVE ATMOSPHERES

SORIN BURIAN[1], JEANA IONESCU[2], MARIUS DARIE[3], TIBERIU CSASZAR[4]

Abstract: The paper aims to identify opportunities for correct association of electrical hand machines for communications in potentially explosive atmospheres.

Keywords: Explosion protection, intrinsic safety, conditions of interconnection.

1. INTRODUCTION

Unprecedented increase in the degree of interconnection of systems and industrial platforms while extending technologies involving combustible revealed a new imperative of maintaining reasonable risk of explosion [1],[3]. Such low current systems have reached a considerable weight in technological systems on industrial sites.

On the other hand according to Directive 99/92/EC approach necessary to maintain acceptable levels of risk of explosion involves the use of atmospheric monitoring systems and explosion protection.

Monitoring systems can contribute both interlock means the process by means of prediction and the time available to the occurrence of events such as exceeding allowable levels [1].

---

[1] *PhD. Eng., IInd degree scientific researcher, INCD INSEMEX Petroşani,*

[2] *PhD. Eng., IInd degree scientific researcher, INCD INSEMEX Petroşani*

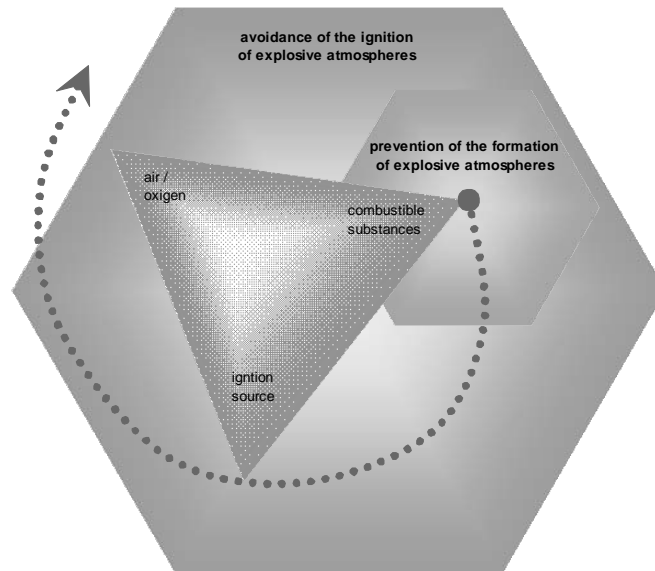[3] *PhD. Eng., IInd degree scientific researcher, INCD INSEMEX Petroşani*

[4] *PhD. Eng., IIIrd degree scientific researcher, INCD INSEMEX Petroşani*

Fig. 1 Basic principles for the protection of explosion

2. TYPES OF PROTECTION

Dramatic accidents in underground mines susceptible to firedamp in Europe have led stakeholders to start a crystallization process research and effective security measures resistance explosions.

Thus the late 19th century the foundations were laid capsular flameproof enclosure protection and early 20th century arises intrinsic safety type of protection. As time went explosion protection solutions have been extended to surface and were diversified.

Currently the types of protection are regulated worldwide through IEC and are grouped into three divisions as follows: for explosion protection of electrical equipment for use in atmospheres of gases, vapors, mists fuel then the explosion protection of electrical equipment operating in spaces powder, lint, fibers, fuel and last subdivision - Non-electrical equipment [5].

Types of explosion protection of electrical applicability of technical solutions are classified as explosion protection: protection types that separate ignition source of potentially explosive atmospheres (p, m, o, q, v, tD); types of protection that controls ignition source (i, e, tD), other types of protection (d, NL, nA, nC,).

Electric utilized communications in potentially explosive atmospheres falls in weak currents. This explosion can be protected with most types of protection. Statistics types of protective equipment use low current prevalence highlights the type of protection flameproof enclosure followed by intrinsic secretion, increased security and encapsulation.

Except protection type intrinsic safety protection all other explosion protection only manifests in the area bounded by carcass equipment.

Type of protection intrinsic safety (i) involves limiting energy and heating at the circuit devices so they can not be the source of ignition for potentially explosive atmospheres. This explains the need to take into account the additional conditions need to be considered when interconnecting circuits concerned gears [1]. Also this particular type of protection intrinsic safety distance determines a possible manifestation of explosion protection.
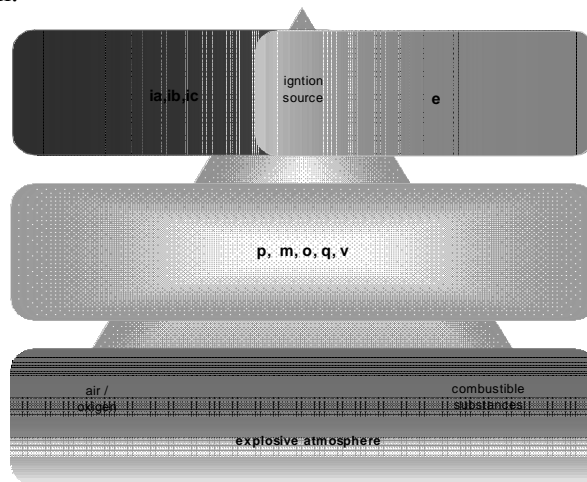
Fig. 2 Types of protection

The technical solutions underlying types of protection, they have affinities for different types of equipment. Such security intrinsic (i) is applicable only low current circuits when equipment for large equipment applies almost exclusively the type of protection encapsulation pressurized (p). Identifying appropriate explosion protection solution from design phase will lead to the development of low-cost equipment and easy to operate.
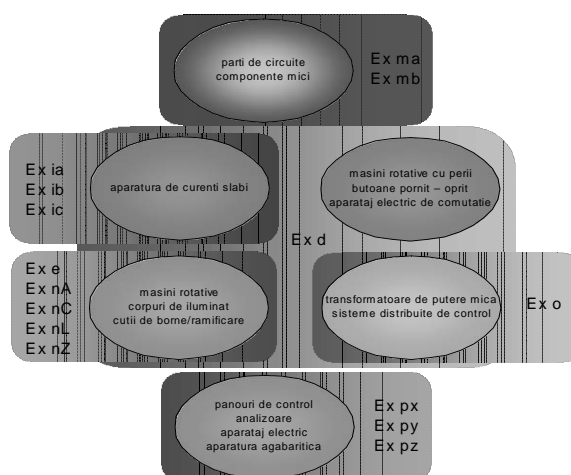
Fig. 3 Apparatus - types of protection

3. CONDITIONS OF ELIGIBILITY

Explosive atmospheres where combustible substances frequency were divided into three zones as follows: Zone 0 - the area where combustible substance is present continuously, Zone 1 - the area where combustible substance is present frequently or periodically as a result of normal operation of the plant technology, Zone 2 - the area where combustible substance is present sporadically due to defective functioning of the system predictable technology.

Explosion protection types and categories (according to ATEX) or levels of protection (IEC) provided allowing electrical apparatus protease only in certain areas in the diagram in Figure 4.

Other eligibility requirements are those relating to employment subgroups and temperature classes.
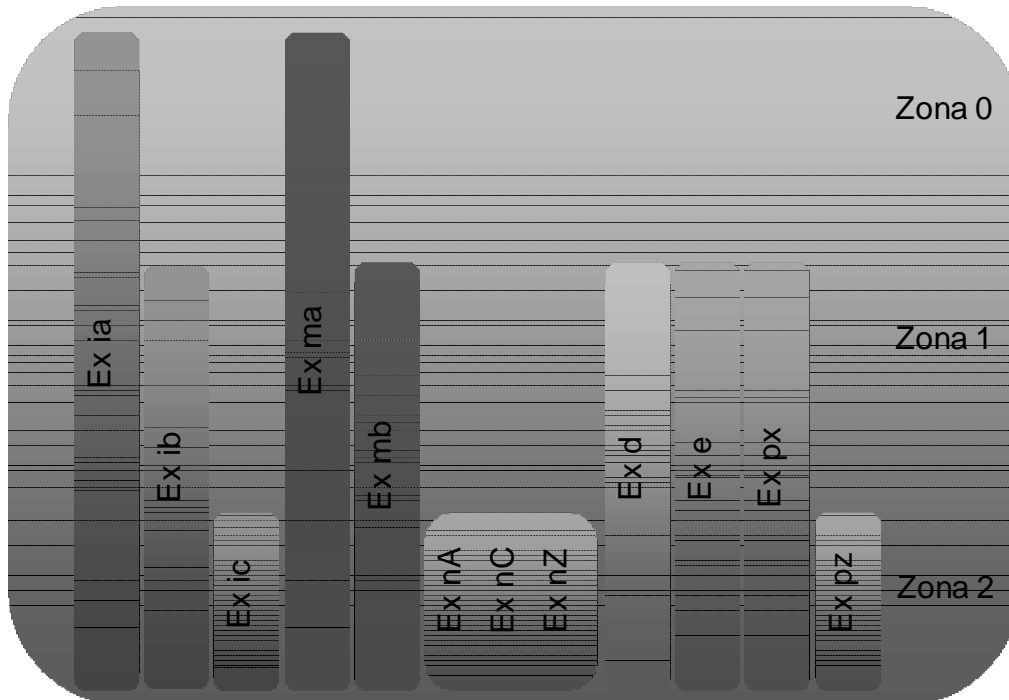
Fig. 4 Eligible types of protection for explosion hazardous areas

4. TYPES OF PROTECTION INTERCONECTING

With few exceptions, circuit protection equipment with type of protection intrinsic safety [3] has electrical connections unprotected parts of electrical explosion known as associated equipment. Due to this, related equipment shall be located outside the explosive atmosphere or otherwise be protected with additional adequate protection. Applications such as dispatching or monitoring plants fall when associated equipment

located outside areas with explosive atmospheres, control circuits and interlocking of switching equipment if the equipment falls associated with other types of protection.
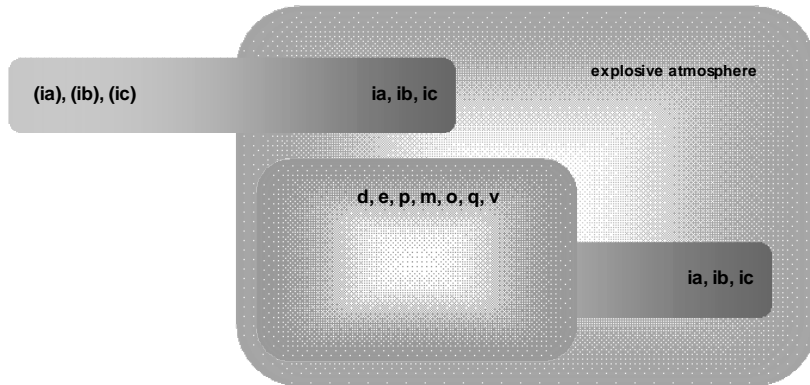
Fig. 5 Associated apparatus

5. INTERCONNECTION CONDITIONS

Interconnection circuits protected equipment protection type intrinsic safety is limited by the conditions of interconnected. These conditions guaranteeing interconnection limitations reflected energy and surface temperature.

Thus for intrinsic safety interface are specified parameters: voltage, current, power, inductance, capacity as maximum values are denoted with the index "a" (out).

The report is specific cable inductance and resistance has implications for not only the type and length of interconnecting cable used.

Parametric specify the index "i" (in) is admissible values for devices with intrinsic safety interfaces for interconnection with other devices protection protected all type of intrinsic safety.

Failure to determine the interconnection conditions invalidation type of protection even if the equipment remains functional.

Fig. 6 Interconnection conditions

6. CONCLUSIONS
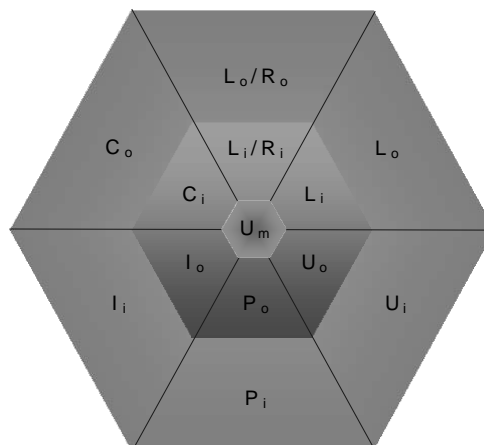
Interconnection circuits protected communication equipment protection type intrinsic safety is limited by the conditions of interconnection.

If used other types of protection such as flameproof enclosure, encapsulation enhanced security and interconnection conditions are applicable only to protected circuits type of protection intrinsic safety.

REFERENCES

[1]. Arad, S., Arad, V., Lupu, L., *The remote control of Electric Devices, Protection, Control and Monitoring Systems*. Industrial Electronics, 2006 IEEE International Symposium on, Proceedings of IEEE, vol I, pp 267-272, Montreal, Que, 2006, ISSN 0018-9219, ISBN 1-4244-0497-5. INSPEC Accession Number: 9132144, DOI 10.1109/ISIE.2006.295604.

[2]. Darie, M., (2009), *Study regarding the ignition capability of potentially explosive atmospheres from low currents electrical installations* – Protection interfaces for low currents installations in areas with hazard of explosive atmosphere, Partnerships Program execution stage I.

[3]. Burian, S., Ionescu, Jeana., Darie, M., Csaszar, T., Andriş, Adriana., (2007) *Requirements for installations in areas with explosive atmosphere, other than mines*, INSEMEX – Petrosani Publishing House, ISBN: 978-973-88590-3-6.

[4]. Simion, S., Baron, Octavia., Basuc, Mariana (2004) *Explosion risk*, Europrint Publishing House, Oradea.

[5]. Lupu, L., Paraian, M., Ghicioi, E., Arad, S., Selection of technical equipment intended for use in underground firedamps mines, Proceedings of MPES2006, pp. 166-172, ISBN 88-901342-4-0, Edited by M. Cardu, R. Ciccu, E. Lovera, E. Michelotti printed in Italy by FIORDO srl-Galliate, Torino, Italy, 2006.

CONSEQUENCES OF CONNECTION OF MICROGENERATORS TO NATIONAL POWER GRID. CASE STUDY

CONSTANTIN BEIU [1], GEORGETA BUICĂ [2], CORNEL TOADER [3]

Abstract: Electric energy production from independent sources is a trend of current period, driven by lower prices than the imports or production of energy from conventional sources. It should be noted that Romania was among the first countries acceding to the EU, who adopted the European Directive 2001/77/EC into national law, regarding Romania's energy strategy for the period 2007-2020. However, these manufacturers of electricity from renewable sources must take into account certain technical and economic requirements, prior to connect the generators. Also the producer of energy must take into account the legal provisions in this field. The case study presented in this paper will detail the effects of connecting the micro-generators to the low voltage public network, calculating the values of induced voltage in the medium voltage network through power transformers, this voltage reaching the rated voltage of the medium network. This case study aims to show that the connection to the public network of the electricity power generators, without the approval of the distribution and system operator may cause dangerous situations for the network and workers.

Keywords: microgenerator, power, system, connection, voltage.

1. GENERAL CONSIDERATIONS

The promotion of producing energy from alternative energy sources is a priority of present times, motivated by environmental protection, limiting energy dependence on imports, by diversifying energy supplying sources and reasons of economic and social cohesion [5].

Romania was among the EU candidate countries which transposed Directive 2001/77/EC into their legislation provisions (GD 443/2003, with the change in GD 958/2005) and set an indicative target for 2012 of 33% representing the share of energy

[1] *PhD. Student Eng. at University Politehnica of Bucharest*
[2] *PhD. Eng , INCDPM "Al. Darabont" Bucharest*
[3] *PhD. Professor Eng. at University Politehnica of Bucharest*

from renewable sources in gross inland consumption of electricity. Subsequently, by GD 1069/2007 on the approval of the Energy Strategy of Romania for 2007-2020 were set targets of 35% in 2015 and 38% for 2020, represents the share of alternative energy in gross inland consumption of electricity.

2. CONDITIONS FOR CONNECTING A DISTRIBUTED GENERATION SOURCES TO NATIONAL POWER GRID (NPG)

2.1. Technical requirements for connection to NPG

We would like to remind the minimal technical conditions known and regulated by parallel implementation of two power sources:

a. The terminal voltages and equal electromagnetic voltage (module and argument);

b. Rigorous equal operating frequency.

c. The difference of phases at the coupling time of sources to be zero (implying the electromagnetic phases to be equal and symmetrical).

Thus, the failure of implementing these minimum requirements does not allow parallel connection to NPG of generators including micro generators.

It states that the solution for connection of power users [6] to NPG must be agreed upon and approved by distribution system operators, as appropriate [7], as follows:

d. The connection to the public network fee assessment

In this respect, as required by law [6] was developed the connection fee, T_{rac}, defined by the relation:

$$T_{rac} = T_{cap\_rac} + T_{inst\_rac} + T_{rl\_pif} \qquad (1)$$

The terms have the meanings:

T_{rac} - is the rate of connection to electric networks of medium and / or low voltage in lei;

T_{cap_rac} - corresponding component of power capacity reserved to the user upstream of the point of connection, its size is determined as the product of the approved power, S, expressed in kVA and a **specific tariff a_i** expressed in lei/ kVA, established based on average costs;

T_{inst_rac} - corresponding component of the connection network, its size is determined by the type of network, connection length of the branch and approved power, based on some **specific indices b_i**, representing average costs per unit (km, kW, pcs. etc.);

T_{rl_pif} - corresponding component of acceptance, and energizing the user's network, determined on the basis of **rates.**

The prices and specific indicators are set according to the methodology, are proposed by distribution operators, approved by the competent authority (ANRE) and they are reviewed annually [8].

e. The comparison of power and energy losses between energizing solutions: from NPG, partly from NPG and partly from local sources, entirely from local sources;

f. The determination of permanent regime and hence the voltage level for the connection configuration of the chosen distributed generation source;

g. The calculation of three-phase short circuit currents due to NPG, for short circuits that occur in the network where distributed generation source are connected;

h. The calculation of all relay protections adjustments involved in case of breakdown;

i. The assessment, by calculation, of all power quality disturbances caused by distributed generation source, connected to the public network, serving the users of electricity.

2.1. Legislative recommendations for connecting to NPG

Taking into account the legislation in force [6, 8], there are the following components:

a. Steps to achieve a power generation plant
- Obtaining the necessary building permits and authorizations,
- Achievement of the objectives,
- Obtain a license to produce electricity,
- Obtaining the qualification for priority production of electricity from the production capacity,
- Registering to Market Operator and to the Green Certificates Market Operator (SC OPCOM SA)
- Signing up to OTS (Transelectrica SA);

b. Documents issued by the county or local public administration
- Certificate of urbanism - including details of all notices to be achieved;
- Building permit.

c. Documents issued by the grid operator where the local source of electricity will be connected to:
- Placement approval - issued according to Methodology for issuing the placement approval accepted by ANRE Order no. 48/2008;
- Connection technical approval - issued under the Connection Regulation of users to local public electric network, approved by GD no. 90/2008.

d. Documents issued de ANRE
- Permit of establishment, according to the Regulation for licensing and authorization in the electricity sector, approved by GD 540/2004, with amendments, approved by GD 553/2007;
- Electricity production license, according to the Regulation for licensing and authorization in the electricity sector, approved by GD 540/2004, with amendments approved by GD 553/2007;
- Qualification for electricity priority production, according to qualification Regulation for priority production of electricity from renewable energy sources, approved by ANRE Order no. 39/2006.

3. CALCULATION OF STEADY STATE OF THE POWER SYSTEMS

3.1. Algorithm for material parameters of local power system components

Figure 1 shows the one-phase diagram of a power system that analyzes the technical conditions for connection of a local generator to the National Grid.

Local synchronous micro generator connected to the consumer's bars has the following rated data:

- Three fase aparent power S_{ngt} = 100 kVA;
- Rated synchronous speed rotation Ω =100·π rad/s (n_n = 3000 rot/min);
- Number of pole pairs p = 1 pole pairs
- Rated frequncy f_n = 50 Hz
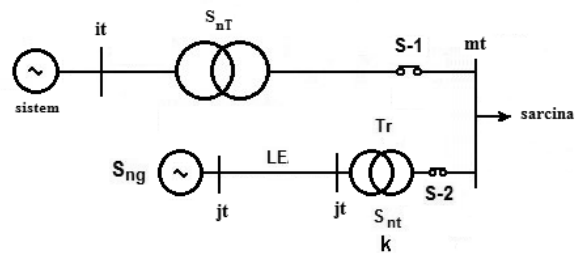- Flowing voltage and curent

Fig. 1. Single-phase diagram of a distribution network

- direct sequence rated percentage syncronous reactance of x_s ;
- Direct sequence rated percentage over - transient reactance x''_d;
- Direct sequence rated percentage transient reactance x'_d .

With the rated data, it can be calculated quantities of material for micro-generator mentioned above. Thus:

- the synchronous resistance of the synchronous micro generator reported to low voltage R_s = 0.
- supratranzitorie directă a microgeneratorului sincron raportată la joasă tensiune R_d = 0.
- direct over-transient resistence of the syncronous micro – generator reported to low voltage R_d = 0.
- inverse transient resistance of the syncronous micro – generator reported to low voltage R_i = 0.
- Syncronous reactance of the syncronous micro – generator reported to low voltage.
- Direct over transient reactance of the syncronous micro-genarator reported to low voltage.
- Inverse transient reactance of the three fase syncronous micro-generator reported to low voltage.

The rated data of the three phase transformer are:

- Primary rated voltage (medium voltage) U_{n1} = 20 kV;
- Secondary rated voltage (low voltage) U_{n2} = 0,4 kV;
- Transformation ratio k_{12} = 50
- Winding conection Δ/y_o or Y/z_o, vector group 5 or 11;
- Aparent power S_{nt} ;
- Rated active power losses for shortcircuit test ΔP_{sc} ;

- The rated percentage voltage for shortcircuit test u_{sc} ;
- Rated active power losses for not loaded test ΔP_o ;
- Percentage electric curent for not loaded test $i_o = 3,1\%$.

With the rated data, it can be calculated the transformer parameters as equivalent diagram adopted for given sequence of the transformer, as follows:

- Transformer windings resistance relative to the medium voltage or low voltage.
- transformer windings impedance relative to medium voltage.
- transformer windings Reactance relative to medium voltage.
- Complex expression of transformer impedance relative to medium voltage.
- No-load apparent power.
- No-load active power P_o.
- No-load reactive power of the transformer.
- Complex expression of no-load power of the transformer.

3.2. Local power system modeling

Single-phase equivalent circuit connected to the system shown in Figure 1 is shown in Figure 2.For single-phase equivalent circuit connected to the system in Figure 1 is drawn the vector diagram in Figure 3, which can model operating equations for the steady state regimes (normal or fault - short circuit) for the analyzed power system. For accurate modeling of the network it is proposed to represent the equivalent circuit in Figure 3, in which are indicated: $\underline{S_o}$ - used power for no-load distribution transformer from the supplier patrimony, $\underline{S_c}$ - equivalent full load of the user connected to the distribution board and is defined by the expression:

$$\underline{S_c} = P_c + j \cdot Q_c \tag{2a}$$

$$\underline{k} = \frac{U_{n\ mt}}{U_{n\ jt}} \cdot \left(1 \pm \frac{p}{100}\right) \cdot e^{j \cdot c \cdot \frac{\pi}{6}} \tag{2b}$$

Where

Un_{mt} and U_{njt} rated voltage transformer windings, p - percentage value of the step voltage control on a plug, c – transformer connection group and x - number of the plug on which the transformer works.
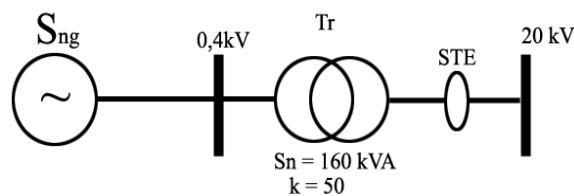

Fig. 2. Connection diagram to the network of a micro-generator

The remaining quantities in Figures 3 and 4 are defined similar as powers $\underline{S_o}$ or $\underline{S_c}$ and have the meanings:
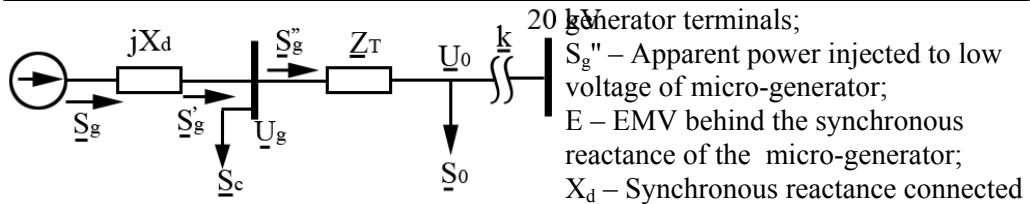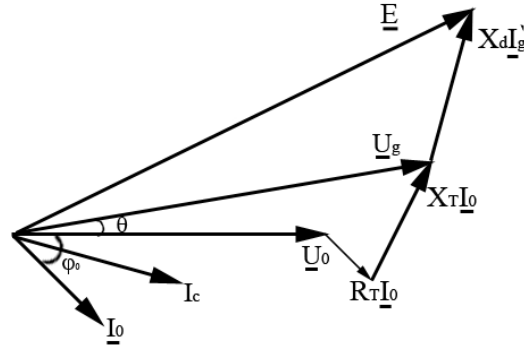
Fig. 3. Single phase diagram of the related system

Fig. 4. Vector diagram of the related system

20 kV generator terminals;

S_g'' – Apparent power injected to low voltage of micro-generator;

E – EMV behind the synchronous reactance of the micro-generator;

X_d – Synchronous reactance connected to the low voltage of the micro-generator;

U_{ng} – Rated voltage of the micro-generator;

S_{ng} – Apparent power of the micro-generator;

x_d – Rated percentage synchronous reactance;

P_{sc} – Rated active power losses of the transformer;

u_{SC} –percentage short circuit voltage of the transformer;

U_{nT} – rated winding voltage to which they are related;

S_{nT} – rated apparent power of the transformer;

$\underline{k}$ – complex transformation operator defined in the relation (2b).

S_g – Flowing apparent power of the Micro-generators;

S_g' – Apparent power to the micro-

Next will be presented relations needed to solve the steady state system. Thus, apparent power of the generator can be defined by the relation:

$$\underline{S}_g = \underline{S}'_g + \Delta\underline{S}_g \tag{3}$$

where the power losses associated with the generator are:

$$\Delta\underline{S}_g = j \cdot X_d \cdot \left|\underline{S}'_g\right|^2 \Big/ \left|\underline{U}_g\right|^2 \tag{4}$$

and the apparent power injected to distribution board is defined as:

$$\underline{S}''_g = \underline{S}'_g - \underline{S}_c \tag{5}$$

If the power losses associated with the transformer are:

$$\Delta\underline{S}_T = \underline{Z}_T \cdot \left|\underline{S}'_o\right|^2 \Big/ \left|\underline{U}_o\right|^{-2} \tag{6}$$

If the voltage U_o, is known, then the rms values of the voltages $\underline{U}_g$ and $\underline{E}$ are determined by relations:

$$\underline{U}_g = U_o + \underline{Z}_T \cdot \frac{S_o^*}{U_o} \qquad\qquad și$$

$$\underline{E} = \underline{U}_g + j \cdot X_d \cdot \left(\underline{S}'_g \big/ \underline{U}_g\right)^* \tag{7}$$

With the above relations, was calculated steady state for three-phase generator whose rated data are shown in Table 1, the data obtained are given below. Thus, Table 1 shows the material and consumption data and Table 2 shows the calculation results of steady state, using appropriate relations [1-4].

Table 1. **Quantities of material and consumption data of a synchronous micro-generator connected to NPG**

Generator connected to 0,4 kV						Load of the generator		
S_{en}	U_{ne}	I_n	x_d	X_e	E_e	P_{3e}	O_{3e}	S_{3e}
kVA	kV	A	%	Ω	kV	kW	kVAr	kVA
200	0,4	166,7	125	1	0,46	8,1	16,8	18,6
200	0,4	166,7	125	1	0,47	18,1	23,5	29,7
200	0,4	166,7	125	1	0,50	33,2	33,6	47,2
200	0,4	166,7	125	1	0,53	48,2	43,6	65
200	0,4	166,7	125	1	0,56	63,3	53,7	83
200	0,4	166,7	125	1	0,59	78,4	63,7	101
200	0,4	166,7	125	1	0,63	93,5	73,8	119
200	0,4	166,7	125	1	0,67	108,5	83,8	137
200	0,4	166,7	125	1	0,71	123,6	93,9	155
Local user						Windings		
P_{3f}	λ		O_{3f}	S_{3f}		ΔP_T		ΔQ_T
kW			kVAr	kVA		kW		kVAr
5,0	0,83		3,4	6,0		2,53		7,26
15,0	0,83		10,1	18,1		2,59		7,24
30,0	0,83		20,2	36,1		2,65		7,22
45,0	0,83		30,2	54,2		2,72		7,19
60,0	0,83		40,3	72,3		2,79		7,17
75,0	0,83		50,4	90,4		2,86		7,14
90,0	0,83		60,5	108,4		2,93		7,11
105,0	0,83		70,6	126,5		3,01		7,07
120,0	0,83		80,6	144,6		3,09		7,04

Table 2. **Results for a synchronous micro-generator connected to NPG**

tablou de j.t.		mers în gol			transformator					
U_e	-θ	ΔP_o	i_o	ΔO_o	S_n	k	U_o	U_2	ΔP_{sc}	u_k
kV	°	kW	%	kVAr	kVA		kV	kV	kW	%
0,421	0,018	0,525	3,1	6,178	200	50	0,420	21	2,9	4
0,415	0,018	0,525	3,1	6,178	200	50	0,415	21	2,9	4
0,410	0,019	0,525	3,1	6,178	200	50	0,410	21	2,9	4
0,405	0,019	0,525	3,1	6,178	200	50	0,405	20	2,9	4
0,400	0,020	0,525	3,1	6,178	200	50	0,400	20	2,9	4
0,395	0,021	0,525	3,1	6,178	200	50	0,395	20	2,9	4
0,390	0,021	0,525	3,1	6,178	200	50	0,390	20	2,9	4
0,385	0,022	0,525	3,1	6,178	200	50	0,385	19	2,9	4
0,380	0,023	0,525	3,1	6,178	200	50	0,380	19	2,9	4

5. CONCLUSIONS

Table 2 leads to the conclusion that the public electrical network connecting micro-generator may lead to the need to the following requirements:

a. Connection to the public network fee assessment

b. The comparison of power and energy losses between energizing solutions: from NPG, partly from NPG and partly from local sources, entirely from local sources;

c. The determination of permanent regime and hence the voltage level for the connection configuration of the chosen distributed generation source;

d. The calculation of three-phase short circuit currents due to NPG, for short circuits that occur in the network where distributed generation source are connected;

e. The calculation of all relay protections adjustments involved in case of breakdown;

f. The assessment, by calculation, of all power quality disturbances caused by distributed generation source, connected to the public network, serving the users of electricity;

g. Detecting dangerous situations that require intervention with trained staff , working with appropriate equipment;

h. The obligation of correct installation of measuring equipment and proper use of the various portable earthing equipment in public distribution networks.

REFERENCES

[1] Eremia M., *Electric Power Systems, Electric Networks*, Editura Academiei Române, Bucureşti (Romanian Academy Publishing House, Bucharest), 2006.

[2] Pătrăşcoiu S, *Stabilitatea sistemelor electroenergetice. Aspecte clasice şi moderne.* Editura MatrixRom, Bucureşti (Stability of power systems. Classical and modern aspects. MatrixRom Publishing House, Bucharest), 2000.

[3] Sorina Costinaş, *Asigurarea calităţii serviciului de alimentare cu energie electrică. Seria Electrotehnică – Electroenergetică*, Editura AGIR, Bucureşti, 2012 (Ensuring quality power supply service. Series Electrical - Power Systems, AGIR Publishing House, Bucharest, 2012).

[4] Toader, C., Golovanov, N., Postolache, P., Porumb, R., Beiu, C., *Conditions of grid connection distributed generation sources*. 8th International Conference on Industrial Power Engineering, April 14-15, 2011 – Bacău, România.

[5] . *** *Legea nr.318 / 2003 - a energiei electrice (Law no 318/2003 – of Electric energy).*

[6] . *** *HG nr.867 / 2003 pentru aprobarea Regulamentului privind racordarea utilizatorilor la reţelele electrice de interes public. (GD no. 867/2003 for approval of the Regulation regarding the users' connection to the public electricity networks).*

[7] . *** *Codul Tehnic al Reţelelor Electrice de Distribuţie, aprobat prin Decizia ANRE nr. 101/2000* (Technical Code of electricity distribution networks, approved by ANRE Decision no. 101/2000);

[8] . *** *Metodologie de stabilire a compensaţiilor băneşti între utilizatorii racordaţi în etape diferite, prin instalaţie comună, la reţele electrice de distribuţie, Ordin ANRE nr.28/2003* (Methodology for determining compensations between connected users at different stages through common installation, at electrical distribution networks, ANRE Order nr.28/2003);

[9] *** *Connection criteria at the distribution network for distributed generation*, Task Force, C6.04.01, October, 2005.

THE MODERN ESTIMATION OF POWER FACTOR

MARIA DANIELA STOCHIȚOIU[1], ALIN CRISTIAN GRUBER[2]

Abstract: *Energy is a product with great economic, social, strategic and political values. It is indispensable for any country's economy as for industries, services and human activities. The power factor is an important quality indicator for efficiency estimation of electrical energy.*

Key words: active energy, reactive factor of distorting, geometrical power factor.

1. INTRODUCTION

The power factor determination is made to estimate the additional power losses in the electrical webs due to the reactive power circulation between the active power transportation. The power factor has a value which is depending by the local electrical web configuration and it is emphases by the supplier agreement of electrical energy for each customer [3].

It is important that the power factor do not be lower than neutral power factor. If the power factor is lower than 0,92 and bigger than 0,65, the value of reactive power quantity is calculated with the reactive energy price corresponding of the voltage from the delimitation node. If the power factor is lower than 0,65 the value of the reactive power quantity is calculated third of energy power price [4].

For the sinus waves, the power factor is:

$$1 \geq \lambda \equiv PF = \frac{P}{S} \geq 0 \tag{1.1}$$

$$\lambda \equiv PF = \frac{P}{S} = \frac{U \cdot I \cdot \cos\varphi}{U \cdot I} = \cos\varphi \ ; \ 0 \leq \cos\varphi \leq 1 \tag{1.2}$$

P – the active power [W];
Q – the reactive power [VAR];

[1] *Associate Professor Eng., Ph.D. at University of Petrosani*
[2] *Professor at School Group Aurel Vlaicu Lugoj*

S – the apparent power [VA].
For the deforming waves, the power factor is:

$$\lambda \equiv PF = \frac{P}{S} = \frac{P}{\sqrt{P^2 + Q^2 + D^2}} \qquad (1.3)$$

D – the distorting power [VAD]

Based on the power factor, the electricity company's manager can monitories the energetic behaviour and can assure the lowest possible cost for the energy supply. The industrial manager also can estimate the efficiency of the electrical energy, avoiding the situations which lead to expensive technologies or to damage the electrical devices.

2. THE MODERN ESTIMATION OF POWER FACTOR

The relation (1.3) can be written using the reactive factor and the distorting factor. [1]
- the **reactive factor of distorting** status is define as the ratio between the reactive power and the active power:

$$\rho = \frac{Q}{P} \qquad (1.4)$$

- the **distorting factor** represents the ratio between distorting power and the undistorting power:

$$\tau = \frac{D}{\sqrt{P^2 + Q^2}} \qquad (1.5)$$

So,

$$\lambda \equiv PF = \frac{P}{S} = \frac{P}{\sqrt{P^2 + Q^2}} \cdot \frac{\sqrt{P^2 + Q^2}}{\sqrt{P^2 + Q^2 + D^2}} = \cos\varphi \cdot \cos\xi \quad (1.6)$$

Where,

$$\cos\xi = \frac{\sqrt{P^2 + Q^2}}{\sqrt{P^2 + Q^2 + D^2}} < 1 \qquad (1.7)$$

In dependence with the reactive power and the distorting power, the relation (1.3) becomes:

$$\lambda \equiv PF = \frac{1}{\sqrt{1 + \rho^2}} \cdot \frac{1}{\sqrt{1 + \tau^2}} \qquad (1.8)$$

The definition of the power factor doesn't show the using level of available power in the electrical web in the deformed regime, because the harmonically sources even are the nonlinear receptors not the generators.

The term $\cos\varphi$ must be use only the variation in time of voltage and the current waves are nonsinusoidal.

- the **fundamental power factor** and the **true power factor** [1]

It is necessary to have in view the electrical energy quality in the interface node of supplier – customer taking in account the extending of nonlinearity of loads.
The supplier has the duty to deliver a voltage which has the wave characterized by the true value of power factor of distorting the accepted limit.

For the low and average voltage webs the total distorting factor must be under 8% conforming the European Standards EN 50160. The accepted levels of harmonics are prescript by the same standard, too.

The supplier requires some limits of perturbation determined on the current wave as the voltage does not be affected and to respect some standards quality indicators. The devices used for monitories an analysis of electrical energy quality are showing two values, one for the fundamental harmonic **DPF** and another one for the total power factor **PF** .

Between these values can appear large difference and an uninformed energetic engineering can take wrong decisions for compensation measurements of reactive power using battery of condensators which can affect the quality energy due to the amplification of harmonics.

DPF – the fundamental power factor at 50/60 Hz:

$$\lambda_1 \equiv DPF = \cos\varphi_1 = \frac{P_1}{S_1} \tag{1.9}$$

PF – the total power factor:

$$\lambda \equiv PF = \frac{P}{S} = \frac{P}{U \cdot I} \tag{1.10}$$

The PF includes the influences of harmonics above the active power and the apparent power giving informations about the efficiency of the active power.

The active power in the no sinus regime is given by the sum of the active powers corresponding of which harmonics:

$$P = \sum_{h=1} U_h I_h \cos(\alpha_h - \beta_h) = \sum_{h=1} U_h I_h \cos(\varphi_h) = P_1 + P_H \tag{1.11}$$

P_1 - is the fundamental active power

$P_1 = U_1 I_1 \cos\varphi_1$

P_H - is the active power of each harmonic

$$P_H = \sum_{h \neq 1} U_h I_h \cos(\varphi_h)$$

S1- is the apparent power of fundamental:

$$S_1 = U_1 \cdot I_1 ; S_1^2 = P_1^2 + Q_1^2 \tag{1.12}$$

S- is the harmonical apparent power

$$S = (U \cdot I)^2 = \left(U_1^2 + U_H^2\right)\left(I_1^2 + I_H^2\right) = S_1^2 + S_H^2 \tag{1.13}$$

The power factor can be defined by introducting the distorting factor **THD** for current and fort the voltage.

$$k_{DI} \equiv THD_I = \frac{I_H}{I_1} = \sqrt{\frac{\sum_{h \neq 1} I_h^2}{I_1^2}} \quad (1.14); \quad k_{DU} \equiv THD_U = \frac{U_H}{U_1} = \sqrt{\frac{\sum_{h \neq 1} U_h^2}{U_1^2}} \tag{1.15}$$

$$\text{So,} \quad \lambda \equiv PF = \frac{P}{S} = \frac{P_1 + P_H}{\sqrt{S_1^2 + S_H^2}} = \frac{\left(P_1 / S_1\right)\left[1 + \left(P_H / P_1\right)\right]}{\sqrt{1 + \left(S_N^2 / S_1^2\right)}} =$$

$$\frac{\left[1 + \left(P_H / P_1\right)\right] \cdot DPF}{\sqrt{1 + THD_I^2 + THD_U^2 + \left(THD_I \cdot THD_U\right)^2}} \tag{1.16}$$

Due to the distorting residue of the active power is more lower than the fundamental active power $P_H \ll P_1$, so $\dfrac{P_H}{P_1} \ll 1$.

For **THD**$_U$ < 5% and **THD**$_I$ > 40%, the relation between the total power factor and the fundamental power factor is :

$$\lambda \equiv PF = \frac{1}{\sqrt{1 + THD_I^2}} \cdot DPF = \frac{I_1}{I} \cdot \cos \varphi_1 \tag{1.17}$$

Where: I_1 - is the effective value of fundamental component of current;

        I-   is the effective value of nonsinusoidal current;

      φ_1 - is the phase between the fundamental component of the current and the voltage waves.

The distribution operator can request some filters in the common coupling node for reduce the electrical perturbation in standard limits, where the customer has nonlinear loads which can produce an important current distortion **THD**$_I$ > 20%.

- the **arithmetical power factor** and **geometrical power factor nonechilibrated systems :**

S_a represents the arithmetical apparent power [VA]

$$S_a = \sum_{x \subset A,B,C} S_x = S_A + S_B + S_C = \tag{1.18}$$

$$S_A = \sqrt{P_A^2 + Q_a^2} \; ; S_B = \sqrt{P_B^2 + Q_B^2} \; ; S_C = \sqrt{P_C^2 + Q_C^2}$$

$S_{A,B,C}$, $P_{A,B,C}$, $Q_{A,B,C}$ - represent the apparent power, active power and the reactive power on the three phases.

S_g - represents the geometrical power [VA]:

$$S_g = \sqrt{P^2 + Q^2} \tag{1.19}$$

$$P = \sum_{x \subset A,B,C} P_x = P_A + P_B + P_C; \quad Q = \sum_{x \subset A,B,C} Q_x = Q_A + Q_B + Q_C$$

$$S_g = \left| P_A + P_B + P_C + j(Q_A + Q_B + Q_C) \right| = \left| P + jQ \right| \tag{1.20}$$

The arithmetical power factor is defined by:

$$\lambda_a \equiv PF_a = \frac{P}{S_a} = (P_A + P_B + P_C)/(S_A + S_B + S_C) \tag{1.21}$$

The geometrical power factor is defined by:

$$\lambda_g \equiv PF_g = \frac{P}{Sg} = (P_A + P_B + P_C)/(\underline{S_A} + \underline{S_B} + \underline{S_C}) \tag{1.22}$$

$$\underline{S_A} = P_A + jQ_A; \quad \underline{S_B} = P_B + jQ_B; \quad \underline{S_C} = P_C + jQ_C$$

3.THE MODERN PROCEEDINGS FOR POWER FACTOR MEASUREMENT

For the apparent power measurement there are two ways:

1) using the based measurement devices with induction counter, where the apparent power is calculated based on the active power measurement and of the reactive power:

$$S_{PQ} = \sqrt{P^2 + Q^2} \; ; P = P_A + P_B + P_C; \quad Q = Q_A + Q_B + Q_C; \tag{1.23}$$

There also was developing digital counter which determ the apparent power in conforming by relation (1.23).

2.) using digital miscellaneous which are measuring the apparent power based on the sectional voltage and current:

$$S = U_A I_A + U_B I_B + U_C I_C \tag{1.24}$$

Where I_A, I_B, I_C and U_A, U_B, U_C are the RMS values of the line currents and the phase voltages. Due to are using two methods for apparent power measurement, the power factor is calculated in two way:

$$PF_{PQ} = \frac{P}{S_{PQ}} = \frac{P}{\sqrt{P^2 + Q^2}} \; (1.25); \; PF_{UI} = \frac{P}{S_{UI}} = \frac{P}{U_A I_A + U_B I_B + U_C I_C} \tag{1.26}$$

When the current wave is unbalanced, the value S_{PQ} will be lower than S_{UI}. This difference is produced that the actual counter give us incorrect information in the distorting regime. The causes which determ a reduced power factor are:

- the asynchronous motors function having a loading factor $\beta < 1$ ($\beta = \dfrac{P}{P_n}$)

$$Q = Q_n \cdot \left[\alpha + (1 - \alpha)\beta^2 \right] \tag{1.27}$$

$\alpha = \dfrac{Q_0}{Q_n}$ Represents the ratio between the reactive power when $\beta = 0$ and the reactive

power when $\beta = 1$. The power factor is decreasing when $\beta < 0,5$.

$$\lambda \equiv PF \equiv \cos\varphi = \frac{P}{\sqrt{P^2 + Q^2}} = \frac{\beta}{\sqrt{\beta^2 + \left[\alpha + (1-\alpha)\beta^2\right]^2 tg\,\varphi_n}} \; ; \; tg\,\varphi_n = \frac{Q_n}{P_n} \tag{1.28}$$

- the transformer operating with an average apparent power lower than nominal

apparent power, $\beta = \dfrac{S}{S_0}$ - represents the loading factor of the transformer;

$$Q = \frac{S_n}{100} \cdot \left(I_0 + k_f \cdot \beta^2 \cdot u_{sc} \right) \tag{1.29}$$

- the existing of transformers on the supply lines;
- the reactive power consumption on the delivery electrical webs.

$$Q_L = \omega \cdot L \cdot I^2 \; ; \qquad Q_C = \omega \cdot C \cdot U^2 \tag{1.30}$$

3. CONCLUSIONS

The apparent power factor can be estimated like the maximum transferable of the active power when the voltages and the line losses are constant. The ratio P/S is an indicator of using the active power. The estimation of the electrical energy cost based on the total power factor doesn't supply information above their electrical behavior and doesn't allow taking in account the losses on electrical webs, for the customers with the emphasing nonlinear characteristics. The PF includes the harmonics influences above the apparent power and give us information about the active power using efficiency $PF \leq DPF$. The optimization of the system (mounting the battery of condensators or the active filters) requires a completed examination of the alternatives because the problem of improvement of power factor is in dependence with the necessity of elimination the unsinus regime.

REFERENCES

[1]. **Ionescu Golovanov C.** *Masurarea marimilor electrice in sistemul electroenergetic,* Editura Academiei Romane, Bucuresti 2009.

[2]. **Dumitriu L., s.a**. *Teoria circuitelor electrice*, Editura Matrixrom, Bucuresti 2007.

[3]. **Orban M.D.** s.a. *Electrotehnica si masini electrice*, Editura Academica Brancusi, Tg Jiu, 2002.

[4]. **Orban M.D., Marcu M.D., Popescu F.G.** *About of electrical energy quality and the deforming state due to electronic devices*. SNET(Simpozionul Național de Electrotehnică Teoretică), 14-16 octombrie 2007, București, UPB.

CONSIDERATIONS REGARDING THE TESTS IN EXPLOSIVE MIXTURES MADE UPON THE ELECTRICAL APPARATUS WITH THE TYPE OF PROTECTION FLAMEPROOF ENCLOSURE "d"

LUCIAN MOLDOVAN[1], MARTIN FRIEDMANN[2], MIHAI MAGYARI[3], DRAGOŞ FOTĂU[4]

Abstract: The type of protection flameproof enclosure applies generally to electrical apparatus which in normal operation produces electrical arcs and sparks, and consists in placing the parts that could ignite an explosive atmosphere inside of an enclosure that can withstand the pressure developed during an internal explosion of an explosive mixture and which prevents the explosion transmission to the explosive atmosphere surrounding the enclosure. The paper presents the most important aspects that must be taken into account when running tests in explosive mixtures (determination of explosion pressure, overpressure test, test for non-transmission of an internal ignition) for verification of flameproof character of the enclosure for explosion-proof electrical equipments with the type of protection flameproof enclosure.

Keywords*:* flameproof enclosure, reference pressure, overpressure, non-transmission.

1. GENERALITIES

Explosion proof electrical apparatus, with the type of protection flameproof enclosure „d", is included in one (or possible both) of the following two groups [6]:
- Group I: electrical apparatus for mines susceptible to firedamp;
- Group II: electrical apparatus for places with an explosive gas atmosphere other than mines susceptible to firedamp.

For the type of protection flameproof enclosure, group II electrical apparatus is divided in 3 subgroups: IIA, IIB and IIC.

---

[1] *PhD.eng. IIIrd degree scientific researcher, INCD INSEMEX Petroşani,*

[2] *PhD.eng. Ist degree scientific researcher, INCD INSEMEX Petroşani,*

[3] *PhD.eng. IInd degree scientific researcher, INCD INSEMEX Petroşani,*

[4] *Eng. scientific research assistant, INCD INSEMEX Petroşani,*

This dividing of group II in 3 subgroups (for the type of protection flameproof enclosure) was made in the basis of the maximum experimental security gap (MESG), which is decreasing in value from group IIA to Group IIC, as follows:
- in IIA subgroup are included gases with MESG > 0,9 mm;
- in IIB subgroup are included gases with 0,5 mm < MESG < 0,9 mm;
- in IIC subgroup are included gases with MESG < 0,5 mm.

The specific elements that ensure the protection to explosion for a flameproof "d" equipment are represented by flameproof joints. A flameproof joint represents the place where the corresponding surfaces of two parts of an enclosure, or the conjunction of enclosures, come together, and which prevents the transmission of an internal explosion to the explosive atmosphere surrounding the enclosure [4],[5].

There are three types of flameproof joints: non-treaded, threaded and special joints.

The non-treaded joints category includes: flanged, cylindrical, spigot and serrated joints.

The threaded joints category includes the cylindrical threaded joints and taper threaded joints.

The special joints category includes the cemented joints, labyrinth joints and floating gland joints.

Non-treaded flameproof joints are characterized by two parameters: the width and the gap of the joint.

The width of flameproof joint, L, represents the shortest path through a flameproof joint from the inside to the outside of an enclosure [1],[5].

The gap of flameproof joint, i, represents the distance between the corresponding surfaces of a flameproof joint when the electrical apparatus enclosure has been assembled. For cylindrical surfaces, forming cylindrical joints, the gap is the difference between the diameters of the bore and the cylindrical component [4], [5].

For certification of electrical apparatus with the type of protection flameproof enclosure, this is subjected to type and routine tests [1].

In the type tests category are included, beside others, the tests in explosive mixtures which are in fact the most important tests in order to verify the safety of this type of protection [1].

In the routine tests category is included the overpressure routine test, which have the purpose of verifying enclosure resistance to pressure and that the enclosure does not contain holes or cracks connecting to the exterior [1].

The tests in explosive atmospheres are divided in 3 categories:

2. DETERMINATION OF EXPLOSION PRESSURE [5]

The reference pressure is the highest value of the maximum smoothed pressure, relative to atmospheric pressure, observed during these tests.

Each test consists of igniting an explosive mixture inside the enclosure and measuring the pressure developed by the explosion.

The number of tests to be made and the explosive mixture to be used, in volumetric ratio with air and at atmospheric pressure, are as follows:
– electrical apparatus of Group I: three tests with (9,8 ± 0,5) % methane;

- electrical apparatus of Group IIA: three tests with (4,6 ± 0,3) % propane;
- electrical apparatus of Group IIB: three tests with (8 ± 0,5) % ethylene;
- electrical apparatus of Group IIC: three tests with (14 ± 1) % acetylene and three tests with (31 ± 1) % hydrogen.

3. OVERPRESSURE TEST [5]

This test shall be made using either of the following methods, which are considered as equivalent.

a) Overpressure test – First method (static)

The relative pressure applied shall be
-   1,5 times the reference pressure, with a minimum of 3,5 bar, or
-   4 times the reference pressure for enclosures not subject to routine overpressure testing, or
-   at the following pressures, when reference pressure determination has been impracticable.

Volume cm^3	Group	Pressure bar
≤10	I, IIA, IIB, IIC	10
>10	I	10
>10	IIA, IIB	15
>10	lIC	20

The period of application of the pressure shall be at least 10 s and the test is made once.

b) Overpressure test – Second method (dynamic)

The dynamic tests shall be carried out in such a way that the maximum pressure to which the enclosure is subjected is 1,5 times the reference pressure, but with a minimum of 3,5 bar.

When the test is carried out with mixtures specified for the determination of the reference pressure, these may be precompressed to produce an explosion pressure of 1,5 times the reference pressure.

The test shall be made once only except for electrical apparatus of Group IIC for which each test shall be made three times with each gas.

4.TEST FOR NON-TRANSMISSION OF AN INTERNAL IGNITION [5]

Gaskets shall be removed and the enclosure is placed in a test chamber. The same explosive mixture is introduced into the enclosure and the test chamber, at atmospheric pressure.

The flamepath lengths (engagement) of threaded joints of the test specimen(s) shall be reduced according to Table 1.

Flanged gaps of spigot joints, where the width of the joint L consists only of a cylindrical part shall be enlarged to values of 1 mm for Groups I and IIA, 0,5 mm for Group IIB and 0,3 mm for Group IIC.

Table 1. **Reduction in length of a threaded joint for non-transmission test**

Type of threaded joint	Reduction in length by			
	Groups I, IIA and IIB		Group IIC	
	3.1 a)	3.1 b)	3.2 a)	3.2 b)
Cylindrical, complying with ISO 965, fit medium or better	No reduction	No reduction	No reduction	No reduction
Cylindrical, with larger tolerances than permitted above	1/3	1/2	1/2	1/3
Taper thread (NPT)	No reduction	No reduction	No reduction	No reduction

4.1 ELECTRICAL APPARATUS OF GROUPS I, IIA AND IIB [5]

a) The gaps i_E of the enclosure shall be at least equal to 90 % of the maximum constructional gaps i_C as specified in the manufacturer's drawings ($0,9\, i_C \leq i_E \leq i_C$).

The explosive mixtures to be used, in volumetric ratio with air and at atmospheric pressure, are as follows:

– electrical apparatus of Group I: $(12,5 \pm 0,5)$ % methane-hydrogen [(58 ± 1) % methane and (42 ± 1) % hydrogen] (MESG = 0,8 mm);

– electrical apparatus of Group IIA: $(55 \pm 0,5)$ % hydrogen (MESG = 0,65 mm);

– electrical apparatus of Group IIB: $(37 \pm 0,5)$ % hydrogen (MESG = 0,35 mm).

If the gaps of a test specimen do not fulfill the above condition, one of the following methods may be used for the type test for non-transmission of an internal ignition:

– a gas/air mixture with a smaller MESG value:

Group	i_E / i_C	**Mixture**
Group I	≥0,75	55 % H_2 ± 0,5
	≥0,6	50 % H_2 ± 0,5
Group IIA	≥0,75	50 % H_2 ± 0,5
	≥0,6	45 % H_2 ± 0,5
Group IIB	≥0,75	28 % H_2 ± 1
	≥0,6	28 % H_2 ± 1
		at 1,4 bar

– precompression of the normal test mixtures according to the following formula:

$$P_k = \frac{i_C}{i_E} \times 0,9 \tag{1}$$

where P_k is the precompression factor.

b) If enclosures of Groups IIA and IIB could be destroyed or damaged by the test for non-transmission of an internal ignition, it is permitted that the test be made by increasing the gaps above the maximum values specified by the manufacturer. The enlargement factor of the gap is 1,42 for Group IIA electrical apparatus and 1,85 for Group IIB electrical apparatus. The explosive mixtures to be used in the enclosure and in the test chamber, in volumetric ratio with air and at atmospheric pressure, are as follows:

- electrical apparatus of Group IIA:

(4,2 ± 0,1) % propane;

- electrical apparatus of Group IIB:

(6,5 ± 0,5) % ethylene.

The test for non-transmission of an internal ignition shall be made five times. The test result is considered satisfactory if the ignition is not transmitted to the test chamber.

4.2 ELECTRICAL APPARATUS OF GROUP LIC [5]

The following methods can be used for this test:

a) First method

All gaps of joints other than threaded joints shall be increased to the value

$i_E = 1,5 \times i_C$ with a minimum of 0,1 mm for flanged joints;

where i_E is the test gap;

i_C is the maximum constructional gap, as specified on the manufacturer's drawings.

The following explosive mixtures, in volumetric ratio with air and at atmospheric pressure, are to be used in the enclosure and in the test chamber:

– (27,5 ± 1,5) % hydrogen, and

– (7,5 ± 1) % acetylene.

Five tests shall be made with each mixture. If the apparatus is intended for use solely with hydrogen or solely with acetylene, the tests shall be made only with the corresponding gas mixture.

b) Second method

The enclosure shall be tested with a test gap i_E according to the following formula:

$0,9\, i_C \leq i_E \leq i_C$

The enclosure and the test chamber are filled with one of the gas mixtures specified for the first method at a pressure equal to 1,5 times atmospheric pressure.

The test shall be carried out five times with each explosive mixture.

Alternatively, if the gaps of a test specimen do not fulfil the above condition, by agreement between the testing station and the manufacturer, the following method may be used.

Precompression of the normal test mixtures according to the following formula:

$$P_k = \frac{i_C}{i_E} \times 1{,}35 \tag{2}$$

where P_k is the precompression factor.

With help of (1) and (2) formulas, the pressure of the explosive mixture could be calculated for different values of i_E/i_C ratio, issue presented in figure 1 [1].
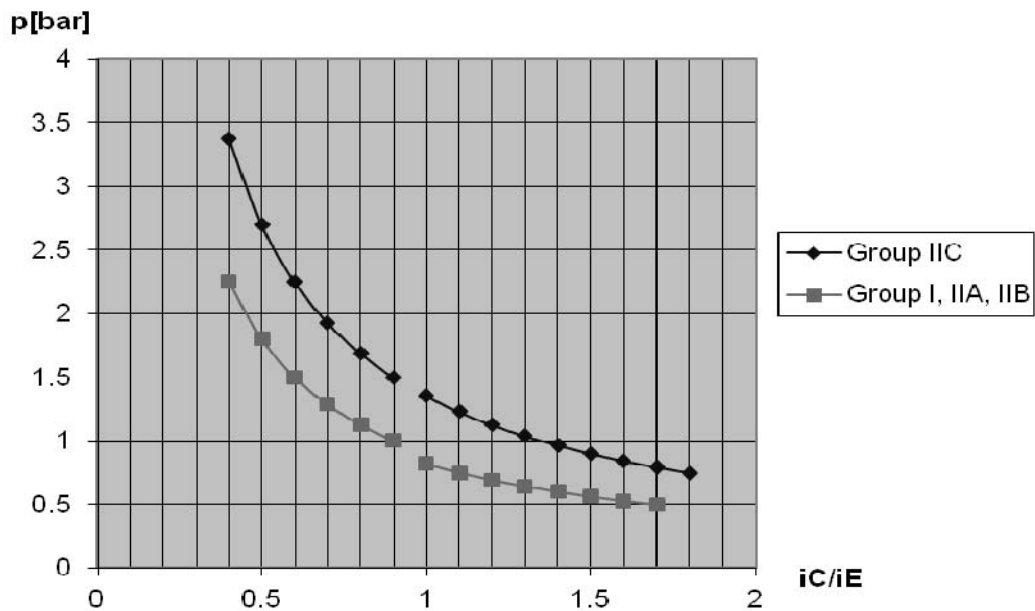

Fig.1. Influence of i_E/i_C ratio over the testing mixture pressure

From the diagram it observes that for small values of the testing gap relative to the constructive gap, high values of the testing mixture pressure are obtained; and for the testing gap values smaller than those of the constructive gap, smaller values of the explosive mixture pressure are obtained, possible smaller even than the atmospheric pressure. Because of this reason, in case of testing gap value higher than the constructive gap value, the non-transmission of an internal ignition test for a IIC group equipment will be done at the overpressure of 1,5 atmospheric pressure [1].

For apparatus with flamepaths, other than threaded joints, and intended for use at an ambient temperature above 60 °C, the non-transmission tests shall be conducted under one of the following conditions [5]:

   – at a temperature not less than the specified maximum ambient temperature;
   – at normal ambient temperature using the defined test mixture at increased pressure according to the factors in Table 2;
   – at normal atmospheric pressure and temperature, but with the test gap i_E increased by the factors noted in Table 2.

Table 2 – **Test factors to increase pressure or test gap (i_E)**

Temperature up to °C	Group I 12,5 % CH_4/H_2	Group IIA 55 % H_2	Group IIB 37 % H_2	Group IIC 27,5 % H_2 7,5 % C_2H_2
60	1,00	1,00	1,00	1,50
70	1,06	1,05	1,04	1,67
80	1,07	1,06	1,05	1,70
90	1,08	1,07	1,06	1,73
100	1,09	1,08	1,06	1,74
110	1,10	1,09	1,07	1,77
120	1,11	1,10	1,08	1,80
125	1,12	1,11	1,09	1,83

During the tests in explosive mixtures it was observed that, when the enclosure of the equipment has the internal free volume in the form of a mono volume regular geometric shape (cylinder, parallelepiped, cube, sphere), the pressure curve resulted after the test for determination of explosion (reference) pressure has a pattern like the one presented in fig. 2.
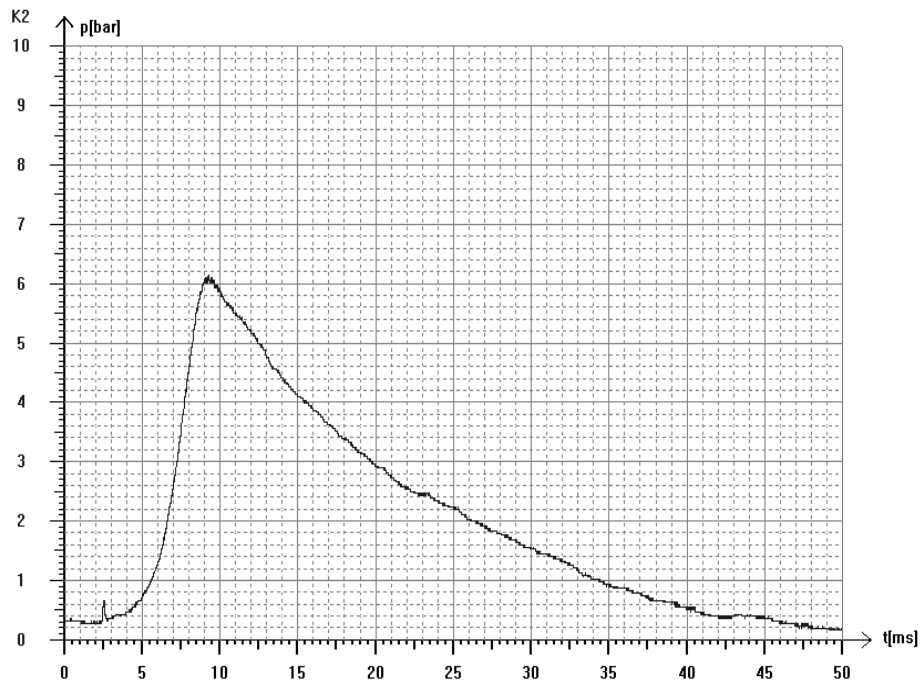
Fig. 2. Pattern of a reference pressure curve obtained when testing a IIC group equipment with internal free volume in the form of a regular geometric shape

Also, in case of equipments with the internal free volume in the form of a regular geometric shape, when performing the overpressure test, with an air-gas mixture at 1,5 bar, the pattern of the pressure curve remains the same as in case of reference pressure determination, and the maximum pressure is approximately 1,5 times higher than in case of reference pressure determination.

When testing equipments with enclosures having the internal free volume divided in two or more compartments that communicate between them through small orifices (for example the enclosure of an electric motor) the pattern of the pressure curve resulted after the test for determination of explosion (reference) pressure is like the one presented in fig. 3.
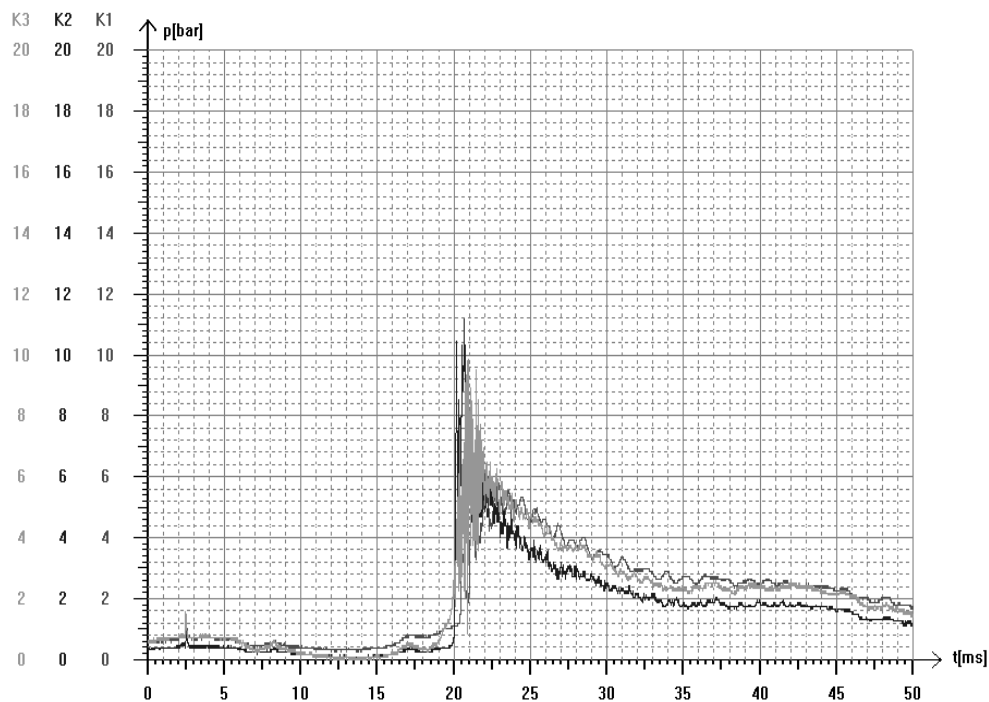
Fig. 3. Pattern of a reference pressure curve obtained when testing a IIC group equipment with multiple compartments communicating between them

In this case the pressure pilling phenomena (which represents the results of an ignition, in a compartment or subdivision of an enclosure, of a gas mixture precompressed, for example, due to a primary ignition in another compartment or subdivision) occurs, resulting in higher values of the pressure than in case of non-compartmented enclosures.

Also, in case of equipments with the internal free volume which is divided in two or more compartments that communicate between them through small orifices when performing the overpressure test with a mixture of air-gas at 1,5 bar, the maximum pressure can be higher than 1,5 times the maximum value obtained in case of reference pressure determination (fig. 4).
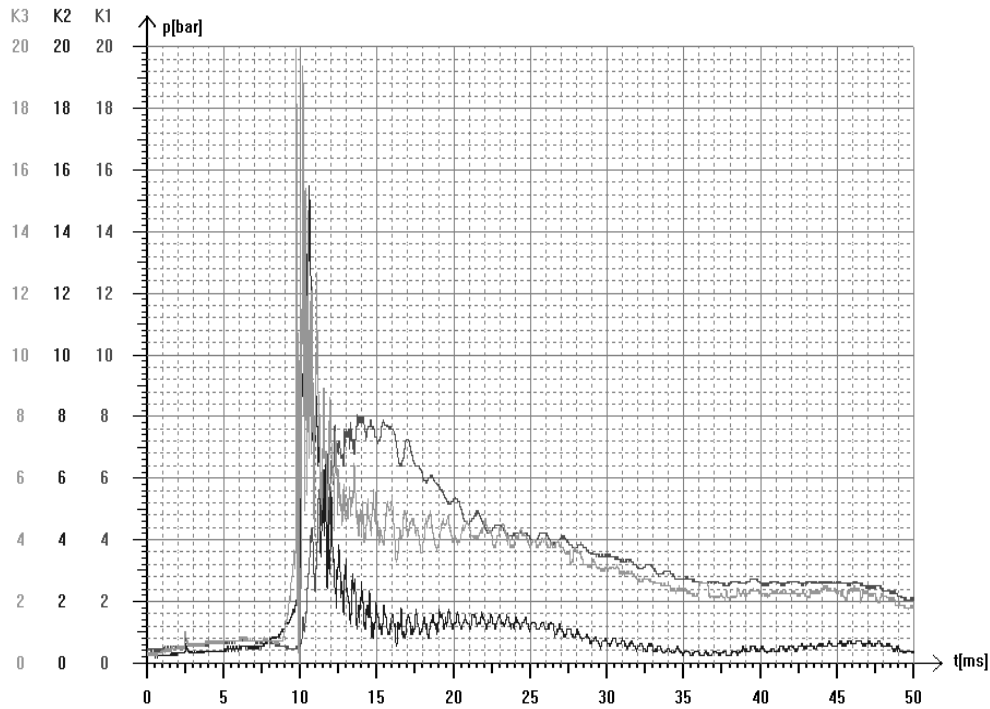
Fig. 4. Pattern of an overpressure curve obtained when testing a IIC group equipment with multiple compartments communicating between them

4. CONCLUSIONS

This paper revealed the influence of the gap over the precompression factor of the explosive mixture for the non-transmission of an internal ignition test.

Also, some pressure curves obtained during testing of flameproof enclosure equipment were analysed in order to underline the pressure pilling phenomena that can occur in case of equipment enclosures with multiple compartments that communicate between them. It is not recommended that the pressure pilling to occur when testing the enclosures in explosive mixture because of the high stresses to which the enclosure is subjected during the tests, higher than in normal conditions (without the precompression of the gas).

It is recommended that the manufacturers to find the best solutions for the enclosures of the flameproof enclosure equipments in order to prevent, as much as possible, the occurrence of pressure pilling when running the tests in explosive mixtures.

It is also recommended for the manufacturers of electrical explosionproof apparatus with the type of protection flameproof enclosure, that all the flameproof joints to have the values of the gap in the range of $0.9\ i_C \le i_E \le i_C$, for the sample that will be tested in explosive mixtures.

REFERENCES:

[1].Arad, S., Stepanescu, I., Lupu, L., *Numerical analysis for heat transfer in normal regime of a flame-proof transformer*, Proceedings Simpozion naţional de Electrotehnică teoretică SNET07 Ed. Printech, pp 198- 203, 567 pgs., sec. E, ISBN 987-973-718-899-1, Bucuresti, 2007.

[2].Lupu, L., Paraian, M., Ghicioi, E., Arad, S., Selection of technical equipment intended for use in underground firedamps mines, Proceedings of MPES2006, pp. 166-172, ISBN 88-901342-4-0, Edited by M. Cardu, R. Ciccu, E. Lovera, E. Michelotti printed in Italy by FIORDO srl-Galliate, Torino, Italy, 2006.

[3].Moldovan L., Friedmann M., Magyari M., *Aspects regarding the influence of the flameproof joints gap on the tests in explosive mixtures for electrical apparatus with flameproof enclosure type of protection,* The works of the VIIIth International Symposia „Young people and Multidisciplinary Research", Timişoara, 2006, ISBN-10 973-8359-39-2, ISBN-13 978-973-8359-39-0.

[4].Moldovan L., Friedmann M., *Underlining the technical and safety characteristics for explosionproof electrical apparatus with type of protection flameproof enclosure*, International Symposia Safety and Health at Work - SESAM 2007, ISSN 1843-6226.

[5].* SR EN 60079-1:2008, *Explosive atmospheres - Part 1: Equipment protection by flameproof enclosures "d",* ASRO, 2008.

[6].* SR EN 60079-0:2010, *Explosive atmospheres - Part 0: Equipment – General requirements,* ASRO, 2010.

INDEX OF AUTHORS

REVIEWERS